



Low Carbon Technologies

Conference proceedings

28th – 30th of June 2021
Czech Republic

Low Carbon technologies

Conference proceedings

ORGANIZED BY



ENERGY
AND ENVIRONMENTAL
TECHNOLOGY CENTRE

ENET
CENTRE

PARTNERS



MISKOLCI
EGYETEM
UNIVERSITY OF MISKOLC



**INSTITUTE FOR CHEMICAL
PROCESSING OF COAL**

SUPPORTED BY

• Visegrad Fund

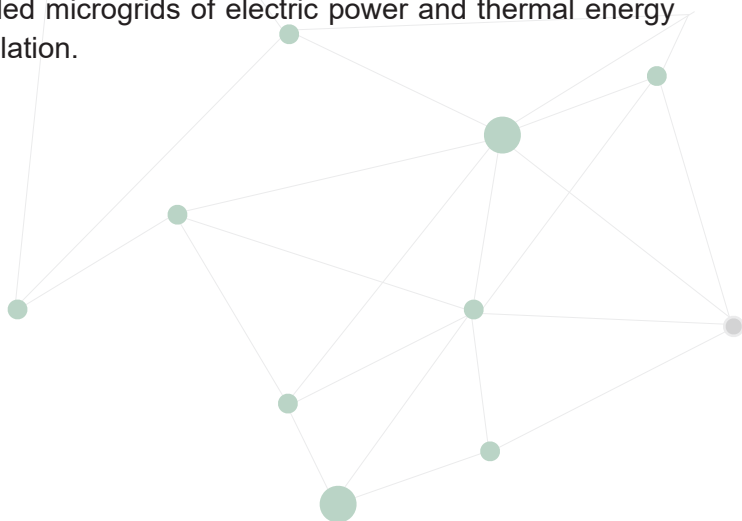
2021

Energy and environmental technology centre

About us

The core of research and development at ENET Centre is energy transformation. The Centre aims to convert feedstock raw materials, particularly waste and alternative fuels, into exploitable forms of energy and investigate their subsequent effective use.

The aim of ENET Centre is research and development in the field of renewable energy resources in order to reduce or eliminate harmful environmental impacts. The efforts focus on new technologies of transport and processing of energy raw materials, on their effective energy transformation and modern solutions of the so-called microgrids of electric power and thermal energy making use of accumulation.



History of the centre

In September 2010 the Ministry of Education, Youth and Sports of the Czech Republic granted VSB – Technical University of Ostrava subsidies at the amount of CZK 316.6 million in order to implement the Project of ENET – Energy Units for Utilization of Non-traditional Energy Sources – CZ.1.05/2.1.00/03.0069 within the Operational Programme for Research, Development and Innovation.

The objective of the ENET Project was to build a university institution CENET – Centre of Energy Utilization of Non-traditional Energy Sources focusing on research and development of interconnected technologies and machinery for compact energy units, including new technologies of transport and processing of energy raw materials, and their effective energy transformation to supply the grid. All the processing and transformation stages also include the technologies of cleaning the combustion products and waste. The research outputs are user-configured (various types of input and output) and performance-scalable facilities for operation/ the industry. The project implementation has contributed to new and higher quality concepts of related educational programmes at VSB-TUO. The project activities were carried out by research teams from four faculties of VSB-TUO and the Nanotechnology Centre. ENET Project has led to the development of a modern European research centre dealing with basic and applied interdisciplinary research of effective and efficient utilization of energy.

Content

1	The Utilization of Coal Gasification Residue as Geopolymer Base Material	6
2	Carbon footprint of coal gasification with carbon capture and storage	16
3	Torrefied biomass as a soil amendment	21
4	Thermal gasification of waste	29
5	Safety aspects of hydrogen fueling stations	36
6	Pellet quality analysis: Torrefaction after pelletization and vice versa	45
7	Recovery of compressor waste heat in Organic Rankine Cycle	52
8	An Examination of Thermal Features' Relevance on Battery-Fault Detection	60
9	The Informative Value of Ash Fusibility Tests	68
10	Complete Syngas Cleaning in a Mobile Wet Scrubber	76
11	Filtration of hot process gases as a key step towards larger industrial uptake of gasification technologies	89
12	Gasification of biomass for the production of electricity and heat in cogeneration	104
13	The utilisation of Vehicle-to-Grid Technology in Power Engineering	111



14

The Using of Fuel Cell
in Micro-Cogeneration Unit in Buildings

120

15

Experimental Investigation of Selected Parameter's Effect on
Solid Biofuels Quality and Densification Process

128

16

Biomass gasification and gas cleaning: combined utilization of
in-situ catalyst and continually working filter for complete gas
cleaning

145

The Utilization of Coal Gasification Residue as Geopolymer Base Material

Roland Szabó¹, Mária Ambrus¹ and Gábor Mucsi¹

¹ Institute of Raw Material Preparation and Environmental Processing/
University of Miskolc, Miskolc (Hungary)

1. Abstract

This study focused on the utilization of the coal gasification residues (cokes) as geopolymer material. In the article, the effect of the replacement of fly ash with 10, 20 and 30 wt.% cokes on the properties of geopolymers is examined. Two types of mechanically activated cokes were used for two sets of experiments to study the changes in the geopolymers. The XRF analysis of the base materials revealed a relative difference in the quantity of the main components. Using a higher density base coal for gasification resulted in higher compressive strength values of the geopolymers, successfully increasing the compressive strength from 11.17 MPa to 15.32 MPa with replacing 30 wt.% fly ash in the mixture. The compressive strength was slightly increased with the use of coke from gasifying lower density base coal, the highest value was only 12.16 MPa with 30 wt.% coke addition. The standard fly ash based geopolymers had the highest specimen density values for both experiments. Applying FTIR spectroscopy, the important geopolymerization reactions could be monitored.

Keywords: coal gasification residue, compressive strength, fly ash, geopolymer

2. Introduction

Considering the global energy mix, coal is considered the second most important energy source utilized via combustion. However, more environmentally friendly uses of coal for fuel production have been investigated in the past decades, such as gasification or liquefaction. Gasification is a thermochemical process that involves the conversion of organic matter to mainly two products: synthesis gas and residual solid matter (such as fly ash or coke). Besides being a more environmentally friendly process than combustion, coal gasification is considered an effective and economical method for coal utilization (Luo et al., 2021, Sebe et al., 2020).

The possible utilization of residual coke from gasification is a significant research topic which led to the determination of numerous potential applications, these include uses as:

- agricultural products, such as soil conditioner or low analysis fertilizer;
- different aggregates, sand substitute;
- landfill and soil stabilization material;
- carbon-silica composite materials;
- industrial material, such as catalyst, filter media, industrial filler, etc.;

- resource for carbon, magnetite, Fe, Al and other metals;
- base material for geopolymer production (Choudhry and Hadley, 1992; Park et al., 2017 Zhu et al., 2020).

Geopolymers are a novel material class which are prepared by the alkali or in some cases acidic activation of a wide variety of alkali-silicate of aluminosilicate base materials. The nomenclature to these 3D structured polymer systems was given by Joseph Davidovits in the late 1970s. The applicable base materials for geopolymer production include numerous primary raw materials, e.g. kaolin or zeolites, and various industrial wastes and by-products as well, e.g. fly ash, ground granulated blast furnace slag, red mud or gasification residues. The advantages of geopolymers include exceptional mechanical properties, fire resistance, good thermal insulation properties, significantly lower CO₂ emissions than OPC concretes, etc. (Davidovits, 1991, Kumar et al., 2017).

In certain cases, the low reactivity of the solid base materials can hinder the geopolymerization process, leading to reduced mechanical properties in the final product. Changes induced in material during the mechanical activation process (such as reduction in particle size, increase in specific surface area, changes in particle morphology, structural defects, decrease in crystallinity degree, implying structural rearrangement) can significantly improve reactivity of raw materials like FA (Temuujin et al., 2009, Marjanović et al., 2014, Kumar et al., 2017, Mucsi et al., 2015).

The application possibilities of coal gasification residue in geopolymers are yet to be profoundly investigated, as there is no extensive literature published about such experiments. The existing literature focuses on cokes produced via integrated coal gasification combined cycle (IGCC) which could be used as cement replacement material, aggregates in geopolymer concrete or for the production of geopolymer composites (Luo et al., 2021, Kim and Chae, 2018, Park et al., 2017).

In the article, coke from brown coal gasification experiments and deposited brown coal fly ash were used to examine the possibility of geopolymer production and the effects of fly ash – coke replacement on the properties of the geopolymers.

3. Materials and methods

3.1. Materials

The materials used for the geopolymer production in this study were landfilled brown coal fly ash (FA) and two brown coal gasification cokes (C1 and C2). The cokes were prepared using brown coal with the same particle size fractions ($1\text{ mm} < x < 20\text{ mm}$) but different densities ($<1.6\text{ g/cm}^3$ and $<1.8\text{ g/cm}^3$) gasified at $900\text{ }^{\circ}\text{C}$ with 10 g/min steam addition. The loss on ignition (LOI) of the base materials was 86.62% for the $<1.6\text{ g/cm}^3$ and 83.62% for the $<1.8\text{ g/cm}^3$ coal. C1 coke was made from coal with density of $<1.8\text{ g/cm}^3$ and C2 coke using coal with density of $<1.6\text{ g/cm}^3$. The chemical composition of the raw materials can be seen in Table 1. According to the results, SiO₂, Al₂O₃, CaO, Fe₂O₃ are the main components

of cokes and FA. There is a considerable divergence in the chemical composition of the two types of raw materials regarding the silica, alumina, CaO, Fe₂O₃, and SO₃ content, but LOI values were also significantly different. Cokes contain more CaO, Fe₂O₃ and SO₃ while FA contains more SiO₂ and Al₂O₃. The comparison of the LOI of the coal samples and the cokes reveals that the coal with lower LOI value resulted in lower LOI for the gasification residue, which is associated with the carbon content of initial brown coal and carbon conversion during the gasification process.

Tab. 1: Chemical composition of raw materials

Sample	SiO ₂	Al ₂ O ₃	MgO	CaO	Na ₂ O	K ₂ O	Fe ₂ O ₃	MnO	TiO ₂	SO ₃	LOI*
C1	15.17	6.90	1.23	4.73	0.42	1.02	11.66	0.09	0.21	4.97	47.70
C2	10.97	5.06	1.07	3.71	0.34	0.72	8.25	0.07	0.17	4.38	61.10
FA	61.32	26.71	0.89	1.50	1.06	1.72	4.27	-	-	0.25	1.92

*LOI at 815 °C

3.2. Sample preparation

Prior to geopolymerization experiments, it was necessary to reduce the particle size of the coke sample materials in several steps. As a first step, the coke samples were crushed with a hammer crusher below 1 mm, and then milled in a ball mill (volume of mill: 5000 cm³; milling media diameter: $d_{\max}=40$ mm, $d_{\min}=12$ mm; milling media filling ratio: 0.3) for 60 min. The amount of feed coke during milling was 147 g. Preliminary experiments revealed that the cokes on their own were not suitable for the production of geopolymer as the specimens disintegrated during the removal from the mold, which could be explained by the low silica and alumina content of the samples. Therefore, it was necessary to use a base material containing higher reactive SiO₂ and Al₂O₃. As a result, the ground cokes were mixed with FA in given amounts (10; 20 and 30 wt.%). FA used for geopolymer production was mechanically activated by milling in a laboratory ball mill for 60 minutes based on the previous work of Mucsi et al. (2015) to improve its reactivity.

The activator used to prepare the geopolymers was a mixture of 12 M NaOH solution and water glass, while the liquid/solid (L/S) ratio was 0.82. First, FA was dry blended with the cokes and then the alkaline activating solution was added. The resulting mixture was then filled into 20×20 mm cubical molds. After that, the specimens were stored at room temperature for 24 hours, then heat cured at 60 °C for 6 hours. After cooling back to room temperature, the specimens were removed from the molds and uniaxial compressive strength tests were performed at 3 days of age. Three specimens were made for each series of measurements.

3.3. Methods

The chemical composition of raw materials was determined by X-ray fluorescence (XRF, Rigaku Supermini X-ray Fluorescence apparatus). The particle size distribution of ground coke samples and FA was investigated by a Horiba LA-950 V2 type laser particle size analyzer in wet mode. Specific surface areas had been calculated from the distributions by

the particle size analyzer, shape factor was 1. Before the measurements, the coke samples were dispersed in sodium-pyrophosphate solution. During the measurement processes, to achieve the appropriate dispersity state, 3-minute ultrasonic treatment was also applied. The chemical bonds in the raw materials and geopolymers were studied by FTIR analysis, which were carried out with a JASCO FT/IR 4220 spectrometer in reflection mode, with diamond ATR. From each sample, 3 measurements were performed, the results of which were averaged. Three days after demolding, the uniaxial compressive strength tests were carried out on 3 specimens using a hydraulic compression-testing machine (SZF-1 type).

4. Results and discussion

4.1. Milling of raw materials

The physical properties of cokes and FA are reported in Table 2. Based on the results, it can be stated that the coke samples had a smaller particle size and a higher specific surface area (SSA), than FA. C1 had the smallest characteristic particle sizes (e.g. median size was 9.22 μm) and the highest SSA (4660 cm^2/g).

Tab. 2: Physical properties of ground cokes (C1 and C2) and FA

Sample	C1	C2	FA
x_{10} [μm]	3.5	4.8	5.5
x_{50} [μm]	9.2	12.6	17.3
x_{80} [μm]	14.3	21.2	49.4
SSA [cm^2/g]	4660.8	2907.3	2293.7
ρ_{particle} [g/cm^3]	2.024	2.340	2.170

The FTIR spectra of the ground cokes and FA are shown in Figure. 1. Based on the Figure, it can be concluded that coke samples are typically dominated by two bands (around 2110 cm^{-1} and 2000 cm^{-1}), which, according to Gerakines et al. (1995), refer to the stretching vibrations of C–O bonds. The intensity of these bands is the highest in the IR spectrum of coke samples. In addition, a band belonging to O–C–O bonds can be observed around 2322 cm^{-1} , indicating the presence of carbon dioxide (Dong et al., 2019), as well as stretching vibrations of T–O–Si (T=Si or Al) bonds around 970 cm^{-1} . In case of FA, this band appeared at around 1048 cm^{-1} . Furthermore, in case of FA, the symmetric stretching vibration of Si–O–Si at 780 cm^{-1} and the Si–O–Si and Al–O–Si stretching bands can be also seen at 547 cm^{-1} (Panias et al., 2007). These bands are common in the ring silicates (Swanepoel and Strydom, 2002).

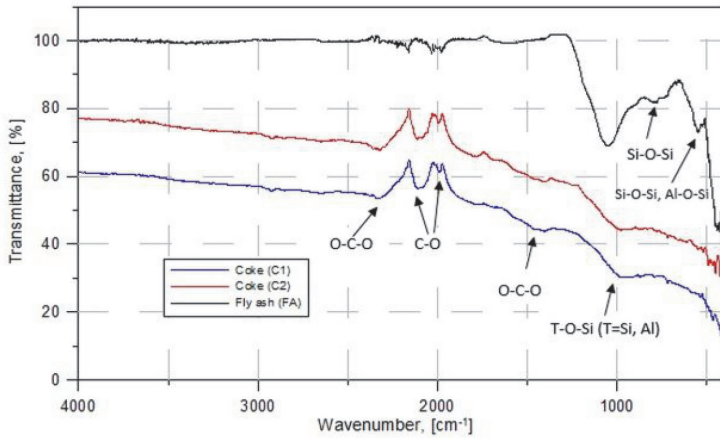


Fig. 1: FTIR spectra of cokes and FA

4.2. Properties of geopolymers

The average uniaxial compressive strength and specimen density values of the geopolymers with C1 addition can be seen in Figure 2. The geopolymers prepared from only FA had the lowest compressive strength value of 11.17 MPa which was increased by around 10% with the addition of both 10 and 20 wt.% C1 and over 30% with 30 wt.% C1. Thus, in case of C1, the highest compressive strength was achieved using 70 wt.% FA and 30 wt.% C1.

Contrary to the compressive strength, the standard FA geopolymer had the highest specimen density value, 1.61 g/cm³. The replacement of 10 wt.% FA with C1 resulted in the lowest specimen density, 1.46 g/cm³, with approximately 10% decrease. However, the increased C1 replacement led to a close to linear increase in specimen density, achieving 1.54 g/cm³ with 30 wt.% C1.

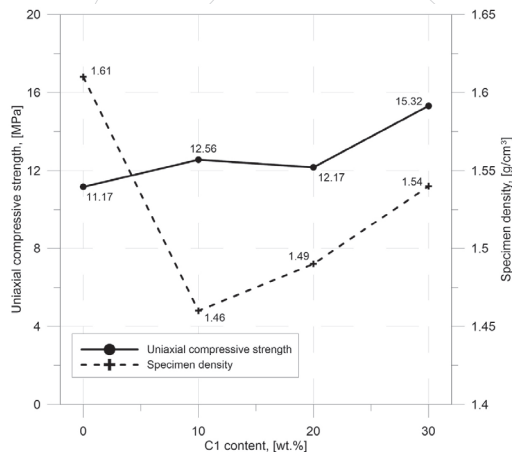


Fig. 2: Compressive strength and specimen density of geopolymers with various C1 contents

In Figure 3, the average uniaxial compressive strength and specimen density values of the geopolymers with C2 addition are illustrated. In contrast to the C1 containing geopolymers, the addition of 10 and 20 wt.% C2 slightly decreased the average uniaxial compressive strength values of the samples, from 11.17 MPa to 10.55 and 10.91 MPa, respectively. Using 30 wt.% C2 increased the compressive strength with almost 10% compared to the FA based geopolymer.

Similarly to the samples with C1, the highest specimen density was observed with the standard geopolymers. However, the replacement of FA with C2 slightly decreased the specimen densities, reaching the lowest value with 30 wt.% C2 at 1.54 g/cm³. Thus, the specimen density of the geopolymer with 30 wt.% C1 and C2 was the same but the mixtures with the two cokes exhibited different trends.

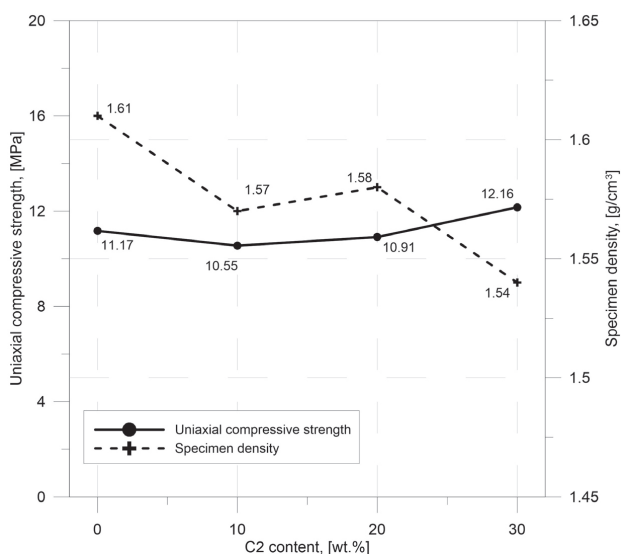


Fig. 3: Compressive strength and specimen density of geopolymers with various C2 contents

The inclusion of the ground C1 had a generally positive effect on the strength of the geopolymers, while the compressive strength was only increased using 30 wt.% of C2 in the mixtures. The addition of only 10 wt.% C1 resulted in similar compressive strength of the geopolymers as 30 wt.% C2. The difference between the effects of the two cokes may be explained by both the high SSA of the C1 sample, and the results of the chemical analysis, as the SiO₂ + Al₂O₃ content of the C2 was only ~70% of the combined silica and alumina content of the C1 sample. Regarding the LOI of the coke samples, the use of C1 (with lower LOI) resulted in better compressive strength values, thus, not only the overall composition and SSA but the LOI values of the base materials can also affect the properties of the final geopolymer products.

Figure 4 and Figure 5 show the effect of C1 and C2 addition on the structure of geopolymers. The band of T–O–Si (T=Si or Al) at 1048 cm^{-1} of the FA (Fig. 1) became sharper and shifted towards lower frequencies ($\sim 970\text{ cm}^{-1}$) in the FTIR spectra of geopolymers (Fig. 4 and 5), which is associated with the dissolution of the fly ash amorphous phase in the strong alkaline activating solution (Panias et al., 2007, Fernández-Jiménez and Palomo, 2005). In both Figures, it can be observed that the intensity of this band at 970 cm^{-1} increased with increasing amount of coke in the geopolymer (up to 20 wt.% coke addition), then showed a decrease. In the geopolymer samples, new bands appeared in the range of 3340 and 1644 cm^{-1} which were attributed to bending vibrations (H–O–H) and stretching vibration (–OH), respectively. These bands refer to the spectrum of adsorbed water (Swanepoel and Strydom, 2002, Fernández-Jiménez and Palomo, 2005). Further difference was found in the intensity of the bands belonging to O–C–O bonds at 1400 cm^{-1} (Panias et al., 2007). This broad band is a result of the presence of Na_2CO_3 sodium carbonate. This may be due to the atmospheric carbonation of the high alkaline NaOH aqueous phase, which is diffused on the geopolymeric materials surface (Swanepoel and Strydom, 2002, Criado et al., 2005, Fernández-Jiménez and Palomo, 2005). The intensity of this band increased with increasing coke content of the geopolymers.

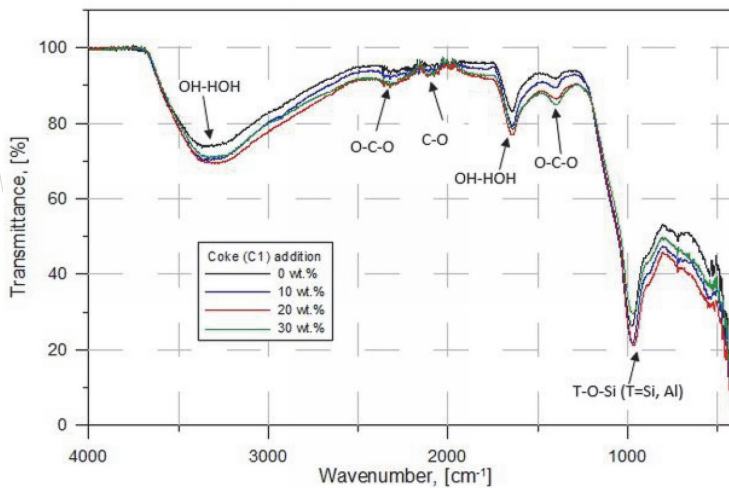


Fig. 4: FTIR spectra of geopolymers containing C1

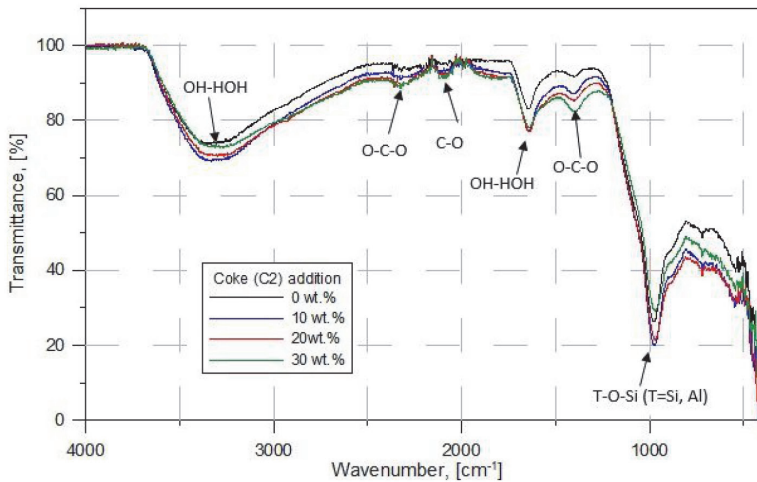


Fig. 5: FTIR spectra of geopolymers containing C2

5. Conclusion

Based on the results of the preliminary experiments, it can be concluded that the coal gasification residue (coke) used was not suitable for the production of geopolymers, as it had a relatively low SiO_2 and Al_2O_3 contents. However, the coke mixed with high aluminum silicate-bearing waste material (such as fly ash) is suitable for the production of geopolymers. The C1 sample with higher SSA and lower LOI values had a more prominent positive effect on the physical properties of the geopolymers, but higher amount of C2 addition could also increase the compressive strength of the specimens. The specimen density values were decreased with the use of FA and coke mixtures compared to the sample FA based geopolymers. FTIR spectroscopy measurements proved the formation of important geopolymerization reaction products in the geopolymer samples.

6. Acknowledgments

The cross-cutting research was conducted at the University of Miskolc as part of the „*More efficient exploitation and use of subsurface resources*“ project implemented in the framework of the Thematic Excellence Program funded by the Ministry of Innovation and Technology of Hungary (Grant Contract reg. nr.: NKFIH-846-8/2019), and within the subsequent „*Developments aimed at increasing social benefits deriving from more efficient exploitation and utilization of domestic subsurface natural resources*“ project supported by the Ministry of Innovation and Technology from the National Research, Development and Innovation Fund according to the Grant Contract issued by the National Research, Development and Innovation Office (Grant Contract reg. nr.: TKP-17-1/PALY-2020).



PROGRAM
FINANCED FROM
THE NRDI FUND

7. References

- Choudhry, V., Hadley, S.R., 1992. Utilization of Coal Gasification Slag. Overview, in Khan M.R. (Ed.), Clean Energy from Waste and Coal. ACS Symposium Series. American Chemical Society, Washington DC. pp 253-263.
- Criado, M., Palomo, A., Fernández-Jiménez, A., 2005. Alkali activation of fly ash. Part 1. Effect of curing conditions on the carbonation of the reaction products. *Fuel* 84, 2048–2054.
- Davidovits, J., 1991. Geopolymers: Inorganic polymeric new materials. *J. Thermal Anal.* 37, 1633-1656.
- Dong, L., Wang, Z., Zhang, Y., Lu, J., Zhou, E., Duan, C., Cao, X., 2019. Study on Pyrolysis Characteristics of Coal and Combustion Gas Release in Inert Environment. *J. Chem.* 2019, 1–9.
- Fernández-Jiménez, A., Palomo, A., 2005. Composition and microstructure of alkali activated fly ash binder: effect of the activator. *Cem. Concr. Res.* 35(10), 1984-1992.
- Gerakines, P.A., Schutte, W.A., Greenberg, J.M., van Dishoeck, E.F., 1995. The infrared band strengths of H₂O, CO and CO₂ in laboratory simulations of astrophysical ice mixtures. *Astron. Astrophys.* 296, 810-818.
- Kim, Y., Chae, T., 2018. Effect of addition of As-received IGCC slag in making geopolymer. *J. Ceram. Process. Res.* 19(5), 378-382.
- Kumar, S., Mucsi, G., Kristály, F., Pekker, P., 2017. Mechanical activation of fly ash and its influence on micro and nano-structural behaviour of resulting geopolymers. *Adv. Powder Technol.* 28, 805-813.
- Luo, F., Jiang, Y., Wei, C., 2021. Potential of decarbonized coal gasification residues as the mineral admixture of cement-based material. *Constr. Build. Mater.* 269, 121259.
- Marjanović, N., Komljenović, M., Baščarević, Z., Nikolić, V., 2014. Improving reactivity of fly ash and properties of ensuing geopolymers through mechanical activation. *Constr. Build. Mater.* 57, 151-162.

- Mucsi, G., Kumar, S., Csőke, B., Kumar, R., Molnár, Z., Rácz, Á., Máдай, F., Debreczeni, Á., 2015. Control of geopolymer properties by grinding of land filled fly ash. *Int. J. Miner. Process.* 143, 50-58.
- Panias, D., Giannopoulou, I.P., Perraki T., 2007. Effect of synthesis parameters on the mechanical properties of fly ash-based geopolymers. *Colloids Surf. A Physicochem. Eng. Asp.* 301, 246-254.
- Park, S., Kim, K. Kang, S., 2017. Fabrication of lightweight geopolymer based on the IGCC slag. *J. Korean Cryst. Growth Cryst.* 27(6), 319-326.
- Sebe, E., Nagy, G., Kállay, A.A., 2020. Co-Gasification of Refuse Derived Fuel Char with Hungarian Brown Coal. *Mater. Sci. Eng.* 45(1), 252-260.
- Swanepoel, J.C., Strydom, C.A., 2002. Utilization of fly ash in a geopolymeric material. *Appl. Geochem.* 17(8), 1143-1148.
- Temuujin, J., Williams, R.P., van Riessen, A., 2009. Effect of mechanical activation of fly ash on the properties of geopolymer cured at ambient temperature. *J. Mater. Process. Technol.* 209(12-13), 5276-5280.
- Zhu, D., Zuo, J., Jiang, Y., Zhang, J., Zhang, J., Wei, C., 2020. Carbon-silica mesoporous composite in situ prepared from coal gasification fine slag by acid leaching method and its application in nitrate removing. *Sci. Total Environ.* 707, 136102.

Carbon footprint of coal gasification with carbon capture and storage

Maciej Weiss¹, Marcin Lutyński²

¹ Pharmaceutical Plant "AMARA" Sp. z o.o., Cracow (Poland)

² Silesian University of Technology, Faculty of Mining, Safety Engineering and Industrial Automation, Gliwice (Poland)

1. Abstract

The article presents calculations of the amount of greenhouse gases emitted into the environment (Carbon footprint) produced in the hard coal gasification plant taking into account the entire chain of technological operations including Carbon Capture and Storage. The analysis of the amount of greenhouse gases emitted to the environment was performed on the basis of the proposed carbon footprint research methodology. Results of the study show that the share of individual processes in the emissions of greenhouse gases, is mainly influenced by two processes, namely the material production process and the hard coal gasification process. On the other hand, the process of transporting materials to the hard coal gasification plant has the lowest carbon footprint. Calculations of carbon footprint show that CCS technology cannot be called a zero-emission since there is always an indirect emission of GHGs. Nevertheless, the overall carbon footprint of the entire process is drastically reduced.

Keywords: carbon dioxide emissions, carbon footprint, coal gasification, Carbon Capture and Storage

2. Introduction

The concept of Carbon Footprint (CF) was created at the 1997 Kyoto Climate Conference, where all European Union countries undertook actions to control and reduce the emission of greenhouse gases harmful to the climate. The calculation method of CF mainly focuses on directly or indirectly induced anthropogenic sources of greenhouse gas emissions. According to the Greenhouse Gas Protocol, three greenhouse gas emissions scopes can be distinguished: Scope 1 - (direct emissions) these are emissions from sources owned or controlled by the company; Scope 2 - (indirect media emissions) these are emissions from the company's operations, but emitted from sources controlled by other parties; scope 3 - (indirect emissions) these are emissions from sources that are not owned and not directly controlled by the reporting company (Wiedmann, Minx 2008). CF is expressed in carbon dioxide equivalent (tCO₂eq). This unit allows the emissions of various greenhouse gases to be converted into tonnes of carbon dioxide equivalent. It is calculated on the basis of the Global Warming Potential (GWP) which was proposed by the International Panel on Climate Change (IPCC) (Radu, Scrieciu, Caracota 2013). The calculation of CF should cover the

entire life cycle of the product / service (LCA), starting from the process of extracting the necessary raw materials, through the production, distribution, use and disposal phase (Kulczycka, Wernicka 2019). In accordance with the applicable rules, a given company determines by itself the limits and scope of the carbon footprint calculations. There are two calculation options: from cradle to gate - this method takes into account all stages from raw material extraction to delivery of the finished product to the customer; from cradle to grave - this method takes into account all stages from extraction of raw materials to disposal (Śleszyński 2016).

In order to reduce GHG emissions into atmosphere and at the same time use fossil fuels a Carbon Capture and Storage concept was introduced. CCS (Carbon Capture and Storage) technology consists of three stages: capturing carbon dioxide, transporting carbon dioxide to the storage site and storing carbon dioxide in deep geological formations, with the possibility of using it to intensify the extraction of raw materials, e.g. crude oil and natural gas (Dubieński, Wachowicz, Koterak 2010). For safe and long-term carbon dioxide storage, it must be injected underground to a depth of over 800 meters. At this depth, due to the increased pressure and temperature, the carbon dioxide enters the supercritical phase. The density of carbon dioxide in the supercritical state is higher than that in the gaseous state, and therefore requires a smaller storage capacity. CCS technology that over 95% of CO₂ will be captured hence it is often called a zero-emission technology.

In this study a true Carbon footprint of hard coal gasification technology combined with CCS is presented. For the purpose of the study the entire chain of technological operations including Carbon Capture and Storage (CCS) process was taken into account.

3. Carbon footprint operational boundaries

For the purpose of the study certain CF operational boundaries were assumed. In this case the cradle-to-gate assumptions were made, these were as follows:

- hard coal gasification process is focused mainly on the production and sale of SNG gas rather than electricity,
- Electricity produced in the plant is mainly consumed for internal operation,
- The gasification plant only uses hard coal from one mine
- Hard coal from the mine to the plant is delivered exclusively via a conveyor belt (approx. 1 km distance),
- The remaining materials used in the gasification process are delivered to the plant by road or rail transport.

The following processes were not included in the CF calculations:

- construction, extension, renovation and decommissioning of plant infrastructure and infrastructure of companies producing materials necessary in the process,
- utilization of waste from the process and the production of other materials,
- transport and processing of finished SNG products.

CF calculations were made in accordance with the proprietary calculation method (Fig. 1). The method focuses on a thorough analysis of all input and output emissions from all stages of the hard coal gasification process (in accordance with the operational boundaries).

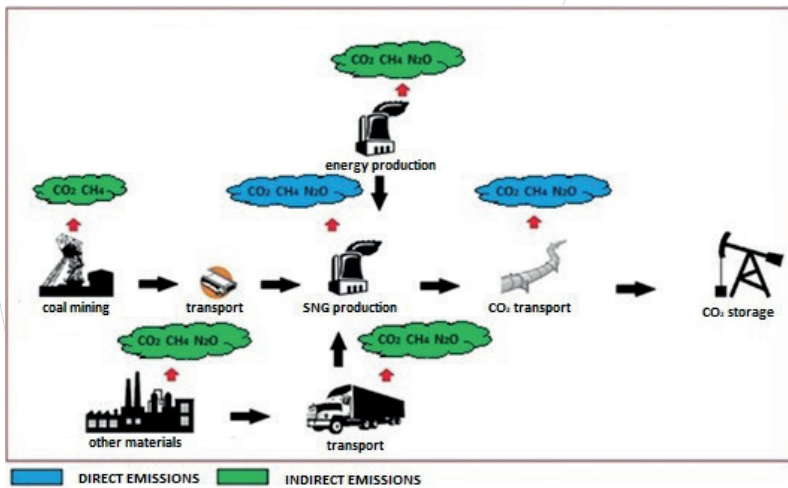


Fig. 1: SNG production in coal gasification plant with CCS and resulting emissions assumed in the study

In terms of materials consumption the following was assumed. The hard coal gasification process in the analyzed period (12 months) for production purposes will use: 1 867 531.9 Mg of hard coal; 10 968 016.256 Mg of air; 13 502 269.8 Mg of process water; 2 401 650.36 MWh of electricity. As a result, the following products will be produced: 1 303 537.43 Mg of SNG; 3 593 149.35 Mg of Carbon dioxide; 8 375 881.63 Mg of Nitrogen; 13 072.723 Mg of Sulfur; 169,044 Mg of ashes.

In addition to the gasification process itself, the following processes were also included in the analysis: hard coal mining (electricity demand - 67,231,148 MWh; heat demand - 176,863 GJ; emission from the production of the necessary amount of heat in a natural gas-fired heat plant is - 9.837 tCO₂eq; emission caused by hard coal mining is 339 890.68 tCO₂eq), transport of hard coal from the mine to the plant (as assumed above, the demand for electricity is 213.832 MWh), the operation of heavy equipment at the plant (the demand for diesel oil is 7 617 258 l, the emission resulting from the diesel oil production process is - 3 315.021 tCO₂eq; the emission from diesel oil transport to the plant is: road transport - 19.14 tCO₂eq, rail transport - 18.464 tCO₂eq; the emission from the use of the necessary amount of diesel oil is: 22 772.602 tCO₂eq).

4. Results and conclusions

The total CF of the hard coal gasification plant with CCS technology was calculated for three different variants resulting from the need to purchase additional electricity. The following variants of additional electricity production were analyzed: in a conventional pulverized coal-fired power plant, in a conventional pulverized coal-fired power plant with CCU technology; in a wind farm.

The carbon footprint of the hard coal gasification process, the carbon dioxide capture and storage process along with other processes (road transport) and the purchase of the necessary amount of electricity in a conventional pulverized coal power plant is 2 461 029.14 tCO₂eq. On the other hand, taking into account rail transport of materials, the carbon footprint slightly lowers to 2 461 028.464 tCO₂eq.

The carbon footprint of the hard coal gasification process, the carbon dioxide capture and storage process along with other processes (road transport) and the purchase of the necessary amount of electricity in a conventional pulverized coal power plant with CCU technology is 424 783. 628 tCO₂eq. However, taking into account rail transport of materials, the carbon footprint is 424 796.029 tCO₂eq.

The carbon footprint of the coal gasification process, the carbon dioxide capture and storage process along with other processes (road transport) and the purchase of the necessary amount of electricity produced in a wind farm is 370 011.87 tCO₂eq. However, taking into account rail transport of materials, the carbon footprint is 370 011.191 tCO₂eq.

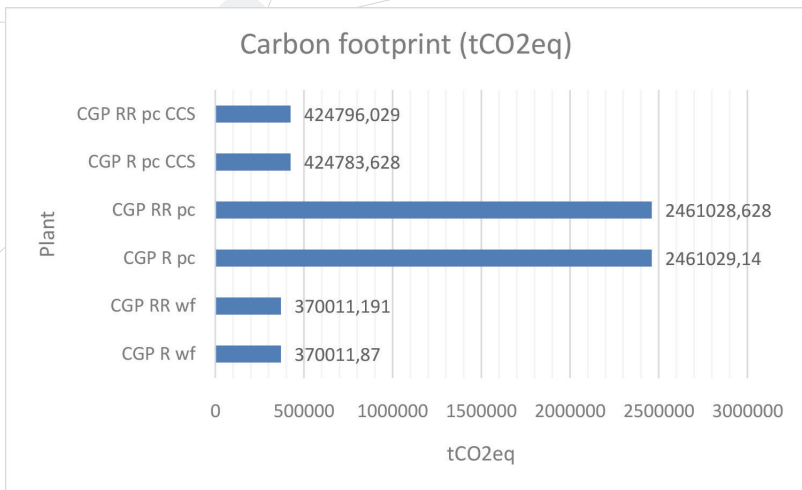


Fig. 2 Total carbon footprint of electricity production in the analyzed installations (CGP - hard coal gasification plant, R - road transport, RR - rail transport, wf - wind farm; pc - conventional pulverized coal power plant, pc CCS - conventional pulverized coal power plant with CCU technology)

The uncertainty of estimating the result of calculating greenhouse gas emissions from the production stage of materials used in the processes is (+/- 5.2%). According to the ranges for assessing the accuracy of the data used in the GHG protocol uncertainty tool, the GHG emission data used for the calculation of the carbon footprint of production, in terms of quality, is considered good (+/- 15%). The data showing the extraction of hard coal have the greatest uncertainty as to the quality (+/- 8.6%).

Taking into account all stages of hard coal gasification, it can be seen that CCS technology will never completely reduce greenhouse gas emissions generated in the gasification process. CCS technology can only significantly reduce greenhouse gas emissions at the gasification stage itself. The emissions from the remaining stages, i.e. the production of the necessary materials used in gasification, the transport of the produced materials, remains at the same level.

When analyzing the percentage share of individual processes in the emission of greenhouse gases, it can be concluded that the emissions are mainly influenced by two processes, namely the material production process and the hard coal gasification process. The process of transporting materials to the hard coal gasification plant has the least impact on the amount of greenhouse gas emissions.

5. References

1. Radu A.L., Sricciu M.A., Caracota D.M., 2013. Carbon Footprint Analysis: Towards a Projects Evaluation Model for Promoting Sustainable Development. *Procedia Econ. Finance* 6, 353–363. DOI:[https://doi.org/10.1016/S2212-5671\(13\)00149-4](https://doi.org/10.1016/S2212-5671(13)00149-4);
2. Bergen F., Pagnier H.J.M., Damen K., Faaij A.P.C., Ribberink J.S., 2003. Feasibility study on CO₂ sequestration and Enhanced CBM production in Zuid-Limburg. NOVEM (the Netherlands Agency for Energy and the Environment);
3. Śleszyński J., 2016. Footprinting, czyli mierzenie śladu pozostawionego w środowisku. *Optim. Stud. Ekon.* 1(79), 56–73. DOI:<https://doi.org/10.15290/ose.2016.01.79.04>;
4. Kulczycka J., Wernicka M., 2015. Metody i wyniki obliczania śladu węglowego działalności wybranych podmiotów branży energetycznej i wydobywczej. *Zesz. Nauk. Inst. Gospod. Surowcami Miner. Energią PAN* nr 89;
5. Dubiński J., Wachowicz J., Koterak A., 2010. Podziemne składowanie dwutlenku węgla - możliwości wykorzystania technologii CCS w Polskich uwarunkowaniach. *Gór.Geol.* 5, 1;
6. Panowski M., Zarzycki R., 2013. Analiza procesowa przygotowania wyseparowanego ze spalin dwutlenku węgla do transportu i składowania. *Polityka Energ.* 16, 4;
7. Luis P., 2016. Use of monoethanolamine (MEA) for CO₂ capture in a global scenario: Consequences and alternatives. *Desalination* 380, 93–99. DOI:<https://doi.org/10.1016/j.desal.2015.08.004>;
8. Rosa M., 2015. Cuéllar-Franca, Adisa Azapagic: Carbon capture, storage and utilisation technologies: A critical analysis and comparison of their life cycle environmental impacts. *J. CO₂ Util.* 9, 82–102. DOI:<https://doi.org/10.1016/j.jcou.2014.12.001>;
9. Wiedmann T., Minx J., 2008. A Definition of Carbon Footprint. *Res. Rep.* 07–01.

Torrefied biomass as a soil amendment

Marcel Mikeska¹, Kateřina Pračke², Jan Najser¹, Václav Peer¹,
Jaroslav Frantík¹ and Pavel Tlustoš²

¹ ENET Centre, VŠB -Technical University of Ostrava, 17. listopadu 15, Ostrava-Poruba CZ-708 33, Czech Republic

² Department of Agro-environmental Chemistry and Plant Nutrition, Faculty of Agrobiography, Food and Natural Resources, Czech University of Life Sciences Prague, Kamýcká 129, 165 00 Prague 6, Suchbát, Czech Republic

1. Abstract

Torrefaction is well known method for enhancement of biomass waste fuel properties. Main benefits of torrefied biomass are reduced water content and increased calorific value. In this study, torrefaction was used as possible method for utilization of biomass to create additive for soil properties improvement. Enormous use of chemical fertilizers is increasing with modern agriculture development, which may results in serious environmental impacts. Therefore finding renewable source of soil properties enhancer, which would improve the retention of nutrients and their accessibility in soils is important. Torrefaction of two types of biomass was carried out in the absence of oxygen in temperature 350 °C. For torrefaction, the batch pyromatic unit was used. Chemical composition of biomass as well as resulted biochar was determined. Levels of heavy metals were also monitored in torrefied biochar to evaluate its possibility of use in agriculture industry.

Keywords: : *torrefaction, biomass, biochar, agriculture*

2. Introduction

Thermochemical conversion methods as combustion, gasification and pyrolysis are promising technologies for utilization of organic materials incl. biomass as renewable source of energy (Honus et al. 2018; Honus and Juchelková 2014). However, these technologies are challenging due to the inferior fuel properties of biomass, such as high water and oxygen contents, low calorific value and strong hygroscopicity (Tong et al. 2018). In most of the researches torrefaction is considered to be pre-treatment technology improving properties of biomass to become preferable solid fuel (Chen et al. 2018; Tong et al. 2018; Wang et al. 2019). Torrefaction is generally carried out in low temperatures around 200 – 300 °C without oxygen presence (for example in N₂ atmosphere) (Gong et al. 2019; Ho et al. 2018; Talero et al. 2019).

Biochar obtained from torrefaction of biomass can be promising soil improver which decompose for long time and which positively influence soil fertility, number of biogenic

components and physical and water properties (Radawiec et al. 2014). Torrefied biomass was also shown to be an effective soil amendment by enhancing plant growth and controlling soil metabolites and microbiota (Ogura et al. 2016). Soil deposit of biochar from lignocellulosic crops has been considered as the method of effective soil improvement and significant element of carbon sequestration in the process of climate change mitigation (Stępień et al. 2017).

Therefore, torrefaction appears to be promising preparation method of additive for improvement of soil properties. The main goal of this study is to prepare soil additive from two types of common biomass and their characterization. Brief overview of the torrefaction process is also presented. Additionally, the effect of additive application to soil and the interaction with plant growth was investigated.

3. Materials and methods

3.1. Raw and torrefied material characterization

Samples of chopped hay and wheat straw (Fig. 1) were used as primary biomass material. To determine the sample composition (elemental analysis) we used a LECO CHN628 analyzer. LECO TGA701 Thermogravimetric Analyzer was used to determine the ash and moisture (proximate analysis). LECO AC600 Semi-Automatic Isoperibol Calorimeter measured the fuel's low heating value (LHV). For analysis of heavy metals, the energy dispersive X-ray fluorescence (Spectro Xepos III) was used.



Fig. 1: Primary biomass material (left- wheat straw, right- hay).

3.2. Experimental operation of torrefaction unit

A Laboratory pyrolysis unit (Fig. 2) is equipped with batch reactor (maximal process temperature up to 900 °C). It consists of four parts: reactor, cooling system, cleaning of pyrolysis gas and gas analysis. The batch reactor volume is 2.3 l for 100 – 500 g of fuel (depending on density and particle size). Independently controlled 3 kW electrical heating element is used for heating the reactor. The hot gas is lead through by heated piping into the tube water cooler. From the bottom, part of the cooler is collected pyrolysis liquid (oil and water). Gaseous phase is then cleaned in three washers with water, oil and mineral wool. Amount of the gas is measured by flowmeter and it is conducted into gas analysis section.

Excess gas is combusted in the burner.

Torrefaction of primary materials was carried out in temperature 350 °C and retention time was 60 minutes.

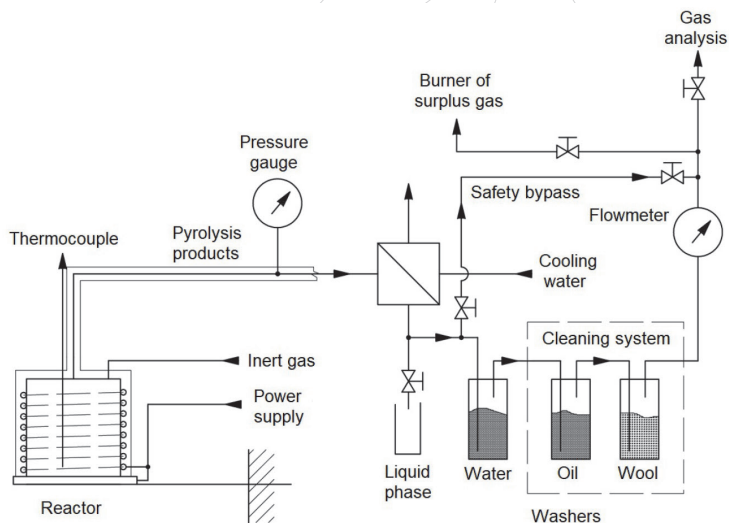


Fig. 2: Scheme of batch pyrolysis unit (Peer, Václav et al. 2018).

3.3. Torrefied additives in vegetation experiment

For the purposes of vegetation experiment sandy soil was chosen. Soil was sampled from topsoil (20cm) of arable land, closed to Sadská (50°14'89N, 14°95'72E). Soil sample was dried and sieved to fraction of 20 mm. Two different types of torrefied material, derived from wheat straw (S) and chopped hay (H), were applied into selected soil in doses of 0.5% and 1.5%, corresponding to real doses of 15 and 30 t/ha. Soil and additive mixtures (5 kg of soil + additive) were put into 5L plastic pots. Nitrogen (N) fertilization, where was applied, was added in dose of 0.5 g N/pot (in NH_4NO_3). Phosphorus (P) and potassium (K) fertilizations, where were applied, were in doses 0,08g (in triple superphosphate) and 0.4 g (in KCl) /pot, respectively. The treatments were followed: i) additive H in dose of 0.5% + NPK fertilization, ii) H 0.5%, no NPK; iii) H 1.5% + NPK; iv) H 1.5%, no NPK; v) S 0.5% + NPK; vi) S 0.5%, no NPK; vii) S 1.5% + NPK; viii) S 1.5%, no NPK; ix) no additive + NPK; x) Control (no additive, no fertilization. Maize, variety CORADI, was used as an experimental plant. Three plants were growth in each pot. The vegetation duration was 91 days. The aim was to compare the influence on cultivated plants and accessibility of the nutrients after harvesting of the plants.

4. Results and discussion

4.1. Raw and torrefied material characterization

Results of raw and torrefied biomass analysis are shown at table 1 and 2. Results of raw biomass materials are consistent with other researches (Biswas et al. 2017). In case of torrefied materials, the lower heating value (LHV) of both torrefied biomass is increased compared to raw samples. The similar increase of LHV of torrefied biomass was reported by other authors (Sadaka and Negi 2009; Tong et al. 2018). In addition, significant loss of moisture content in torrefied samples was observed. Most noticeable changes in elemental analysis between raw and torrefied materials is increased content of carbon and decreased oxygen levels. It is thought that these changes are mainly caused by releasing water content and partial oxidation.

Tab. 1: Biomass elemental and proximate characterization (raw basis)

Biomass	Proximate analysis [Wt%]		Elemental analysis [Wt%]					LHV [MJ/kg]
	Water	Ash	C	H	S	N	O	
Wheat straw	9.5	5.1	45.6	5.66	0.14	0.54	33.6	15.407
Hay	12.7	3.6	44.8	6.21	0.23	0.40	32.9	14.309

Tab. 2: Torrefied biomass elemental and proximate characterization (raw basis)

Biomass	Proximate analysis [Wt%]		Elemental analysis [Wt%]					LHV [MJ/kg]
	Water	Ash	C	H	S	N	O	
Wheat straw	1.8	7.1	58.9	5.27	0.17	0.78	17.3	18.317
Hay	2.1	6.0	58.4	5.01	0.12	0.69	17.6	17.115

4.2. Torrefaction product yields

The solid residue yield is most interested in field of torrefaction as preparation method of additive for improvement of soil properties. In both biomass materials, the solid residue yield was quite low (Table 3). It is common that in woody biomass torrefaction the solid residues yields are much higher (about 80 Wt% (Wannapeera and Worasuwannarak 2012)). But in case of non woody biomass such as straw the solid yield are significantly lower (rice straw torrefied at 300 °C had solid yield 44.8 Wt% (Tong et al. 2018)). In our case where temperature 350 °C was used, the wheat straw and hay had solid residue of 48.26 and 55.25 Wt%, respectively. In this research, the composition of produced gases and composition of liquid phase has not been studied.

Tab. 3: Torrefaction product yields

	Gaseous phase [Wt%]	Liquid phase [Wt%]	Solid residue [Wt%]
Wheat straw	12.61	39.13	48.26
Hay	6.44	38.31	55.25

4.3. Heavy metals content in torrefied biomass

The heavy metals content in torrefied biomass samples (Table 4) has been investigated for meeting the limits set by Decree of the Ministry of Agriculture No. 131/2014 Coll. This decree set limits for use of biomass ash as additive (fertilizes) into the soils. In both samples, the measured values of heavy metals did not exceed established limits. These results proved that use of torrefied biomass, as additive to soils is possible. As addition another condition must be met and its concentration of polyaromatic hydrocarbon (PAH) in torrefied biomass to be less than 20 mg/kg. This is going to be subject of following research.

Tab. 4: Limits and measured values of heavy metal in torrefied biomass

Measured values (dry basis) [mg/kg]					
	Cd	Pb	Hg	As	Cr
Limits	5	50	0.5	20	50
Wheat straw	5	1.1	< 0.5	< 0.5	7
Hay	2.7	2	< 0.5	< 0.5	19.2

4.4. Torrefied additives in vegetation experiment

Fig. 3 showed the maize biomass yield. The highest biomass yields were observed at treatments, where fertilizers were applied, with no regards to type of additive and application dose. No significant differences were determined at treatments, where no fertilizers were added. The highest biomass yield was observed at treatment, where torrefied straw in dose of 0.5% was applied together with NPK fertilizer, however statistically, the difference was not significant comparing other fertilized treatments. The effects of biochar on plant biomass production have been characterised ambiguously in literature (Kavitha et al. 2018). In our experiment, strong dependence of fertilization was showed. However, the improvement of soil properties and follow-up increase in biomass production could be visible after longer additive exposure, or repeated application (Kavitha et al. 2018). The nitrogen uptake was calculated as determined nitrogen concentration*biomass yield. However, significantly highest nitrogen uptake was determined at treatment, where NPK was applied, and treatments with torrefied additives showed satisfactory nitrogen uptake. Similarly to biomass yield, there was observed no influence of type of additive and its dose. Gale and Thomas (Gale and Thomas 2019) explained that nitrogen is rather in unavailable forms in biochars and plants growth is supported by available potassium or magnesium. It can happen that nitrogen is fixed by biochar. In our case, application of fertilizers together with additives was successful method for maize production.

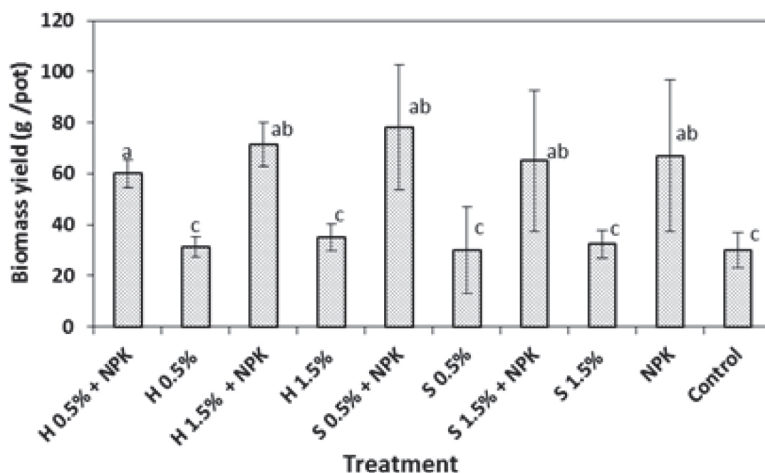


Fig. 3: Maize biomass yield. (Values are means of 4 replicates, error bars shows standard errors of the means.)

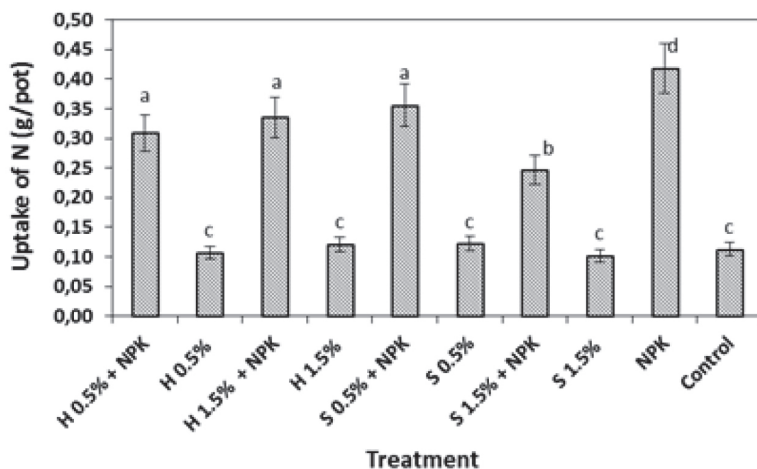


Fig. 4: Nitrogen uptake by plants. (Values are means of 4 replicates, error bars shows standard errors of the means.)

5. Conclusion

In this research, the two types of biomass were torrefied to obtain biochar and use it as additive for improvement of soil properties. Torrefaction has been carried out in batch laboratory pyrolysis unit with temperature 350 °C and retention time of 60 minutes.

Characterization of torrefied biomass revealed usual changes in composition reported by other researches. Low heating value has increased as expected. In case of product yields,

the biochar was around 50 % mass fraction of primary samples. The heavy metals content in biochar did not exceed the limits set by Decree of the Ministry of Agriculture No. 131/2014 Coll. Thus, the resulted biochar can be use as additive to soils but additional analysis of PAH in biochar is needed.

To summarize vegetation experiment, it was found that application of torrefied material together with fertilizer in sandy soil represent effective method for maize growth. The self effect of biochar addition should be further observed in future vegetation season and supported by more detailed analyses of soil and soil microbiota.

6. Acknowledgments

This article was supported by Project: CZ.02.1.01/0.0/0.0/16_019/0000753 Research centre for low-carbon energy technologies, CZ.01.1.02/0.0/0-0.0/15_019/0004771 Torrefaction, Czech Republic and specific research SP 2019/160.

7. References

- Biswas, B., Pandey, N., Bisht, Y., Singh, R., Kumar, J., & Bhaskar, T. (2017). Pyrolysis of agricultural biomass residues: Comparative study of corn cob, wheat straw, rice straw and rice husk. *Bioresource Technology*, 237, 57–63. <https://doi.org/https://doi.org/10.1016/j.biortech.2017.02.046>
- Chen, D., Gao, A., Cen, K., Zhang, J., Cao, X., & Ma, Z. (2018). Investigation of biomass torrefaction based on three major components: Hemicellulose, cellulose, and lignin. *Energy Conversion and Management*, 169, 228–237. <https://doi.org/https://doi.org/10.1016/j.enconman.2018.05.063>
- Gale, N. V., & Thomas, S. C. (2019). Dose-dependence of growth and ecophysiological responses of plants to biochar. *Science of The Total Environment*, 658, 1344–1354. <https://doi.org/https://doi.org/10.1016/j.scitotenv.2018.12.239>
- Gong, S.-H., Im, H.-S., Um, M., Lee, H.-W., & Lee, J.-W. (2019). Enhancement of waste biomass fuel properties by sequential leaching and wet torrefaction. *Fuel*, 239, 693–700. <https://doi.org/https://doi.org/10.1016/j.fuel.2018.11.069>
- Ho, S.-H., Zhang, C., Chen, W.-H., Shen, Y., & Chang, J.-S. (2018). Characterization of biomass waste torrefaction under conventional and microwave heating. *Bioresource Technology*, 264, 7–16. <https://doi.org/https://doi.org/10.1016/j.biortech.2018.05.047>
- Honus, S., & Juchelková, D. (2014). Mathematical models of combustion, convection and heat transfer in experimental thermic device and verification. *Tehnicki Vjesnik*, 21, 115–122.
- Honus, S., Kumagai, S., Molnár, V., Fedorko, G., & Yoshioka, T. (2018). Pyrolysis gases produced from individual and mixed PE, PP, PS, PVC, and PET—Part II: Fuel characteristics. *Fuel*, 221, 361–373. <https://doi.org/https://doi.org/10.1016/j.fuel.2018.02.075>
- Kavitha, B., Reddy, P. V. L., Kim, B., Lee, S. S., Pandey, S. K., & Kim, K.-H. (2018). Benefits and limitations of biochar amendment in agricultural soils: A review. *Journal of Environmental Management*, 227, 146–154. <https://doi.org/https://doi.org/10.1016/j.jenvman.2018.08.046>

jenvman.2018.08.082

Ogura, T., Date, Y., Masukujane, M., Coetzee, T., Akashi, K., & Kikuchi, J. (2016). Improvement of physical, chemical, and biological properties of aridisol from Botswana by the incorporation of torrefied biomass. *Scientific Reports*, 6, 28011. <https://doi.org/10.1038/srep28011>

Peer, Václav, Frantík, Jaroslav, Kielar, Jan, & Masek, Drahomír. (2018). Substrates for slow pyrolysis. *MATEC Web Conf.*, 168, 8004. <https://doi.org/10.1051/mateconf/201816808004>

Radawiec, W., Dubicki, M., Karwowska, A., Żelazna, K., & Gołaszewski, J. (2014). Biochar from a digestate as an energy product and soil improver. *Agricultural Engineering*, 18(3), 149--156. <https://doi.org/http://dx.medra.org/10.14654/ir.2014.151.067>

Sadaka, S., & Negi, S. (2009). Improvements of biomass physical and thermochemical characteristics via torrefaction process. *Environmental Progress & Sustainable Energy*, 28(3), 427–434. <https://doi.org/10.1002/ep.10392>

Stępień, P., Pulka, J., & Białowiec, A. (2017). Organic Waste Torrefaction – A Review: Reactor Systems, and the Biochar Properties. <https://doi.org/10.5772/67644>

Talero, G., Rincón, S., & Gómez, A. (2019). Torrefaction of oil palm residual biomass: Thermogravimetric characterization. *Fuel*, 242, 496–506. <https://doi.org/https://doi.org/10.1016/j.fuel.2019.01.057>

Tong, S., Xiao, L., Li, X., Zhu, X., Liu, H., Luo, G., et al. (2018). A gas-pressurized torrefaction method for biomass wastes. *Energy Conversion and Management*, 173, 29–36. <https://doi.org/https://doi.org/10.1016/j.enconman.2018.07.051>

Wang, Z., Lim, C. J., & Grace, J. R. (2019). Biomass torrefaction in a slot-rectangular spouted bed reactor. *Particuology*, 42, 154–162. <https://doi.org/https://doi.org/10.1016/j.partic.2018.02.002>

Wannapeera, J., & Worasuwanarak, N. (2012). Upgrading of woody biomass by torrefaction under pressure. *Journal of Analytical and Applied Pyrolysis*, 96, 173–180. <https://doi.org/https://doi.org/10.1016/j.jaap.2012.04.002>

Thermal gasification of waste

Jitka Hrbek¹ and Christoph Pfeifer¹

1 University of Natural Resources and Life Sciences, Vienna
Institute of Chemical and Energy Engineering
Muthgasse 107/1
1190 Vienna, Austria

1. Abstract

Waste streams suitable for thermal gasification processes can be divided into following groups: forest waste, agricultural waste, residential and industrial waste streams.

Gasification of woody based feedstock can be seen for decades as state of the art. The confirmation could be over 2000 operational gasification units, most of them in small scale, distributed all over Europe, which employ waste wood as a feedstock.

On the other hand, gasification of agriculture, or residential and industrial waste streams involves mostly more complex gasification systems because of higher content of alkali- and/or heavy- metals causing operational problems.

The residential and industrial waste streams, which are relevant for gasification are primarily refuse derived fuel (RDF) and solid recovered fuel (SRF) as waste streams. In this paper, the chemical characteristics of RDF and SRF are presented as well as some implementation examples of waste gasification systems.

Keywords: waste, gasification, refuse derived fuel, solid recovered fuel

2. Introduction

Waste treatment is of high importance to all societies as it is linked to other issues such as health, pollution of land, air and water as well as climate change and unsustainable resource utilization.

In the 20th century, the landfilling was the most common way for waste disposal. Today, the situation is changing and an effort to recycle or to increase the waste value (e.g. thermal treatment and production of power and heat) can be observed.

In the figure below, the waste treatment situation in the EU can be seen. It is obvious, that landfilling is decreasing and incineration or thermal disposal is increasing with the years.

To utilize waste for thermal gasification to produce power and heat or even value-added

products, such as biofuels or biochemical is a brilliant idea for waste disposal and fossil-free products generation at the same time.

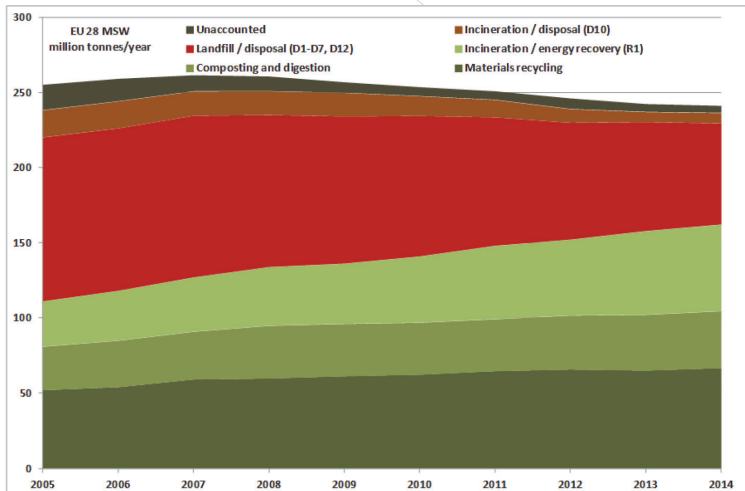


Figure 1: Different ways of MSW treatment in EU between 2005-2014¹

3. Waste as a feedstock

Feedstock suitable for thermal gasification can be generally divided into 3 categories:

- 1. Woody biomass, residues and waste
 - (e.g. soft wood, hard wood, bark, demolition wood, waste wood, etc.)
- 2. Agricultural waste
 - (e.g. straw, maize, husks, manure, etc.)
- 3. Residential and industrial waste streams
 - (e.g. MSW, RDF, SRF, black liquor, sewage sludge, etc.)

The gasification of woody biomass or woody waste is already for decades the state of the art. The proof is the fact that there are over 2000 operational gasification facilities all over Europe utilizing (waste) wood as a feedstock. IEA Bioenergy Task 33 – Gasification of biomass of waste², which provides the monitoring of gasification facilities worldwide manages also a database³ with reference facilities in small, medium as well in large scale. It should be pointed out, that not all small scale gasification facilities could be found in the database, but only the reference ones.

¹ Eurostat data

² www.task33.ieabioenergy.com

³ <http://task33.ieabioenergy.com/?database=true>

More challenging than woody feedstock is the gasification of agricultural waste. The reason is the high content of alkali metals causing slagging and fouling during the gasification process. Alkali metals play an important role in the ash melting process, they decrease the melting temperature of the ash, which could be a problem by e.g. fluidized bed gasification.

Anyway, the gasification of residential or industrial waste streams could be even more challenging than gasification of agricultural waste. The reason is mainly the variability of these waste streams. This variability is caused by many different factors, such as time - seasonal variations, spatial availability - uptake areas, socio-economic factor - collection practices and waste sorting.

In fact, not all fractions of e.g. municipal solid waste (MSW) can be used for thermal gasification. In the practise, the sorted waste as RDF and SRF are the waste streams used for the conversion.

Refuse derived fuel (RDF) is produced from domestic and business waste, which includes biodegradable material as well as plastics. Non-combustible materials such as glass and metals are removed, and the residual material is then shredded.

Solid recovered fuel (SRF) is a high-quality alternative to fossil fuel and is produced from mainly commercial waste including paper, card, wood, textiles and plastic. This type of waste stream has gone through additional processing to improve the quality and value. It has a higher calorific value than RDF.

In the following table the characteristics of RDF and SRF are shown as indication, calculated as average of 16 resp. 17 samples.

Table 1: RDF and SRF characteristics⁴

Phyllis 2 Database ⁵	RDF, 16 samples in total				SRF, 17 samples in total			
N denotes number of samples RDF, 16 samples in total	Mean	Min.	Min.	N	Mean	Min.	Max.	N
Net CV MJ/kg (daf)	21.54	16.13	27.80	16	25.33	18.96	32.46	17
Gross CV MJ/kg (daf)	22.72	17.40	26.57	15	27.10	20.28	34.75	17
Moisture cont. wt. %	13.12	2.82	38.70	10	28.46	1.90	59.00	13
Ash cont. wt. % (dry)	17.47	9.30	27.72	14	8.27	4.90	10.90	7
C wt. % (daf)	52.11	42.50	61.62	16	61.74	51.49	75.56	12
H wt. % (daf)	7.40	5.84	8.91	16	8.42	6.08	10.73	13
N wt. % (daf)	0.85	0.31	1.49	15	0.52	0.10	2.18	17
S wt. % (daf)	0.46	0.12	0.98	14	0.14	0.02	0.42	17
O wt. % (daf)	37.06	24.60	43.73	16	32.47	30.60	35.02	4
Cl mg/kg (daf)	7 265	55.0	14 341	14	0.5	0.5	0.5	1
Br mg/kg (daf)	50.1	50.1	50.1	1	n.a.	n.a.	n.a.	0
F mg/kg (daf)	88.2	88.0	88.5	2	n.a.	n.a.	n.a.	0
Al mg/kg (dry)	5 201	1 600	7 300	3	n.a.	n.a.	n.a.	0
K mg/kg (dry)	1 593	1 364	1 823	2	n.a.	n.a.	n.a.	0
Na mg/kg (dry)	2 772	2 590	2 955	2	n.a.	n.a.	n.a.	0
Ca mg/kg (dry)	23 915	21 936	25 895	2	n.a.	n.a.	n.a.	0
Si mg/kg (dry)	18 272	9 641	26 903	2	n.a.	n.a.	n.a.	0
Mg mg/kg (dry)	1 688	1 410	1 966	2	n.a.	n.a.	n.a.	0
Fe mg/kg (dry)	2 477	768	4 689	3	n.a.	n.a.	n.a.	0
P mg/kg (dry)	379	279	480	2	n.a.	n.a.	n.a.	0
Ti mg/kg (dry)	1 359	1 063	1 654	2	n.a.	n.a.	n.a.	0
As mg/kg (dry)	6.4	5.0	9.0	3	n.a.	n.a.	n.a.	0
Cd mg/kg (dry)	1.9	0.8	3.0	2	n.a.	n.a.	n.a.	0
Co mg/kg (dry)	5.6	4.2	7.0	2	n.a.	n.a.	n.a.	0
Cr mg/kg (dry)	168.4	8.0	429.0	3	n.a.	n.a.	n.a.	0
Cu mg/kg (dry)	386.0	35.0	610.0	3	n.a.	n.a.	n.a.	0
Mn mg/kg (dry)	83.2	57.0	126.0	3	n.a.	n.a.	n.a.	0

⁴ Lars Waldheim: Gasification of waste for energy carriers: A review, IEA Bioenergy Task 33 Project
<http://www.task33.ieabioenergy.com/content/Task%2033%20Projects>

⁵ <https://phyllis.nl/>

Ni mg/kg (dry)	100.3	2.0	266.0	3	n.a.	n.a.	n.a.	0
Pb mg/kg (dry)	134.4	50.0	260.0	3	n.a.	n.a.	n.a.	0
V mg/kg (dry)	4.7	3.1	7.0	3	n.a.	n.a.	n.a.	0
Zn mg/kg (dry)	232.1	85.0	393.0	3	n.a.	n.a.	n.a.	0
Ba mg/kg (dry)	341.7	142.4	541.0	2	n.a.	n.a.	n.a.	0
Mo mg/kg (dry)	9.2	1.4	17.0	2	n.a.	n.a.	n.a.	0
Se mg/kg (dry)	0.3	0.3	0.3	1	n.a.	n.a.	n.a.	0
Hg mg/kg (dry)	0.2	0.2	0.2	1	n.a.	n.a.	n.a.	0
Sn mg/kg (dry)	20.1	17.0	23.1	2	n.a.	n.a.	n.a.	0
Sr mg/kg (dry)	103.3	63.5	143.0	2	n.a.	n.a.	n.a.	0
B mg/kg (dry)	63.1	44.2	82.0	2	n.a.	n.a.	n.a.	0
Sb mg/kg (dry)	45.0	29.0	61.0	2	n.a.	n.a.	n.a.	0

4. Examples of waste gasification implementation

4.1. ESKA gasification facility, the Netherlands

Eska is the leading global manufacturer of recovered paper based substrates for a wide variety of industries and applications, including hardcover books, stationery, luxury packaging, puzzles and games and many more.

One of the latest implementations is the use of gasification for replacement of natural gas. Eska is using air blown - circulating fluidized bed (CFB) technology operating at atmospheric pressure to gasify paper rejects and using the product gas as a feed to a boiler. The installation is a 12 MWth CFB boiler processing 25 kton/year of reject to produce steam for the onsite processes. The boiler produces 5 –16 ton/h steam (196°C, 13.6 barg). The producer gas is combusted in a waste heat recovery boiler to produce saturated steam with an overall thermal efficiency of the plant of 85%. In this way, 18 million of m³ of natural gas per year are substituted. The plant was supplied by Leroux & Lotz and started October 2016, more information can be found at ESKA website⁶.

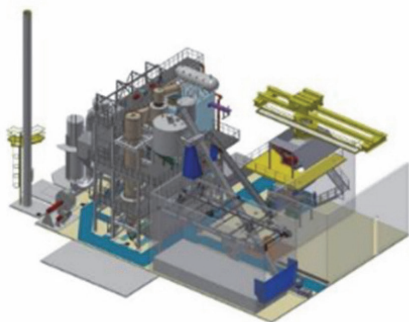
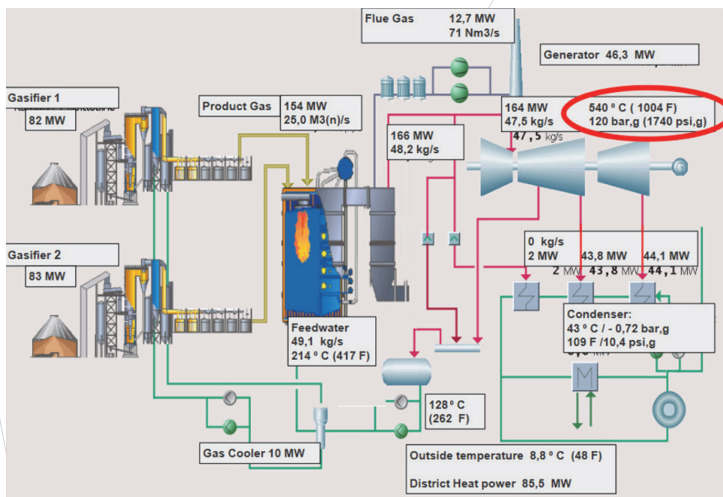


Fig. 2: 3D model (left) of the plant at Eska and a photo of the site erection

⁶ www.eska.com

The plant in the Kymiäarvi power plant area is based on the CFB gasification technology equipped with an innovative gas cooling and cleaning system before combusting the product gas in a specially designed gas fired boiler. Valmet delivered the CFB gasification process, together with gas cooling and cleaning, steam boiler and flue gas cleaning system. The SRF is gasified at 850-900°C in two CFB-gasifier units (2x80 MW) and it is converted into product gas, the gas is then cleaned and the resulting gas is combusted in an ordinary natural gas boiler. In the gasification of SRF, impurities, that could cause boiler corrosion, are transferred to the product gas. The product gas is cooled down from 900°C to about 400°C. Thus, compounds causing corrosion turn from gas into solid particles. Then, the solid particles can be filtered out to gain clean gas. The total fuel input of the plant is 160 MW; the power plant produces 50 MW of electricity and 90 MW of district heat for the city of Lahti.



The Waste2Value project is based on upcycling of residual waste, such as sewage sludge, residues from the pulp and paper industry and damaged timber into eco-friendly, CO2-neutral fuels.

A 1MW pilot plant based on a dual fluidized bed (DFB) gasification process employs waste materials for syngas production. In a second process step, the syngas can be converted into a wide range of fuels – including green diesel and kerosene, green natural gas and green hydrogen – which can subsequently be used in the transport sector and/or the energy industry. These fuels are 100% renewable if the feedstock is from renewable sources. However, another option would be to add also fossil-based waste such as non-recyclable plastics. In this way the plastics “recycling” could be achieved.



Fig. 4: Waste2Value pilot plant in Vienna

The plant is the first of its kind in the world designed to research the entire process chain, from waste materials through syngas production and synthesis of the fuel, through to fleet trials by Vienna's public transport operator "Wiener Linien".

The project findings will pave the way for industrial-scale application of this technology by the energy supplier in Vienna "Wien Energie". Through the various conversion pathways, the production of CO₂-neutral green diesel and kerosene, mixed alcohols, synthetic green natural gas and green hydrogen will be possible.

The pilot plant was designed by BEST[®]– Bioenergy and Sustainable Technologies GmbH and built by the SMS Group. Other project partners include paper producer Heinzl Paper, Wiener Linien, the local utility company Wiener Netze and the Austrian Forest Authority, with TU Vienna and Luleå University of Technology in Sweden as the scientific partners.

The start-up of the gasification facility will be in Fall 2021.

5. Conslusions

Waste gasification could be seen a part of circular economy with zero waste strategy. The technology employs waste feedstock for production of gas, which could be used in different ways: for co-firing and replacement of fossil fuels such as natural gas, for production of heat and power or even for production of biofuels and biochemicals. In this way the waste disposal and generation of value-added products could be managed in one way.

Ján Vereš¹

¹Energy and Environmental Technology Centre, Energy Research Centre, VSB-TU Ostrava, 708 33 Ostrava Poruba, Czech Republic

1. Abstract

Fuel cell vehicles (FCVs) have been developed for years to cut dependence on fossil fuel and significantly reduce carbon dioxide emissions toward a sustainable society. One of the major problems in the hydrogen infrastructures is to put in place and spread hydrogen fueling stations throughout society. Furthermore, it is essential to address safety issues of hydrogen fueling stations to ensure safety of workers, customer and the public for stable supply of hydrogen to FCVs. Hydrogen has hazards such as embrittlement and detonation. To control hydrogen hazards leads to prevent accidents involving hydrogen. Risk assessment is a useful tool to identify hazards and prevent and mitigate accidental risks. Therefore, the purpose of this study is to propose effective safety measures for a gas station with a liquid hydrogen fueling system by risk assessment.

Keywords: hydrogen fueling station, safety, risk assessment, compression, explosion.

2. Introduction

Hydrogen is enjoying a renewed and rapidly growing attention in Europe and around the world. Hydrogen can be used as a feedstock, a fuel or an energy carrier and storage, and has many possible applications across industry, transport, power and buildings sectors. However, deploying hydrogen in Europe faces important challenges that neither the private sector nor Member States can address alone. Driving hydrogen development past the tipping point needs critical mass in investment, an enabling regulatory framework, new lead markets, sustained research and innovation into breakthrough technologies and for bringing new solutions to the market, a large-scale infrastructure network that only the EU and the single market can offer, and cooperation with our third country partners. Hydrogen is a leading fuel for a renewable and environment-friendly energy carrier. It can simultaneously reduce a country's dependence on foreign oil and significantly reduce greenhouse gases. Hydrogen station systems play as a key bridgehead in commercializing fuel cells and fuel cell powered vehicles. Several studies related to the safety of hydrogen stations have been concerned with the diffusion of leakage, explosion, deflagration or detonation of hydrogen and jet flames from hydrogen fueling stations (Kim et al., 2013). Hydrogen is dangerous due to its properties of low ignition temperature, small ignition energy, wide explosion limit and fast combustion speed. In a confined space, the hydrogen is dangerous, like any other flammable gas. In an open space, the probability of hydrogen explosion is lower as compared to that occurring in a confined space, as buoyancy speed is high (Sakamoto et al.,

2019). To reduce the risk, reliable risk analysis methodology is required so that appropriate control measures can be planned and required safety standards can be established. This is particularly important especially when the population at large is involved such as in the case of hydrogen stations (Al-Shanini et al., 2014).

3. Hydrogen properties and production processes

The safe handling and use of hydrogen requires an appreciation of its physical properties, both as a gaseous fuel and as stored in a liquid or adsorbed state. Hydrogen is colourless, odourless and is the lightest gas made up of the smallest molecules. The main physicochemical properties are shown below in table 1.

Tab. 1: Main physical and chemical properties of hydrogen

Field	Characteristic values
Substance name	Hydrogen
CAS number	1333-74-0
Molecular formula	H ₂
Density	0,084 kg/m ³
Boiling point	-253°C
Melting point	-259°C
Ignition temperature	500°C
Explosive limits	4-75%

The extremely low melting and boiling points result from weak forces of attraction between the molecules. The existence of these weak intermolecular forces is also revealed by the fact that, when hydrogen gas expands from high to low pressure at room temperature, its temperature rises, whereas the temperature of most other gases falls. According to thermodynamic principles, this implies that repulsive forces exceed attractive forces between hydrogen molecules at room temperature—otherwise, the expansion would cool the hydrogen.

Hydrogen can be produced using a number of different processes:

Thermochemical Processes

Some thermal processes use the energy in various resources, such as natural gas, coal, or biomass, to release hydrogen from their molecular structure. In other processes, heat, in combination with closed-chemical cycles, produces hydrogen from feedstock's such as water.

- Natural gas reforming (also called steam methane reforming or SMR)
- Coal gasification
- Biomass gasification
- Biomass-derived liquid reforming
- Solar thermochemical hydrogen (STCH)

Electrolytic Processes

Electrolysers use electricity to split water into hydrogen and oxygen. This technology is well developed and available commercially, and systems that can efficiently use intermittent renewable power are being developed.

- Polymer Electrolyte Membrane Electrolysers
- Alkaline Electrolysers
- Solid Oxide Electrolysers

Direct Solar Water Splitting Processes

Direct solar water splitting, or photolytic, processes use light energy to split water into hydrogen and oxygen. These processes are currently in the very early stages of research but offer long-term potential for sustainable hydrogen production with low environmental impact.

- Photoelectrochemical (PEC)
- Photobiological

Biological Processes

Microbes such as bacteria and microalgae can produce hydrogen through biological reactions, using sunlight or organic matter. These technology pathways are at an early stage of research, but in the long term have the potential for sustainable, low-carbon hydrogen production.

- Microbial biomass conversion
- Photobiological

4. Overview of hydrogen fueling stations

Hydrogen fueling stations supply high-purity, high-pressure hydrogen fuel primarily to fuel cell vehicles. Hydrogen stations are in operation and under construction for light-duty vehicles (passenger vehicles), heavy-duty vehicles (trucks and buses), and material handling equipment. The actual map of H₂ fueling stations in EU is presented in Fig.1

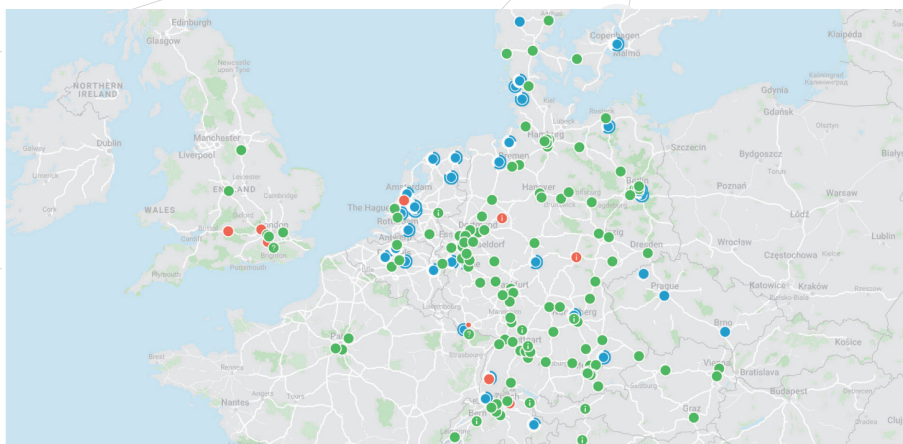


Fig.1: Map of H2 fueling stations in Europe (green, red-in operation; blue-in progress)(h2.live)

Stations dispense hydrogen as a compressed gas at pressures of 700 bar for light-duty vehicles and 350 bar for all other vehicles. All stations generally have the same equipment, but station employs different designs depending on how the hydrogen is produced, delivered, stored and dispensed. Each station includes (Fig.2), at minimum:

- Hydrogen storage equipment – based on the station's location and capacity, hydrogen can be stored as a liquid, a low-pressure gas, or a high-pressure gas.
- Compressor – Hydrogen is compressed to reduce volume and increase pressure. Typically, a compressor is used to replenish the buffer storage. Liquid and low-pressure storage tanks may use multiple compressors.
- Chiller – Hydrogen is cooled as to not exceed the temperature threshold of the industry standard fueling protocol. (Stations for heavy-duty vehicles and material handling equipment may not use chillers.)
- Dispenser – Dispensers look similar to gasoline dispensers. They may sit on the same island as other fuel dispensers, or sit on their own island. Dispensers for material handling equipment are usually inside the warehouse.

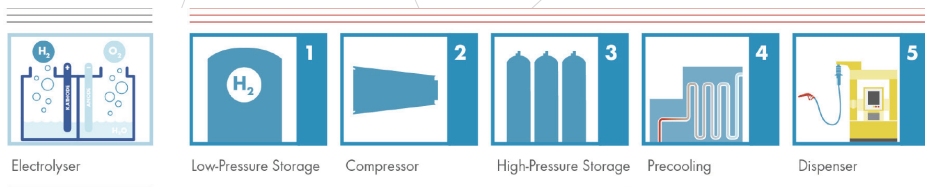


Fig.2: Hydrogen fueling station scheme (www.kobelco.co.jp)

Hydrogen fueling stations can be classified by type of installation into stationary and mobile. The stationary type can be further classified into on-site and off-site types depending on the type of hydrogen production. The on-site type refers to stations that produce hydrogen within the station (Fig.3). Examples of the stationary type include the standalone type, parallel installation type and satellite type.



Fig.3: Stationary hydrogen fueling station (www.itm-power.com)

The mobile type is non-stationary, including stations where all processes are on board a vehicle, as well as stations without hydrogen production facilities assuming they will receive in the compressed hydrogen (Fig.4).



Fig.4: Mobile hydrogen fueling station (www.motor1.com)

Hydrogen fueling stations comprise components such as dispenser with a nozzle to supply hydrogen, a pressure accumulator to store hydrogen, a compressor to compress hydrogen, and a pre-cooler for cooling the hydrogen.

5. Hazard identification and risk management

The development and growth of the hydrogen economy is highly dependent on the process safety and public perception of the refuelling process and therefore the safe design of the station is paramount. The safety philosophy is that the process has to be inherently safe so that the risks are minimised to the “as low as reasonably practicable level”. Hydrogen is reported to be one of the safest gases as it is non-toxic and since hydrogen is the lightest gas, it can easily disperse and get diluted in the atmosphere below the flammability limit. Studies have shown that the general public perception on the use of hydrogen is neutral and only a minority relate it to the Hindenburg incident. The acceptance of hydrogen as the fuel of the future is strongly related to public understanding of the safety and cost of hydrogen. The hydrogen fuelling station installation should be sited to minimise risk to users, operating personnel, properties, and the environment to an acceptable level (Kikukawa et al., 2009).

The following elements of a hydrogen fuelling station shall be considered potential hazard sources:

- on-site hydrogen production unit as applicable;
- hydrogen delivery system, including mobile storage and remote fill points as applicable;
- compressors;
- storage;
- piping connections (non-welded);
- dispensers.

The hydrogen fuelling station shall include measures to reduce the risk of harm from fires, deflagrations, detonations and blast waves to an acceptable level. Risk assessment is the overall process of risk identification, risk analysis, risk evaluation, and risk mitigation. Use of risk assessment may allow station owners and designers to flexibly define station-specific mitigations that achieve an equal or better level of risk to those of prescriptive recommendations or to relax existing prescriptive mitigation measures as long as the total system risk remains below the selected tolerability threshold (risk acceptance criteria). A risk assessment shall be performed for the hydrogen fuelling station except when the stations comply with prescriptive regulations that address relevant risks. The risk assessment should demonstrate that the mitigation measures employed are appropriate to achieve the desired level of risk of the station. The physical modeling can contribute to the risk identification and consequence analysis in Fig. 5.

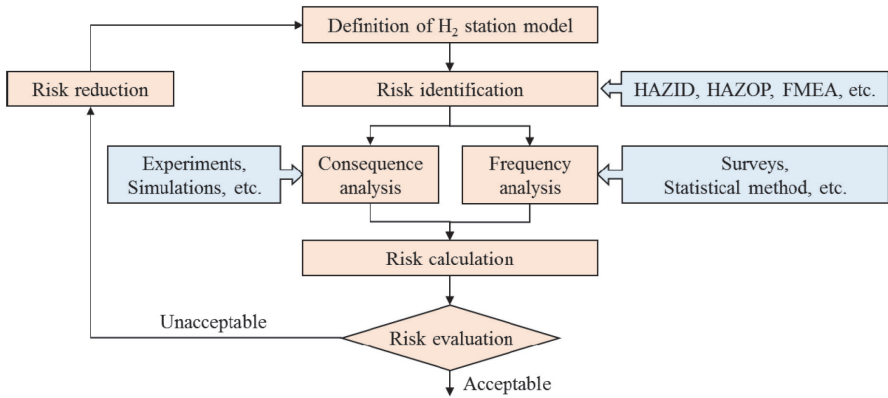


Fig.5: Schematic of risk assessment of hydrogen fueling station

A hazard and operability study (HAZOP) was carried out to identify all possible hazards and possible ways of handling them. A complete HAZOP analysis needs a detailed process and instrument diagram, and with the process flow diagram a simplified HAZOP analysis was carried out to the best of our knowledge about the process and based on the historical incident record related to hydrogen refuelling stations (h2tools.org). This HAZOP analysis is presented in Table 2.

Tab. 2: List of possible hazards of the H2 station

FAILURE MODE	SOURCE OF FAILURE	EFFECT	SEVERITY (1-10)	PROBABILITY OF OCCURRENCE (1-10)
Fire and explosion	Ignition in the vicinity of H2 and O2 mixture	Equipment damage and possible injuries	10	2
Hydrogen leak in piping	Mechanical failure/improper joints and fittings	Potential fire and explosion	7	3
Hydrogen leak in electrolyser	Overpressure causing rupture of membrane	Potential fire and explosion	8	3
Hydrogen leak in storage tank	Mechanical failure/improper joints and fittings	Potential fire and explosion	8	3
Compressor failure	Equipment failure, worn out seals	Potential H2 leaks	5	6

FAILURE MODE	SOURCE OF FAILURE	EFFECT	SEVERITY (1-10)	PROBABILITY OF OCCURRENCE (1-10)
Hose pressure rating verification error	Human error	Overpressure in vehicle tank, potential H2 leaks	6	3
Leak at breakaway fitting	Equipment failure at dispenser	Potential fire	7	2
Improper fill speed at fuel dispenser	Failure to follow standard operating procedures, deficiency in procedures, software failure	Overheating on receiving fuel tank	5	4
Incorrect check valve installation	Human error, inadequate inspections	Property damage	7	2
Vehicle crashing into refuelling system	External factor	Property damage and injuries	7	2

6. Conclusions

H2 fueling station scenarios representing significant hazards and significant risk were identified. These scenarios need to be analysed in more detail to obtain a more accurate estimate of the actual risks. Common for all concepts are releases of hydrogen from high pressures leading to large hazard distances, and hydrogen releases in confined areas leading to risk of explosions. This is a challenge, especially in densely populated and crowded areas. Risk reducing measures are suggested and should be taken into consideration in the development of standards. Due to lack of experience and specific data, there is clearly a need for further research related to hydrogen hazards and development of safe systems.

7. Acknowledgments

This study was carried out as part of the project, CEET - Center of Energy and Environmental Technologies (identification code TK03020027).

8. References

- Eunjung K., Jaedeuk P., Jae H.C., Il M. Simulation of hydrogen leak and explosion for the safety design of hydrogen fueling station in Korea, *International Journal of Hydrogen Energy* 38, 2013.
- Al-Shanini A., Arshad A., Faisal K. Accident modelling and analysis in process industries, *Journal of Loss Prevention in the Process Industries* 32, 2014.
- Sakamoto J., Misono H., Nakayama J., Kasai, N., Shibutani T., Miyake A. Evaluation of Safety Measures of a Hydrogen Fueling Station Using Physical Modeling, *Sustainability* 11, 2019.
- Kikukawa S., Mitsunashi H., Miyake A. Risk assessment for liquid hydrogen fueling stations, *International Journal of Hydrogen Energy* 34, 2009.
- ISO 19880-1: Gaseous Hydrogen-Fuelling stations, 2020.

Pellet quality analysis: Torrefaction after pelletization and vice versa

Lucie Jezerska¹, Jiri Zegzulka^{1, 2} and Jan Necas^{1, 2}

¹ VSB-Technical University of Ostrava, ENET Centre, Ostrava, Czech Republic

² VSB-Technical University of Ostrava, Faculty of Mining and Geology, Ostrava, Czech Republic

1. Abstract

Oilseed rape is widely cultivated to produce biofuel. Waste straw can be considered an energy source. But the downside is its low energy density. One way to process waste straw efficiently is to convert it into pellet form. Another, currently studied, alternative appears to be pellet torrefaction or pelletization of already torrefied rape straw. Both process ways were therefore examined for the treatment of waste rapeseed straw. First, pellets were produced without any thermal treatment (PWT – pellets without torrefaction). In the next step, these pellets were torrefied (TAP – torrefaction after pelletization). The waste rapeseed straw itself was also torrefied and then pelletized (PAT – pelletization after torrefaction). Basic mechanical properties such as mechanical resistance, hardness, resistance to moisture and density have been determined for all pellets. These parameters were compared and evaluated. The TAP way produced pellets were found to be suitable in terms of mechanical resistance parameters, resistance to moisture and calorific value. They were easier to process compared to PAT way. The PAT pellets were parametrically consistent with calorific value, moisture resistance and hardness. Energy parameters showed a clear increase in the calorific value of pellets processed by both process paths.

Keywords: *pellets; biomass; torrefaction; pelletization; rapeseed straw*

2. Introduction

Various biomass processing technologies have been introduced over the years. But only a few have been fully described and demonstrated. These include torrefaction. During the torrefaction process, heat is transferred to the surface of the individual particles, which then passes to their center, where they are subsequently decomposed (Ribeiro et al., 2018). The origin of the word torrefaction is in Latin. Latin for „torrefacere“. This association was formed from the two Latin words „torrere“, which means roast/dry and the word „facere“, which means do/perform. This whole process can be divided into five (Chen et al., 2021):

1. Initial heating — at the beginning, the biomass is heated until it reaches the desired drying temperature.

2. Drying — at this stage the temperature is kept constant until the rate of evaporation of the water is reduced so-called critical moisture content. Free water from biomass evaporates at constant rates.
3. Additional drying — in the subsequent drying phase, the biomass is heated to 200 °C. Physically bonded water is removed.
4. Torrefaction – when a temperature of 200 °C is exceeded, the biomass is torrefied.
5. Cooling — in the cooling stage, the temperature of the torrefied product is cooled to ambient temperature.

The torrefaction temperature is 200 to 300 °C. Torrefaction can be categorized into light torrefaction (200 °C to 235 °C), mild torrefaction (235 °C to 275 °C), and severe torrefaction (275 °C to 300 °C), according to torrefaction temperature (Chen and Kuo, 2011). Hemicellulose decomposes at 200-235 °C. After torrefaction, the volume density of the biomass decreases and thus the various methods to compact the fuel are advantageous. This will facilitate the use of torrefied biomass as a globally tradable energy raw material. The use of this biomass densification technology (pelletization, briquetting) can be used as an interesting substitute for coal. Especially with today's trend away from burning this fossil fuel (Manouchehrinejad and Mani, 2018). Furthermore, the biomass that has undergone the torrefaction process is an excellent feedstock to other thermal processes. Like pyrolysis and gasification. The resulting chemicals and biofuels were found to be of much higher quality.

During torrefaction, the primary structural components of biomass decompose. The breakdown of hemicellulose results in a decrease in the weight of input material and therefore a greater representation of lignin and Lignin cellulose remains degradingly incomplete. For cellulose, there is a distinct percussion depolymeration at a temperature of about 340 °C (Chen et al., 2021).

Nowadays, research work is more concerned with the torrefaction of biomass before pelletization. The main problem with this technology is that torrefied biomass loses its natural binding characteristic in lignin. Increasing the temperature of the matrix, using binders or increasing compression pressures are ways of dealing with this problem. The lifespan of the matrix is also shorter due to the high abrasive effect of the torrefied biomass. It is possible to pellet both the torrefied and the unsorted biomass on the same pelletization press. Another possible way is to torrefaction already produced pellets. Torrefaction of wood pellets is already known to increase calorific value and resistance to water absorption. But the density, hardness and durability/mechanical resistance of the pellets will decrease (Siyal et al., 2020). Researchers from Canada have made two process ways. They torrefied before and after pelletization. The material was a chip of Douglas tisolist. It has been shown that it was more energy efficient to first compact the wood chips and then torify them. Pellets were superior in terms of their high stability in water, increased calorific value, higher carbon content and reduced moisture content (Ghiassi et al., 2014).

The aim of this study is to analyse the quality of pellets which have been produced by two different process ways. Either the biomass was first pelletized and then torrefied (PAT) or the biomass was first torrefied and then pelletized (TAP).

3. Material and methods

Oilseed rape straw Odeon was used in this study as a raw material. Oilseed rape straw is produced as waste during the harvesting of oilseed rape seeds (Figure 1).



Fig. 1: Oilseed rape. Left – flowers, middle – seeds, right – oil and pellets.

At present, according to statistics from the Ministry of Agriculture in the Czech Republic, rapeseed is grown on an area of about 400,000 hectares of land. It has a growing season of 300 – 350 days. After this it is harvested and what remains is so-called rapeseed straw, which is biological rapeseed waste, and which retains energy potential for further use. Therefore, it is important to address the possibilities of processing this type of bio waste.

Oilseed rape straw were crushed in the Green Energy 9FQ 50 hammer crusher, Pest Control Corporation (engine output 11 kW, crusher capacity 800–1200 kg/h). Particle size distributions, moisture and bulk density were determined for the crushed samples. For particle size analysis, a Retsch AS 200 Control vibrating machine (20 minutes, amplitude 4 mm) with standard sieves (DIN ISO 3310-1) was used. The moisture content was determined by means of an air oven at $105 \pm 2^\circ\text{C}$ to a constant weight, following EN 14774-1. To determine the bulk density, the volume and weight of the samples of the raw materials were measured according to EN 15103, using a graduated cylinder and laboratory balance. Particle density of pellets was determined on the Mettler Toledo JEW-DNY-43 tester.

Pellets durability index (PDI) was measured on a Holmen NHP 1000 instrument. During the test, a sample of 100 g of pellets pneumatically circulates at 70 mbar in a chamber with perforated conical walls for 60 seconds. The pellets hit each other and the walls of the chamber, creating crumble. After the test, the sample is sieved through a 3.15 mm sieve. PDI was calculated as a proportion of the weight of the pellet sample after the test to the weight of the pellet sample before the test expressed in percentage. The procedure was repeated five times.

The hardness of the pellets was expressed as the weight load in kg, without cracking or crushing of the pellet being tested. Hardness was measured by the Amandus Kahl ak-14 tester. The hardness value was determined as the mean value of the ten tests of one sample. This test simulates the compressive stress due to the weight of the pellets underneath them during storage in silos and crushing pellets in different types of conveyors.

The resistance to moisture, the so-called wettability index (WI) was performed according to Equation (1) defined by (Mahadeo, 2014)

$$W \quad (eq. 1)$$

where m_1 is the weight of the pellet before the test and m_2 is the weight of the pellet after the test. The test consists in immersing the pellet in distilled water for 30 seconds. The procedure was repeated ten times. The average value was subsequently calculated from the results.

Oilseed rape straw samples were pelleted on the Kahl 14 - 175 flat-bed pelleting press. For all samples identical palletizing matrices were used. Throughout the process, the matrix temperature was always monitored by the built-in temperature sensor.

Torrefaction was carried out in a small experimental reactor. In this reactor thermochemical processes of various materials can be carried out. The main part of the plant is the reactor, cooler and purifier of the gas produced, and the measuring fittings. The weight of the test material was around 1000 g for pellets and 750 g for raw straw. The reactor consists of a lid, a vessel body and a liner. The heating of the reactor is provided by a resistance wire which is wound to the outside of the reactor vessel, and a heating element which heats the bottom of the vessel. The entire reactor is then encased in temperature resistant Sibril insulation to reduce heat sharing to the surrounding area. Temperature control is possible in the range of 200 to 900 °C. At the top of the reactor there is an inert gas supply, a process gas drain and a thermocouple to measure the process temperature. Liquid components condense in the upstream gas cooler, which is cooled by water. Process gas is purified in three washing vessels.

4. Results and discussions

4.1. Material characterization

There was no additional drying of input material. The moisture content was on average 10.93%. Particle size distribution is shown in Figure 2.

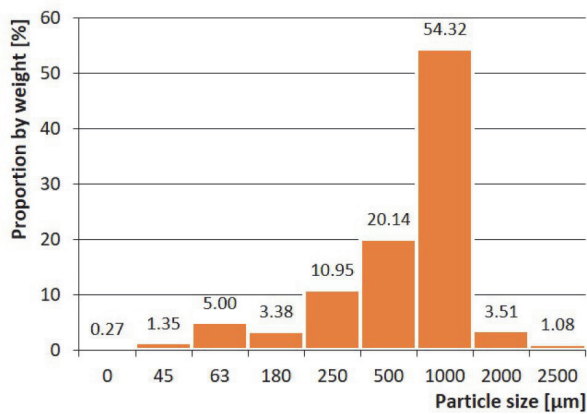


Fig. 2: Particle size distribution of input material

The mean value of repose angle for the raw input mixture of straw was determined. This value corresponded to 49.56 ± 2.00 . Based on this value, the material was placed in a cohesive material mode due to its flowability. This characteristic suggests that there may be process problems arising from the coherence of the material when it is transported. There was also pelletization according to section 3, and torrefaction of the input Oilseed rape straw.

4.2. Torrefaction

During the torrefaction process, the temperature was kept between 220-270 °C. The process took place in an inert nitrogen atmosphere. The heat conversion time was 90 min. The percentage of each component is shown in Figure 3.

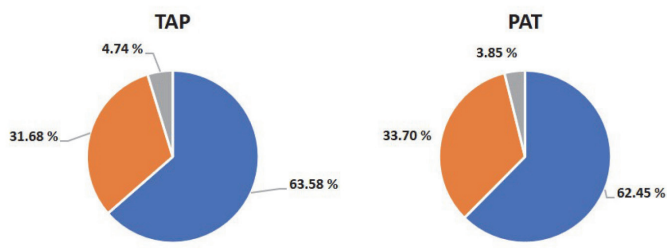


Fig. 3: Percentage of each component after torrefaction for TAP and PAT pellets. Blue part – solid residue, orange part – bio-oil, gray part – gas

4.3. Pellet analysis

For all type pellets, bulk and particle density, pellets durability index, hardness and wettability index were determined. The results are shown in Table 1.

Tab.1.: Pellet mechanical parameters

	Pellets without torrefaction	TAP pellets	PAT pellets
Bulk density, kg.m ⁻³	607±16	451±16	501±13
Particle density, kg.m ⁻³	1410±27	1038±30	1262±25
PDI, %	96.1±0.5	96.0±0.7	82.9±2.0
Hardness, kg	43.5±9.0	19.5±3.2	32.3±3.6
WI, %	25.8±2.3	4.1±2.1	4.6±1.8

Torrefaction has always reduced the bulk and particle density of the pellets. In some cases, when measuring TAP pellets, some pellet samples remained floating on the surface of the water. It is due to their higher hydrophobicity. Particle density is not a standardized quantity for pellets. It can be concluded that torrefaction reduced pellets durability index produced by the PAT process. The process-produced pellets of TAP will be more suitable for transport and handling. From the results of the hardness values, the pellets, that were not torrefied have a very good hardness, which decreases due to torrefaction. In determining the WI, some pellets swelling, as shown in Figure 4.

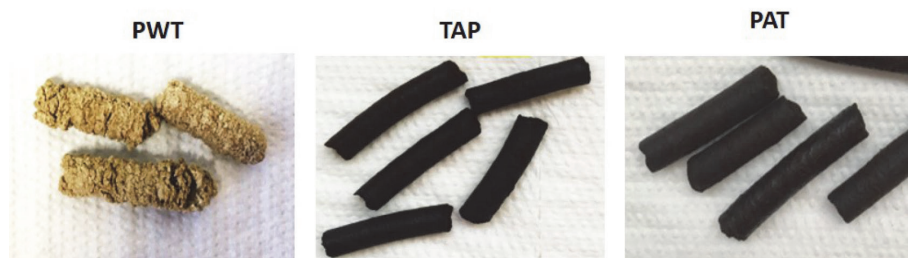


Fig. 4: Pellets appearance after determination wettability index (WI). PWT – pellets without torrefaction, TAP – Torrefaction after pelletization, PAT – pelletization after torrefaction.

The results of the WI values indicate that torrefaction has a positive effect on water resistance. Again, these measurements confirm that torrefaction improves pellet hydrophobicity. They will therefore be better resistant to moisture and mould.

4.4. Energy parameters

Torrefaction increased the calorific values. The input mixture had a higher heating value 16.03 MJ.kg-1 and a lower heating value 15.89 MJ.kg-1. The values after torrefaction were 19.90 MJ.kg-1 and 19.84 MJ.kg-1, respectively. Torrefaction also caused the amount of ash to increase from 7.23% to 11.38%, but it also logically reduced the moisture content to 0.9% relative to the material that was not torrefied. There has also been an increase in the proportion of fixed flammable versus volatile flammable.

5. Conclusion

The aim of this study was to evaluate the quality parameters of the pellets produced by different process ways. The first one was pellet torrefaction after pelletization (TAP) and the second reverse, i.e. pelletization after torrefaction of the input material. The Odeon rapeseed straw was tested. All manufactured pellets from both ways were subjected to mechanical testing. The results indicate that pellets produced without the thermal torrefaction process are already of good quality and can be used as an alternative fuel. They have good mechanical-physical properties that suggest their potential for use. Pellets that have undergone a torrefaction process have very good resistance to water absorption, lower wettability index. Because this thermal process causes the materials to become hydrophobic. Torrefaction increased the amount of ash, but it also decreased moisture relative to the material that was not torrefied. There has also been an increase in the proportion of fixed flammable versus volatile flammable. Furthermore, the calorific value of materials and pellets increased significantly. TAP pellets have lower hardness and only slightly lower pellets durability index. Torrefaction reduced durability index significantly for PAT pellets. It should be noted that no additives were used during the pelletization of the material.

TAP pellets have lower values of bulk density and hardness. PAT pellets correspond to lower

values of bulk density and mechanical resistance/durability index. Material processing is worse for the PAT way. Torrefied material clung to the walls of the hopper. The calorific value is higher for TAP pellets. Overall, TAP can be seen as an easier process way.

6. Acknowledgments

This paper was supported by the Ministry of Education, Youth and Sports of the Czech Republic under OP RDE grant number CZ.02.1.01/0.0 /0.0 /16_019/0000753 "Research centre for low-carbon energy technologies".

7. References

- Chen, W. H. et al. (2021) 'Progress in biomass torrefaction: Principles, applications and challenges', *Progress in Energy and Combustion Science*. Elsevier Ltd, 82. doi: 10.1016/j.pecs.2020.100887.
- Chen, W. H. and Kuo, P. C. (2011) 'Torrefaction and co-torrefaction characterization of hemicellulose, cellulose and lignin as well as torrefaction of some basic constituents in biomass', *Energy*. Elsevier Ltd, 36(2), pp. 803–811. doi: 10.1016/j.energy.2010.12.036.
- Ghiasi, B. et al. (2014) 'Densified biocoal from woodchips: Is it better to do torrefaction before or after densification?', *Applied Energy*. Elsevier Ltd, 134, pp. 133–142. doi: 10.1016/j.apenergy.2014.07.076.
- Mahadeo, K. (2014) 'Study on Physical and Chemical Properties of Crop Residues Briquettes for Gasification', *American Journal of Energy Engineering*, 2(2), p. 51. doi: 10.11648/j.ajee.20140202.11.
- Manouchehrinejad, M. and Mani, S. (2018) 'Torrefaction after pelletization (TAP): Analysis of torrefied pellet quality and co-products', *Biomass and Bioenergy*. doi: 10.1016/j.biombioe.2018.08.015.
- Ribeiro, J. M. C. et al. (2018) 'Future perspectives of biomass torrefaction: Review of the current state-of-the-art and research development', *Sustainability (Switzerland)*, 10(7), pp. 1–17. doi: 10.3390/su10072323.
- Siyal, A. A. et al. (2020) 'Torrefaction subsequent to pelletization: Characterization and analysis of furfural residue and sawdust pellets', *Waste Management*. doi: 10.1016/j.wasman.2020.05.037.

Recovery of compressor waste heat in Organic Rankine Cycle

Jaroslav Frantík¹, Jan Kielar¹ and Ondřej Němček¹

¹ VSB – Technical University of Ostrava, ENET Centre, 17. listopadu 15/2172, 70833 Ostrava-Poruba, Czech Republic

1. Abstract

The paper deals with the recovery of waste heat arising during air compression in a screw compressor ALUP LARGO 90 kW. This compressor was fitted with temperature and pressure sensors to determine the energy balance of the facility. Waste heat quantities were determined in dependence on the compressor output set-ups, to be subsequently used in the Organic Rankine Cycle system.

Keywords: compressor, energy, waste heat, organic rankine cycle.

2. Introduction

The production of compressed air is a process intense in energy but low in efficiency (Nehler, 2018; Saidur et al., 2010). Up to 75 % of the energy needed for air compression is converted to heat, which is wasted. In rare cases the heat is used to heat buildings in winter or to heat water. The research deals with the recovery of waste heat from air compression in Organic Rankine Cycle (ORC), being a conventional condensation cycle. However, instead of water vapour, an organic substance is used as the medium (Mahmoudi et al., 2018). Based on the type of the facility, this medium drives the turbine, for example, which generates electric power in the generator (Lecompte et al., 2015). An organic substance is used as the medium because of low temperature drops and temperature levels, where the use of water vapour is excluded. The advantages of ORC are the automated technology and minimum maintenance (Rahbar et al., 2017).

3. Measuring “stand”

The “measuring stand” comprises of four components: ALUP LARGO 90 kW compressor station (Fig. 1), fittings for the air inlet and outlet, compressed air of the appliance, and the measuring system. The different process parameters of the compressor station were selected to simulate real operation conditions, namely the construction elements, air-handling inlet elements, the outlet section, compressor unit case, including the cooling circuit.

The compressor station was fitted with an inlet and outlet port and sensors. However, its function was not modified. We aimed to collect data without exerting any influence on the

measured quantities in the important points of the system. The different sensors were located in order to record the major operation parameters and quantities in the important points of the overall system. This way, we were able to evaluate medium flow rates, temperatures and consumptions of the different nodes.



Fig. 1: ALUP LARGO 90 Kw compressor.

The appliance was an air chamber of 500 l in volume, fitted at the inlet with two slide valves and pressure valve with a control range from 9 to 2 bar. Thanks to the system, we were able to alter the consumption of compressed air from the compressor and, thus, to simulate the real needs of the operation in the conditions of the industry and other applications.

The system of sensors is connected to the measuring distributor, where the data measured in real time during the testing operation go to the data-logger Ahlborn Almemo 710 via the measuring interface WASBORN. The data processed in the data-logger are visualised in a PC software. A PC is also used to regulate the basic quantities of the system – e.g. cooling liquid pump in the oil / water circuit.

Before own measurements, it is necessary to make sure the “measuring stand” runs without any problems to avoid undesirable operation trends and potential system damage. When the compressor station is switched on and pre-pressurised, the required pressure is set using the reduction valve and slide valves downstream the air chamber. Thanks to the regulation elements of the pump, the required temperature is set on the oil return into the oil/ water cooler. Next, it is important to steady the system to reach the required / operational parameters to be able to carry out the measurements. The approximate time to reach the steady state varies in dependence on the required and set operational parameters, and may last tens of minutes. Therefore, the stabilisation time was set to 1 hour in order to prevent possible breakdowns. The time of measurements was also set to 1 hour. After the measurements, the different energy balance flows were evaluated - see Fig. 2.

Based on the compressor energy balance results, we evaluated the waste heat production and proposed the subsequent ORC.

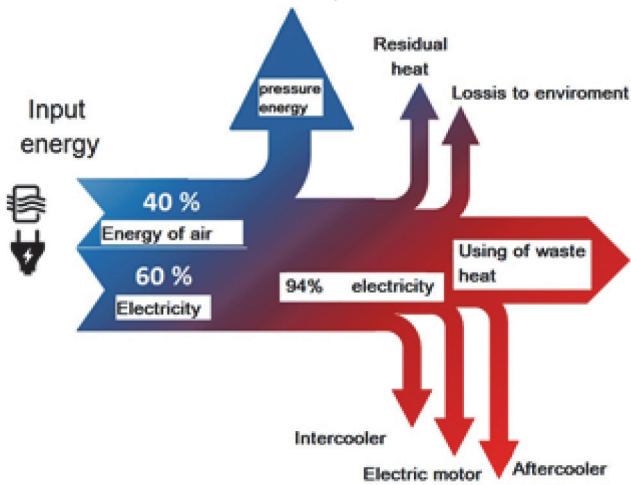


Fig. 2: Scheme of the different energy balance flows.

3.1. Location of the measuring points in the “measuring stand”

The measuring points were selected to determine the energy flows as accurately as possible – see Fig. 3. When determining the air flow in the ducts (air speed), it is important to position the measuring points correctly. These were determined using a set of measurements during which, using Prandtl tube measuring of air ports, each point of average speed was determined. Calorimetric anemometer sensors were placed at each of the points. The points were verified by subsequent measurements.

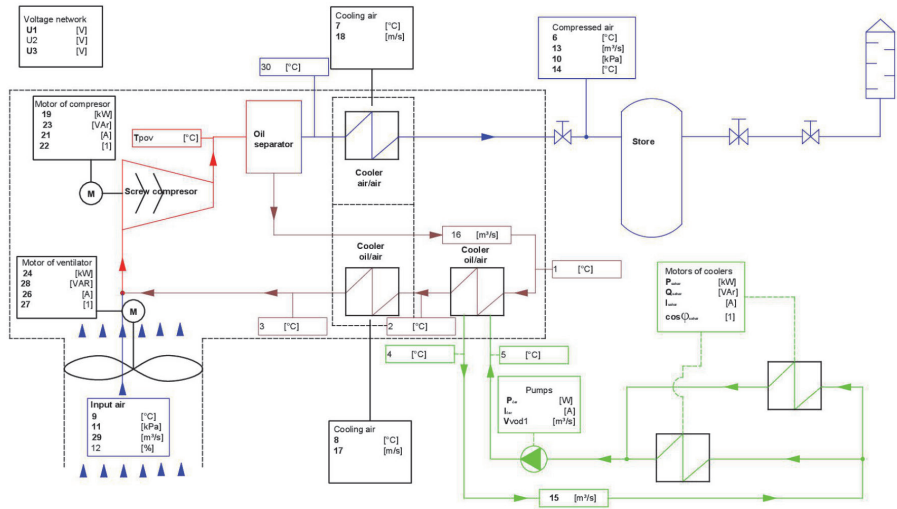


Fig. 3: Scheme of the measuring equipment set-up.

Fig. 3. shows the scheme of the measuring points: green – water; blue – compressed air, intake; red – water + oil, dark red – oil.

The different energies were determined according to Equation 1. Enthalpy and densities for the different states and substances determined using the EES programme.

(eq. 1)

where: E_x – energy of component x

$(m_x)'$ – mass flow of component x

i_{xTp} – enthalpy of component x at temperature T and pressure p

4. Determination of a compressor energy balance

The energy balance was determined for the ALUP LARGO 90 kW compressor (Fig. 1). Having fitted the temperature and pressure sensors and connected to the control system, we carried out a series of measurements under various output set-ups. The heat arising from the air compression was passed into the water circuit via the oil/ water exchanger. The compressor output is 14.3 m³/min and the maximum quantity of exploitable heat was determined as 74 kW.

There were several complications during the testing of the different parameters. It was utmost difficult to determine the air flow rates. These were verified by means of Prandtl tube measuring. To measure the speed of air flow and compressed air volumes, we used the method of Prandtl tube measuring combined with a mercury U-tube. The measurements of oil flow rates were burdened by a considerable error caused by the formation of bubbles, which influenced the final values of the fitted flowmeter. Despite all the complications, the energy balance of the compressor was determined for its different output set-ups.

The below stated energy balance states the balance between the energies entering the facility and leaving the facility in kW.

$$E1 + PK + PV = E2 + E3 + E5 + QV + EZ \quad (\text{eq. 2})$$

where: $E1$ - energy of the inlet air

PK - compressor input

PV - fan input

$E2$ - inlet air energy (air/ air exchanger)

$E3$ - compressed air energy

$E5$ - outlet energy (oil/ air exchanger)

QV - energy in the cooling water (oil/ water exchanger)

EZ - energy of the losses

For illustration, we calculated the energy balance of the compressor at the air compression set-up of 5 bar. The values are given in kW.

$$179 + 82.5 + 0.004 = 91 + 29 + 84.7 + 52.6 + 4.1 \quad (\text{eq. 2})$$

The energy balance implies that at the compressor output set-up of 5 bar, the quantity of the heat exploitable in the ORC system is 52.6 kW. The determined quantities of the exploitable heat in dependence on the compressor set-up are given in the chart in Figure 4 below.

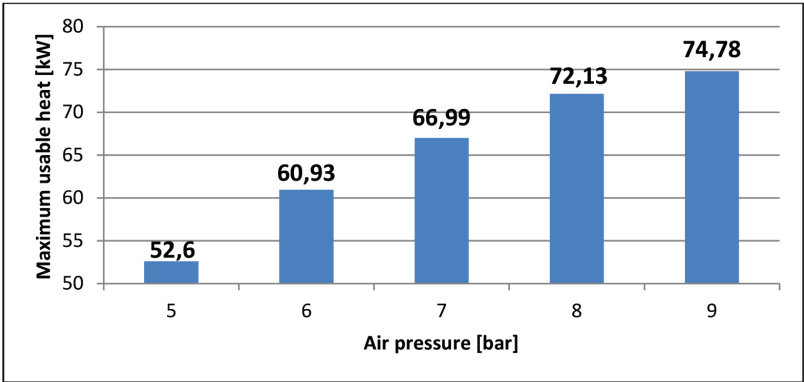


Fig. 4: Chart of the dependence of the exploitable heat quantity on the compressor output.

5. ORC system design

The Organic Rankine Cycle system was proposed on the basis of the model in the EES programme. We selected the relevant cooling agents, using which the efficiency of the overall system will be tested. When selecting the cooling agents, we assessed the parameters such as T-S diagram, toxicity, minimum environmental impact, availability in the EU, and the price.

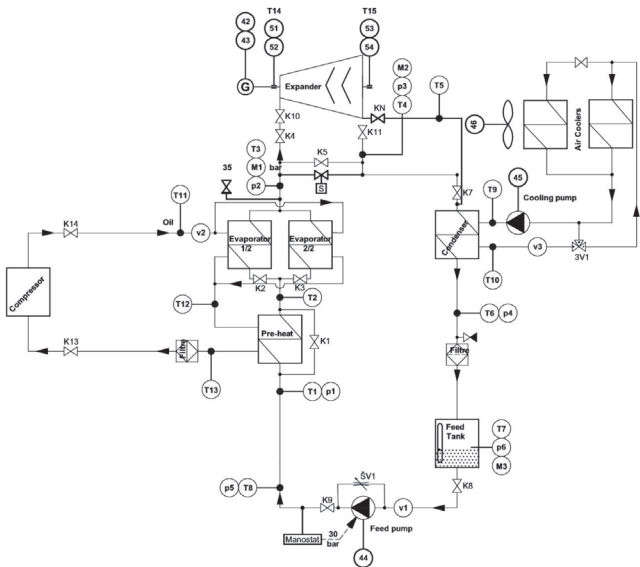


Fig. 5: Organic rankine cycle prototype scheme

ORC consists of 3 closed systems, which are interconnected by means of an exchangers. The whole system is equipped with a number of sensors, especially pressure, temperature and flow meters.

5.1. Coolant circuit

The coolant is gradually heated by three exchangers: preheater, evaporator 1/2 and evaporator 2/2. The exchangers are countercurrent and transfer heat from the oil to the coolant. The coolant then enters the expander with parameters p_2 and T_3 . On the expander, the coolant transmits part of its enthalpy and it converts it into mechanical energy, which is measured using a dynamometer (G).

The expander is equipped with two bypasses. The first is operational and serves to gradually increase the pressure ratio. The second is an emergency and is equipped with a solenoid valve. The valve is controlled by a dynamometer and opens when voltage is lost.

After the expander, the coolant has temperature T_4 and pressure p_3 . The coolant condenses in a water-cooled condenser which acts as a countercurrent exchanger. After complete condensation of the coolant, there is a significant reduction in pressure caused by a reduction in the volume of the coolant.

A filter is connected in the circuit behind the condenser to ensure the purity of the coolant. The filter performs 2 tasks, capturing fine particles that got into the circuit during production and as a dehydrator.

After cleaning, the coolant continues to the supply tank. It provides a coolant supply for all ORC operating conditions. The tank is equipped with 3 sight glasses to check the coolant level and equipped with temperature sensors T_7 and pressure p_6 .

The entire ORC is powered by a gear pump controlled via a frequency converter to selected flow, measured by a propeller flow meter v_1 . For fine-tuning of the flow, there is the throttle needle valve ŠV1, which passes the outlet to the pump suction. After the pump, the coolant continues at pressure p_5 and temperature T_8 to the pre-heat.

5.2. Oil circuit

The oil enters the ORC at temperature T_{11} with a flow rate v_2 and transfers its internal energy through the exchangers and exits at temperature T_{13} . The oil circulates by means of a different pressure between the compressor itself and the oil separator.

5.3. Water circuit

The water circuit removes heat from the condensation from the ORC system. The heat from the water is dissipated by two air coolers, which dissipate it into the air. Due to the low energy potential, we can no longer use it in any way, and therefore we discharge it into the air to maintain the highest possible enthalpy gradient on the turbine. Water circulation is ensured by a circulating pump and the flow is measured by a flow meter v_3 . The whole circuit is equipped with two temperature sensors T_{10} and T_9 to determine the size of the

thermal gradient.

6. ORC system efficiency measurement

The efficiency of the ORC was determined on the basis of measurements, where the energy that enters the ORC in the form of thermal energy in oil and energy output from the system in particular was monitored: the power input of the coolant circulation pump and the power of the expander. The ORC efficiency measurement was performed when the compressor output was set-up of 5 bar. Energy output from ORC was measured by dynamometer TK-1. Efficiency of system was calculated based on the input and output energy.



Fig. 6: ORC system

Based on these measurements, the efficiency of the entire ORC system was determined in the range of 5.45 to 5.7 %. The highest achievable thermodynamic efficiency without any losses at a temperature drop of $26^{\circ} - 80^{\circ} \text{C}$ in the Carnot cycle is 15%. Since our device had an expander, which was originally designed as a screw compressor (for the purposes of the expander it was connected in reverse) and the whole ORC stand was only a prototype, we can consider the measured results achieved as good.

7. Conclusions

The recovery of waste heat arising from air compression using an ORC system is an innovative direction of research. Considering the fact that compressor stations use several tens of compressors of outputs analogous to the compressor used in this research, it is a huge potential energy source with a number of applications.

The paper reports research using ALUP LARGO 90 kW compressor fitted with a number of sensors and control system, together representing a “measuring stand”. Using the “measuring stand” we determined the energy balance for the different compressor output set-ups.

The major focus was to recover the energy from the waste (exploitable) heat, which was determined for all the compressor output set-ups. It shows that at the maximum compressor output, it is possible to recover as much as 74.7 kW of energy in the ORC system.

Efficiency of ORC system was measured when the compressor output was set-up of 5 bar and corresponds to maximum 5.7 %. Since the measurement was performed on a prototype device, we can consider the results as good.

Energy recovery and possible applications of ORC system will be the subject of subsequent research. Nevertheless, after modifications to the system, especially the use of a new type of expander, a significant improvement in efficiency is expected.

8. Acknowledgments

This contribution was supported by the project TH02020183: Increasing the efficiency of compressed air production in compressor stations using the ORC compressor, SP2018 / 54 and LO 1404: Sustainable development of the ENET Center.

9. References

- Lecompte, S., Huisseune, H., van den Broek, M., Vanslambrouck, B., Paepe, M. De, 2015. Review of organic Rankine cycle (ORC) architectures for waste heat recovery. *Renew. Sustain. Energy Rev.* 47, 448–461. <https://doi.org/https://doi.org/10.1016/j.rser.2015.03.089>
- Mahmoudi, A., Fazli, M., Morad, M.R., 2018. A recent review of waste heat recovery by Organic Rankine Cycle. *Appl. Therm. Eng.* 143, 660–675. <https://doi.org/https://doi.org/10.1016/j.applthermaleng.2018.07.136>
- Nehler, T., 2018. Linking energy efficiency measures in industrial compressed air systems with non-energy benefits – A review. *Renew. Sustain. Energy Rev.* 89, 72–87. <https://doi.org/https://doi.org/10.1016/j.rser.2018.02.018>
- Rahbar, K., Mahmoud, S., Al-Dadah, R.K., Moazami, N., Mirhadizadeh, S.A., 2017. Review of organic Rankine cycle for small-scale applications. *Energy Convers. Manag.* 134, 135–155. <https://doi.org/https://doi.org/10.1016/j.enconman.2016.12.023>
- Saidur, R., Rahim, N.A., Hasanuzzaman, M., 2010. A review on compressed-air energy use and energy savings. *Renew. Sustain. Energy Rev.* 14, 1135–1153. <https://doi.org/https://doi.org/10.1016/j.rser.2009.11.013>

An Examination of Thermal Features' Relevance on Battery-Fault Detection

Ondřej Kabot, Stanislav Mišák, Jan Fulneček

VSB – Technical University of Ostrava, Ostrava (Czech Republic)

1. Abstract

Uninterruptible power supplies (UPS) play an important role in industry. They secure various kind of industrial technologies from being damaged by an interruption of electric power supply. This paper describes an experiment focused on the possibility of an infrared thermography for a long-term monitoring and fault detection of UPS. Such method can be used as a supplement for lead-acid battery-based UPS monitoring, providing their higher reliability and reducing maintenance costs.

Keywords: infrared thermography; uninterruptable power source; lead-acid battery; fault detection

2. Introduction

Typical large scale uninterruptible power supply usually consists of high number of elementary batteries, connected in series strings or series-parallel groups. Nowadays, most advanced UPS are equipped with a complex battery management system (BMS). Voltage of each battery is evaluated and the charging and discharging current of every battery in a string is controlled by balancers. This approach is necessary especially for Li-ion batteries, which are sensitive to overcharging and deep discharging [1]. In industrial purpose UPS, lead acid batteries are usually the most common because of their low price. Most of the lead acid-based UPS are operated without any BMS, charging process is completely controlled only by the voltage of a battery string. There is an economic reason for this: lead acid batteries are relatively cheap and resistant to overcharging and deep discharging processes [2], so there is a long payback period for BMS. Estimation of condition of the battery only according to their temperature will enable to create a cheap monitoring system. It was decided to use infrared thermography instead of contact temperature sensors, because an extensive wiring work around is usually necessary to additional installation of temperature sensors to an existing UPS. The whole battery string must be usually disconnected, and UPS must be temporarily turned off. In compare, an infrared camera can be easily installed next to existing battery without any string disconnections or manipulations. Decreasing cameras prices are making them more available for individual small-scale projects.

1.1. Voltage distribution in a battery string

During UPS normal operation (stand-by), batteries are permanently connected to the charger, which is represented by the voltage source. Voltage of the charger is set according

to the float charge voltage of the battery (constant voltage charging). In ideal case, all the cells in a string has the same properties, which leads to uniform distribution of voltage on each cell.

If UPS is not equipped with BMS, periodical checks of UPS batteries voltage are necessary. This is usually done by a maintenance personnel. Goal of this paper is to describe the possibility of infrared thermography for long term monitoring and estimation of the condition of batteries in a string of UPS. Whole experiment was driven by the idea of creation of infrared thermography supplement to maintenance.

1.2. Current approach

Modern BMS evaluates condition and charge level of batteries according to their voltage, charging or discharging current and temperature [3]. When the cell is damaged, overloaded or being overcharged, it generates heat [4]. This is a reason why the temperature monitoring also represents an important part of modern BMS. It improves safety of the battery operation, increases charging and discharging performance and prolongs the battery lifetime. Temperature sensors must be placed right on the surface of a cell, or inside the cell itself for proper function. In most of the applications, simple thermistors are used for temperature monitoring. But there are other types of sensors, developed especially for BMS purposes. Semiconductor CMOS sensors can provide high accuracy and linearity [5]. Flexible micro temperature sensors can be fabricated into the cells, providing high accuracy measurement with short response time [6]. Temperature sensors can be also produced by printed electronics technology [7]. In special applications, an optical fiber can be used for external and also internal cell temperature monitoring [8]. This method is suitable especially for an aggressive environment.

3. Experiment description

12V/63 Ah lead-acid batteries were used in this experiment. All measured batteries were diagnosed before the experiment for their actual capacity estimation (tab. 1). First of all, high resolution thermograms were captured to discover any significant temperature differences during battery malfunction. As it was presumed, thermal map inhomogeneity is detectable for a battery with internal defect (fig. 1).

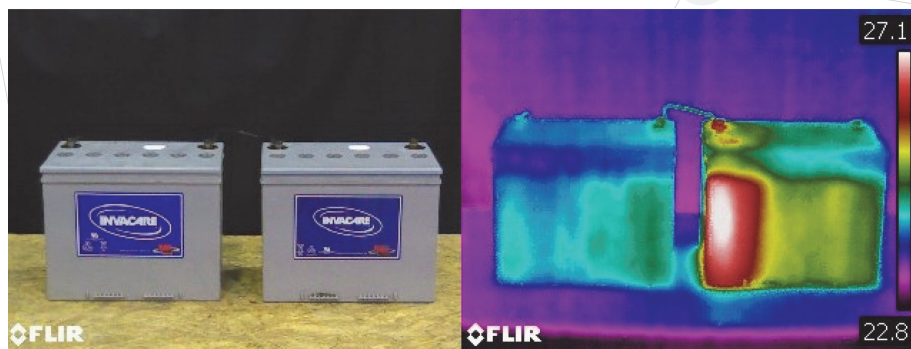


Figure 1. Thermogram of damaged and undamaged battery

After this confirmation, experiment itself was conducted. Batteries were connected into series string, containing from three to five batteries according to the experiment configuration. Infrared camera was mounted on the ceiling of laboratory (fig.3) for automatic data acquisition with period of 1 minute, its temperature range was set manually. Lower limit was set according to the ambient temperature, upper according to the battery maximal allowed temperature. Voltage of each battery was measured with the same period with data acquisition card. Value of the battery surface emissivity was estimated with the emissivity tape and set to 0.96.

Table 1. Percent values of battery actual capacity (from nominal value)

Configuration	1	2	3	4	5	6
Bat 1	47 %	47 %	47 %	47 %	47 %	47 %
Bat 2	56 %	56 %	56 %	56 %	56 %	2 %
Bat 3	56 %	56 %	56 %	56 %	5 %	5 %
Bat 4	33 %	2 %	4 %	-	-	-
Bat 5	45 %	45 %	45 %	-	-	-

Voltage source was used as a charger. Its voltage was set according to the number of batteries in a string, multiplied by float charge voltage of the battery (13.6 V). Charging and discharging current was limited to 15 A to prevent the damage of batteries.



Figure 2. Example of acquired thermogram

4. Statistical testing

The correlation coefficient among multivariate variables or towards categorical variable is not directly obtainable. What we can examine, is the correlation between the range of temperatures and voltages during all measurements. The range is simply the difference between maximal and minimal values (temperature or voltage) of the configuration at the measured time. If their progress is correlated, the implication about thermal features relevancy could arise. On the other hand, in case of uncorrelated behaviour, we can only confirm no presence of redundancy among these variables.

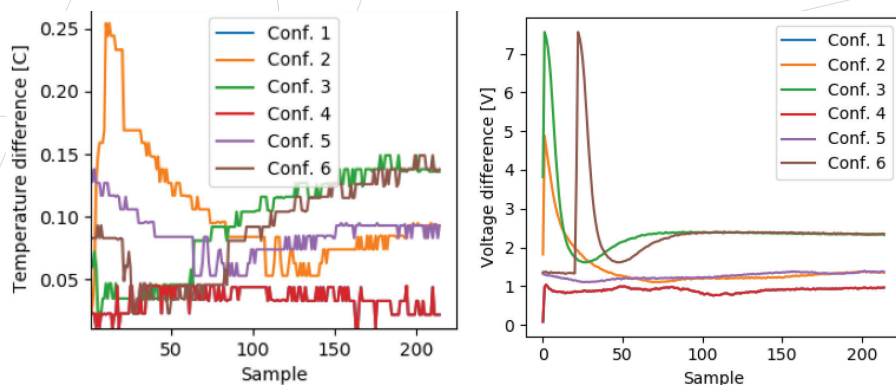


Figure 3. The differences between minimal and maximal measured values on the given battery configuration at the given time. The temperature data are used on left side and voltage data on right side

On the Figure 3 we can see that ranges of temperature and voltage vectors does not possess similar behaviour, which is also confirmed by their correlation coefficients. They are listed in Table 2 and their values were calculated between each pair of all configurations and (dis)charging processes. The obtained coefficients mean that most of the time, there is no correlation between these variables. This fact does not say anything about relevancy of thermal feature, it only confirms that this data is not redundant in statistical manner with voltage vectors.

Table 1. Correlation coefficients

Configuration	1	2	3	4	5	6
Charging	-0.0623	0.362	-0.0759	0.1981	0.1568	0.5509
Discharging	-0.2319	0.4762	0.7371	-0.4414	-0.2845	-0.5877

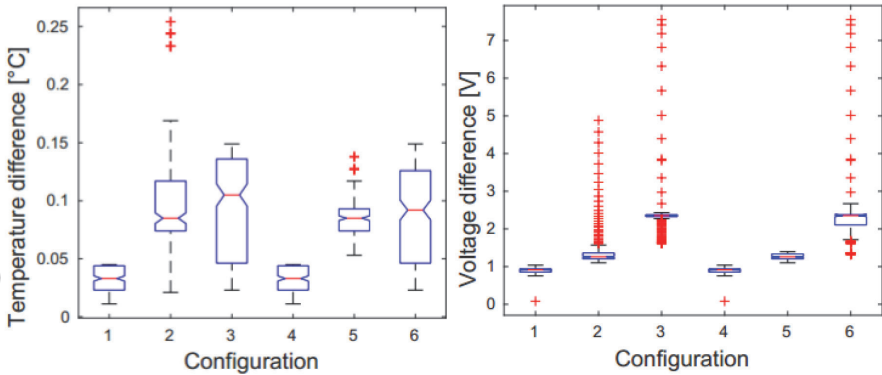


Figure 4. The analysis of variance of temperature (left) and voltage (right) ranges during charging period

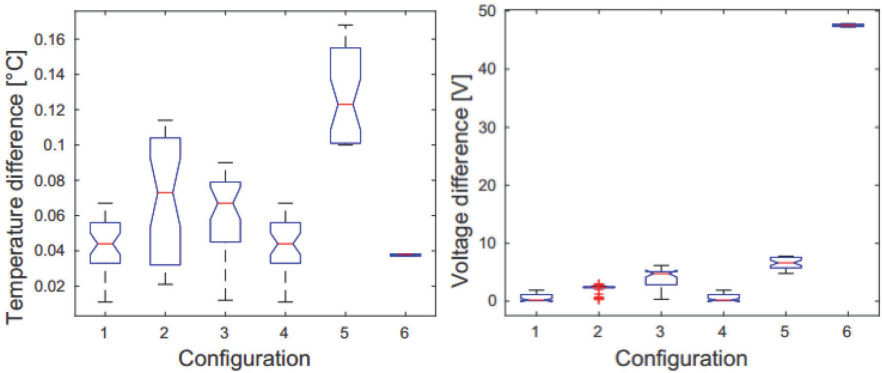


Figure 5. The analysis of variance of temperature (left) and voltage (right) ranges during discharging period

On the same ranges, the ANOVA test was executed to examine the statistical similarity among the configurations. As it was mentioned previously, the result of ANOVA test is the rejection of null hypothesis, which states about statistical equality of means of the observed variables. In case of no rejection of this hypothesis, it would be difficult to use variables without distinguishing ability for classification. This test was performed on voltage and temperature data again and also on charging and discharging measurements. In all cases, the resulted p-values dropped under the level of significance (voldischarge: $2.71\text{E-}226$, tempdischarge: $1.13\text{E-}171$, voldischarge: $1.1\text{E-}239$, tempdischarge: $6.11\text{E-}47$) which implies the rejection of the null hypothesis in all cases. The graphical representation of ANOVA means comparison is depicted on Figures 4 and 5.

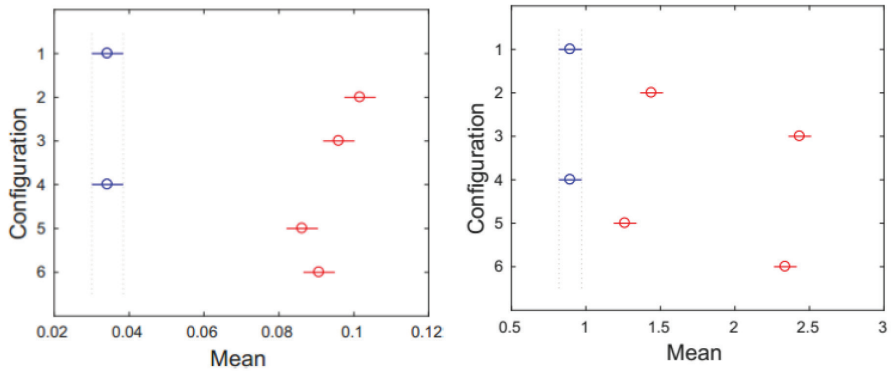


Figure 6. The post-hoc analysis of means of temperature (left) and voltage (right) ranges during charging period

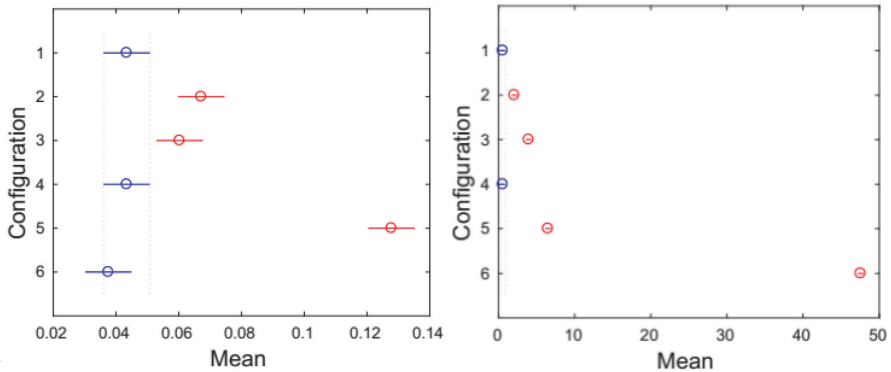


Figure 7. The post-hoc analysis of means of temperature (left) and voltage (right) ranges during discharging period

Because the statistical difference among the groups of data was observed, we are allowed to perform an additional post-hoc analysis that will uncover which group is significantly different from others. This test will also reveal which configurations are distinguishable only by their means. The graphical representations of the results from the post-hoc analysis is depicted on Figures 6 and 7. In case of charging process, the configurations 1 and 4 are clearly distinguishable from the rest of the configurations by both variables, the temperature range and the voltage range. These configurations do not contain defected batteries which is reflected by their smaller ranges.

In case of discharge process, the configurations 1, 4 and 6 have their means significantly different from the means of the rest in case of temperature range variable. It could be caused by overall high temperature and relatively small range on the entire battery configuration 6, which mostly consisted only of defected batteries. The voltage range was able to clearly distinguish this configuration from the rest. Voltage ranges performed very well in distinguish ability between fault and failure-free configurations also during discharge process.

These results confirms that values of examined variables are significantly different among

configurations and some of them are able to be distinguished by their means. So far we do not have any comparison whether the temperature data are more or less relevant than voltage data. This fact should be revealed by further tests.

5. Discussion

Results of statistical analysis shows strong correlation between the voltage and thermal distribution in battery string. Thermal data vector describes the voltage distribution in string almost as precisely as a voltage vector itself. Thus, it is possible to create infrared thermography monitoring system for battery fault detection, which can replace maintenance personnel. Correlation of vectors is more significant during charging process and less significant during discharging.

Differences between thermal and voltage vectors can be explained by thermal capacity of the battery. If the battery is defective, its voltage is influenced almost immediately after the start of charging or discharging. But it takes some time of heat generation to increase the surface temperature of the battery. This time delay is reason of the difference.

Disadvantage of this method is the necessity of free space in UPS surrounding area. Camera's angle of view is limiting factor, so it is not suitable for container-type UPS. But it can be easily applied in accumulator rooms, where sufficient distance between batteries and camera can be reached. In this case, such monitoring system could provide almost the same results as voltage monitoring, but with lower investment price. Experiment was realized with lead-acid batteries. Probably, similar correlation could be found for Ni-Cd batteries too.

6. References

1. Andrea, Davide; Battery Management Systems for Large Lithium Ion Battery Packs; Arttech House: USA, Massachusetts, 2010; pp. 6, ISBN 1608071043.
2. Thomas Crompton, P.J.; Lead-acid secondary batteries. In Battery Reference Book, 3rd ed.; Newnes, 2000; ISBN 075064625X.
3. Zhou, S.; Battery Management Systems BMS. In Advances in Battery Manufacturing, Service and Management Systems, 3rd ed.; John Wiley & Sons, 2016; ISBN 1119056497.
4. IEEE Draft Guide for the Ventilation and Thermal Management of Batteries for Stationary Applications, IEEE: 2011; ISBN 978-0-7381-6614-8.
5. Wang, C.C.; LU, W. J; Wu, T. C. A CMOS wide-range temperature sensor with process compensation and second-order calibration for Battery management Systems. Proceedings of the Circuit and Systems Symposium, Melbourne, Australia, 1-5 June 2014; IEEE: 2014. DOI 10.1109/ISCAS.2014.6865203
6. Chi-Juan, L.; Shuo-Jen, L.; Yu-Ming, L. In situ monitoring of temperature using flexible micro temperature sensors inside polymer lithium-ion battery. Proceedings of the Nano/Micro Engineered and Molecular Systems (NEMS), Kyoto, Japan, 5-8 March 2012; IEEE: 2012. DOI 10.1109/NEMS.2012.6196871
7. Grosch, J.; Teuber, E.; Jank, M. Device optimization and application study of low cost printed temperature sensor for mobile and stationary battery-based Energy Storage

Systems. Proceedings of the Smart Energy Grid Engineering (SEGE), Oshawa, Canada, 17-19 Aug. 2015; IEEE: 2015. DOI 10.1109/SEGE.2015.7324599

8. Novais, S.; Nascimento, M. Internal and External Temperature Monitoring of a Li-Ion Battery with Fiber Bragg Grating Sensors. *Sensors* 2016, vol. 16. DOI 10.3390/s16091394

Jakub Lachman¹, Marek Baláš¹ and Hana Lisá¹

¹ Energy Institute – Department of Power Engineering, Faculty of Mechanical Engineering,
Brno University of Technology, Technická 2, 616 69 Brno, Czech Republic

1. Abstract

Slagging and fouling are some of the more prominent problems associated with firing solid fuels. The vast experience with firing coal led to the creation of fouling and slagging indicators based purely on the chemical composition of ash. These indicators are usually based on the results of ash fusibility tests. Other than actual long-term fuel firing, ash fusibility tests are the only empirical indicator of slagging and fouling propensity. Both the predictive indices and ash fusibility tests have been shown to be inaccurate when directly used with biofuels and alternative fuels. Several changes have been made to the tests to better suit the different nature of biomass ash composition and behavior. However, certain standardized procedures in the ash sample preparation as well as in the actual ash fusion temperatures evaluation are still somewhat questionable. To that end, the results of an extensive study of ash fusion temperatures and ash composition have been evaluated and the discussion and conclusions are presented in this article. Severe problems in the standardized procedures are listed in the discussion part of the article and are further elaborated upon. Several new methods have already been proposed within the scientific community, however, the ash fusibility tests remain the technical standard, despite their somewhat flawed nature.

Keywords: *Ash Fusion Temperatures, Ash Fusibility Tests, Slagging and Fouling*

2. Introduction

One of the more prominent technical obstacles when it comes to biomass thermal utilization is the formation of ash deposits on the heated surfaces of the boiler. In fact, all solid fuels contain a mineral fraction that is mostly non-combustible and made of inorganic matter, whether bound to organic matter or present as distinct inclusions. Formation of deposits depends mainly on fuel quality, boiler design and boiler operation. The two general mechanisms or types of ash deposition are slagging and fouling and are described below.

2.1 Slagging

Slagging is the formation of molten or partially fused deposits on furnace walls of the boiler or on convective surfaces exposed to radiant heat. Slag is formed from molten or partially molten ash particles. When these particles come in contact with the cooled boiler wall, they might adhere to the surface and form the initial deposits on which further slagging occurs through entrapment of more particles. If the particles re-solidify before

the impact, they often re-bounce and are again entrained in the flue gas stream. If, however, the temperatures inside the furnace exceed the ash fusion temperatures, excessive slagging might occur. Steam or air soot blowers can inhibit the formation of ash deposits, depending on the strength and physical characteristics of the deposit. However, the initial base deposit generally remains attached to the tube, allowing subsequent deposits to accumulate more rapidly. Excessive slagging not only hinders the performance of the water-tube wall, but it can also cause severe combustion problems through inhibition of air/fuel mixing. This is especially the case in small scale boilers, such as those for household heating firing agro-pellets. The grate and furnace wall deposits are almost identical to the original ash composition and retain most silica present in the fuel. Aluminum and silica often form a glassy matrix that can entrap other minerals or trace elements. Phosphorus was shown to further amplify this effect (Vassilev et. al, 2015). When char becomes entrapped within the glassy matrix, incomplete combustion (as mentioned above) often occurs. This is often accompanied by excessive CO emissions.

2.2 Fouling

Fouling is defined as the formation of deposits on convective heat surfaces such as the superheater or reheater tubes. It is generally attributed to ash cinders and accumulations that form on the leading edges of the tubes. These deposits can again be partially dislodged by soot-blowing. Fouling deposits tend to be rich in volatile salts (usually chlorine and alkali metals compounds) and consist mostly of potassium, calcium, and sulfur (Miles et. al, 1996). The most prominent mechanism of deposit formation when it comes to fouling is through condensation of these inorganic vapors upon contact with the cooler superheater tubes. Similarly, as with slagging, the deposits formed through fouling hinder the heat transfer intensity and could lead to accelerated corrosion.

2.3 Ash fusibility tests

Boiler design manuals and handbooks take both slagging and fouling into account. Design is based on a range of ash deposition indices and on experience. The deposition indices are based on the ash chemical composition and on the results of laboratory tests on small samples of ash. As these values are often unreliable, boiler manufacturers have to rely on experience. This is especially true when it comes to biomass, as the vast experience from large-scale coal-fired boiler design cannot be directly translated to biofuels and alternative fuels. It is therefore imperative that empirical results of biomass ash behavior are obtained and compared with industrial installations. To that end, the technical standard for coal ash fusibility tests have been altered to better fit biofuels and alternative fuels. Ash fusibility tests are currently the only empirical evidence for many biofuels as there are often no industrial boilers that utilize them. Standards ČSN EN ISO 21404 and ČSN P CEN/TS 15404 are recommended for ash fusion temperatures (AFT) evaluation for solid biofuels and solid alternative fuels respectively. The methods themselves are described briefly in chapter 3.2. The characteristic ash fusion temperatures obtained through the tests are SST (shrinkage starting temperature), DT (deformation temperature), HT (hemisphere temperature) and FT (flow temperature). The aim of the article presented below was to analyze different biofuels and alternative fuels and discuss the differences, uncertainty and general precision and applicability of the standardized ash fusibility tests. The results of the analyses have already

been published elsewhere (Lachman et. al, 2021). This article, however, uses the results as a baseline and further elaborates upon them, drawing conclusions about the experimental procedure and informative value of ash fusibility tests both presented here and in general.

3. Materials and methods

The samples presented in this study were divided into two groups: biofuels and alternative fuels, with biofuels being further divided into woody and non-woody (herbaceous) biomass. The woody samples comprise the commercially available A1 spruce pellet, a representative softwood and hardwood sample for comparison and finally amaranth wood, all in the form of chips. The non-woody samples are composed mostly of agricultural residues, some in the form of pellets (hay, straw, sunflower) and some raw and unprocessed (rye grains, camelina seed etc.). The two alternative fuels selected were sludge acquired from a municipal sewage treatment plant and digestate as a solid fermentation residue from a biogas plant.

3.1 Ash content and composition

The ash content was analyzed in accordance with ČSN EN ISO 18122 for both the woody and non-woody biofuels and ČSN EN 15403 for the two alternative fuels. Each fuel was sampled and analyzed twice, and the ash content was established as the mean value of the two results. The ash samples were then analyzed by an accredited external laboratory through ICP-OES in accordance with ČSN EN 72 0101 and ČSN EN ISO 11885.

3.2 Ash fusion temperatures

The ash fusion temperatures were analyzed in accordance with ČSN EN ISO 21404 for all the biofuels and ČSN P CEN/TS 15404 for the two alternative fuels. A muffle furnace was used to prepare the ash samples at 550 °C. The ash was then pressed into cylinders in a manual hydraulic press and exposed to a uniform heating rate of 10 °C/min in oxidizing conditions. The decomposition was recorded using a high-definition camera that monitored changes in the shape and size of the silhouette. Each fuel was again sampled and analyzed twice, and the individual AFT's were established as the mean value of the recorded temperatures.

4. Results and discussion

The results of the experiments are presented in the following tables. **Tab. 1** shows the observed ash fusion temperatures and the measured ash content (dry basis). The ash composition of the different biofuels and alternative fuels is presented in **Tab. 2** (here given in weight percentages). The ash content in woody-biomass is generally low (the commercially available A1 spruce pellet shows the least amount of ash). The softwood and hardwood chips show comparatively higher ash content. This is most likely caused by the inclusion of bark, whereas the A1 pellets are probably produced without it. The non-woody fuels show much higher ash content, only safflower and straw pellets are similar in ash content to amaranth wood. The highest ash content was, as expected, found in sewage sludge. Sunflower pellets show the second highest ash content. This could be caused by the natural phytoextraction and hyperaccumulation of sunflower, as its ability to extract

minerals from the soil is much stronger than with the other analyzed plants.

Tab. 1 Ash fusion temperatures (°C) and ash content of the selected biofuels and alternative fuels

Sample	SST	DT	HT	FT	Ash content Ad [%]
<i>Woody biomass</i>					
Wood pellet A1 (spruce)	670	930	-	-	0.329
Softwood chips	1310	1320	1370	1390	3.010
Hardwood chips	1480	1500	-	-	2.441
Amaranth wood	1380	1450	-	-	7.704
<i>Non-woody biomass</i>					
Hay pellets	870	1080	1160	1230	17.729
Straw pellets	800	840	1000	1040	6.639
Sunflower pellets	890	1140	1210	1270	34.623
Quinoa waste	610	680	750	910	15.161
Flax	970	1170	1350	1470	17.900
Rye grains	620	750	900	970	13.675
Camelina seed	680	950	-	-	13.360
White mustard seed	730	970	1170	1450	17.088
Safflower grains	740	840	1010	1060	6.085
<i>Alternative fuels</i>					
Sewage sludge	980	1160	1260	1270	49.103
Digestate	1180	1240	1260	1270	15.947

The ash fusion temperatures of all the herbaceous biofuels are way below those of wood, indicating severe slagging and fouling propensity. The A1 spruce pellet shows uncharacteristically low SST and DT when compared to woody samples presented both here as well as in other studies (Garcia-Maraver et. al, 2017). This is further discussed in the following section. If the woody samples presented here are to be taken as a reference base, then the thermal utilization of all the non-woody biomass samples cannot be recommended due to their low AFTs. The ash composition can offer valuable insight into the behavior of the fuels. The hay pellets have been found to be rich in K₂O content. Potassium in most its forms is one of the more volatile major ash elements. High slagging and fouling propensity are therefore to be expected when firing hay or other fuels rich in potassium. This has been observed in another experiment conducted by the research team. Several of the other fuels, such as safflower grains and white mustard seed, have shown exceedingly low ash fusion temperatures and could therefore cause major slagging problems when used as organic binders in wood pellet making.

Tab. 2 The chemical composition of ash from selected samples given in wt%

Sample	K ₂ O	Na ₂ O	CaO	MgO	Fe ₂ O ₃	Al ₂ O ₃	SiO ₂	P ₂ O ₅	MnO	SO ₃	TiO ₂	S	Cl
<i>Woody biomass</i>													
Wood pellet A1 (spruce)	12.5	0.25	32.1	10.9	0.71	0.51	2.72	1.99	6.43	2.47	0.036	0.99	0.1
Softwood chips	8.71	0.4	39.3	3.03	0.94	1.56	8.62	5.55	0.18	1.86	0.096	0.74	0.1
Hardwood chips	9.81	0.17	42.2	4.34	0.49	0.55	2.8	5.47	0.18	2.17	0.041	0.87	0.1
Amaranth wood	14.4	0.29	39.2	6.74	0.48	0.22	2.38	3.7	0.027	1.87	0.27	0.75	0.17
<i>Non-woody biomass</i>													
Hay pellets	20.9	0.65	11.6	4.28	1.58	3.91	36.3	5.72	0.26	5.05	0.27	2.02	0.86
Straw pellets	18.8	0.58	8.1	3.2	1.94	4.97	45	5.07	0.19	3.22	0.31	1.29	1.51
Sunflower pellets	14	2.62	9.92	3.51	3.73	5.94	46.8	6.14	0.28	2.61	0.4	1.05	1.16
Quinoa waste	36	0.33	11.4	5.75	0.27	0.11	1.18	4.79	0.067	3.43	0.017	1.37	1.61
Flax	5.48	0.7	2.35	1.45	0.85	3.88	76.9	3.98	0.084	0.86	0.35	0.34	0.17
Rye grains	28.1	0.19	3.13	11.3	0.56	0.45	2.65	45.4	0.18	1.48	0.031	0.59	0
Camelina seed	27.4	0.089	8.12	12.6	0.6	0.12	1.04	34.8	0.089	8.97	0.015	3.59	0.1
White mustard seed	14.6	0.34	12.4	7.72	0.52	2.23	19.6	31.1	0.057	5.93	0.032	2.38	0.1
Safflower grains	23.9	0.28	11.7	14.3	0.56	0.01	0.54	39.3	0.09	2.55	0.009	1.02	0.1
<i>Alternative fuels</i>													
Sewage sludge	7.33	1.22	11.6	3.07	11.5	7.52	37.3	9.5	0.15	3.69	0.58	1.48	0.43
Digestate	10.6	2.38	22.7	11.8	0.87	0.33	14	17.2	0.34	4.58	0.031	1.83	1.42

4.1 Problems with ash fusibility tests

The ash fusibility tests, and their informative value have been subject to some controversy in the scientific community with some authors proclaiming them inaccurate and misleading (Kleinhans et. al, 2018). This generally stems from the artificial preparation and analysis of the sample. The samples themselves are prepared under uniform heating rate and subsequent retention at temperature of 550 °C. This temperature is well above the melting point of some low-temperature eutectics and can cause minor evaporation of more volatile inorganic matter (Miles et. al, 1996). This volatile inorganic matter is then absent in the prepared specimen that is tested for ash fusion temperatures. The resulting temperatures are therefore higher than those of the actual raw fuel. The size and shape of the specimen are also defined differently among the available technical standards with no indication of the effect they might have on the AFTs. The mechanical properties of the produced sample can also affect the AFTs. The A1 spruce pellet presented in this study showed problematic behavior both during preparation and subsequent analysis. This can be attributed to the low ash content in the pellet as well as its composition, which is uncharacteristically rich in potassium (possibly due to additives contained in binders). The sample was brittle and would deform poorly, making it almost impossible to identify all the AFTs. This could be caused by the release of gaseous CO₂ that is contained in dolomite and other carbonates. The SST is sometimes difficult to identify as this release of CO₂ can often occur without partial melting, causing the specimen to shrink. On the other hand, certain samples rich in silica can cause swelling instead. The specimen can then appear swollen on the outside (hence not shrinking under the 95% silhouette size defined as SST) while partial melting possibly already occurs underneath. The technical standards do not further specify this behavior and leave the identification of SST to the judgement of the personnel. This procedure then gives the empirical results of the test a somewhat subjective value, rather than an exact objective one.

The arguably flawed sample preparation is still the only procedure in which to obtain an ash sample in a reasonable timeframe. The possible release of volatile salts and alkali compounds should be investigated to validate the sample preparation methodology. Furthermore, certain physio-chemical transformations inside the inorganic matter can occur during the sample preparation, affecting the subsequent behavior of the AFT specimen. The produced specimen for the AFT evaluation is also much more homogenous and sizeable than the actual particles and mineral inclusions found in general application. The reducing and oxidizing conditions in which the tests can be carried out are also subject to some debate. While the volatile compounds mix well with air and are therefore present in oxidizing conditions, the larger particles react heterogeneously through diffusion while the core of the particle is being decomposed in reducing conditions. The ash fusibility tests can be carried out in both oxidizing and reducing conditions with reducing conditions often showing lower temperatures. It is possible to relate the industrial firing observations to the laboratory obtained results; however, it is inadvisable to design boilers based solely on the laboratory obtained AFTs. Unlike the ultimate or proximate analysis of the fuel, the ash fusion temperatures only give a slight indication of the expected behavior and can only be compared among other laboratory obtained AFTs to estimate the slagging and fouling propensity. The construction of the burner and the boiler itself have a much stronger impact

on complete combustion and operational quality than the laboratory obtained AFTs.

5. Conclusion

Ash fusibility tests are currently the only empirical evidence of inorganic matter behavior for many biofuels and alternative fuels. Their informative value is, however, questionable as the actual firing conditions vary drastically from those in the artificial lab environment. Unlike the results of proximate or ultimate analysis, the results of ash fusibility tests are purely indicative. It is impossible to estimate slagging and fouling tendency based solely on the results of fusibility tests. Boiler design, burner or grate type, fuel feed and operational conditions have much stronger impact on the slagging tendency and combustion quality. Fouling can to some extent be estimated based on the ash composition. However, the reported elemental content neglects important chemical associations and structural formations. It was shown that higher alkali content can cause severe fouling due to evaporation and subsequent condensation of inorganic vapors. The rate of deposit formation on the other hand, cannot precisely be estimated. Moreover, the alkali metals associations can vary from low temperature melting chlorides to high temperature melting silicates or many other different compounds. Therefore, the content reported as the percentage of a stable oxide can be somewhat misleading when trying to predict slagging and fouling tendency. Several new methods have been proposed in the scientific community, however, the ash fusibility tests remain the technical standard, despite their somewhat flawed nature. For further information, the reader is referred to (Horák et. al, 2013), (Lindberg et. al, 2013) or (Fernández et. al, 2005).

6. Acknowledgements

This research was financially supported by the Brno University of Technology, Faculty of Mechanical Engineering in frame of the Specific Research Fund, grant no.: FSI-S-20-6280

7. References

- ČSN P CEN/TS 21404: Solid biofuels - Method for the determination of ash melting behaviour - Part 1: Characteristic temperatures method. Praha, Czech Republic: UNMZ, 2020.
- ČSN P CEN/TS 15404: Solid recovered fuels - Methods for the determination of ash melting behaviour by using characteristic temperatures. Praha, Czech Republic: UNMZ, 2007.
- ČSN EN ISO 18122: Solid biofuels - Determination of ash content. Praha, Czech Republic: UNMZ, 2016.
- ČSN EN 15403 (838307): Solid recovered fuels - Determination of ash content. Praha, Czech Republic: UNMZ, 2011.
- Vassilev, Stanislav V, David Baxter, Lars K Andersen, and Christina G Vassileva. 2010. "An Overview Of The Chemical Composition Of Biomass". Online. Fuel 89 (5): 913-933. <https://doi.org/10.1016/j.fuel.2009.10.022>.
- Lachman J., M. Baláš, M. Lisý, H. Lisá, P. Milčák, and P. Elbl. 2021. "An overview of

slagging and fouling indicators and their applicability to biomass fuels.” Fuel processing technology 217. <https://doi.org/10.1016/j.fuproc.2021.106804>

Kleinhans, Ulrich, Christoph Wieland, Flemming J Frandsen, and Hartmut Spliethoff. 2018. “Ash Formation And Deposition In Coal And Biomass Fired Combustion Systems: Progress And Challenges In The Field Of Ash Particle Sticking And Rebound Behavior”. Online. Progress In Energy And Combustion Science 68 (C): 65-168. <https://doi.org/10.1016/j.pecs.2018.02.001>

Garcia-maraver, Angela, Jesus Mata-sanchez, Manuel Carpio, and Jose A Perez-jimenez. 2017. “Critical Review Of Predictive Coefficients For Biomass Ash Deposition Tendency”. Online. Journal Of The Energy Institute 90 (2): 214-228. <https://doi.org/10.1016/j.joei.2016.02.002>.

Miles, Thomas R, Larry L Baxter, Richard W Bryers, Bryan M Jenkins, and Laurance L Oden. 1996. “Boiler Deposits From Firing Biomass Fuels”. Online. Biomass And Bioenergy 10 (2): 125-138. [https://doi.org/10.1016/0961-9534\(95\)00067-4](https://doi.org/10.1016/0961-9534(95)00067-4)

HORÁK J. et al. PROBLEMATIKA STANOVENÍ CHARAKTERISTICKÝCH TEPLŮT TAVITELNOSTI POPELA BIOMASY. www.chemicke-listy.cz. [Online] 2013. Available at: http://www.chemicke-listy.cz/docs/full/2013_06_502-509.pdf.

Lindberg, Daniel, Rainer Backman, Patrice Chartrand, and Mikko Hupa. 2013. “Towards A Comprehensive Thermodynamic Database For Ash-Forming Elements In Biomass And Waste Combustion — Current Situation And Future Developments”. Online. Fuel Processing Technology 105: 129-141. <https://doi.org/10.1016/j.fuproc.2011.08.008>.

Fernández Llorente, M.J, and J.E Carrasco García. 2005. “Comparing Methods For Predicting The Sintering Of Biomass Ash In Combustion”. Online. Fuel 84 (14): 1893-1900. <https://doi.org/10.1016/j.fuel.2005.04.010>.

Complete Syngas Cleaning in a Mobile Wet Scrubber

Martin Lisý¹, Marek Balas¹, Patrik Elbl¹, Hana Lisá¹ and Pavel Milčák¹

¹ Energy Institute – Dept. of Power Engineering, Faculty of Mechanical Engineering, Brno University of Technology, Technická 2, 616 69 Brno, Czech Republic

1. Abstract

Gasification is one of the promising alternative technologies for heat and electricity production from renewable and alternative fuels. However, tar and dust present in the gas do not enable the direct utilization. Known cleaning technologies used in well-known industrial applications (coal gasification) are not suitable and acceptable due to the high investment costs and the loss of process efficiency. This work describes particularly mobile pilot plant wet scrubber with gas flow $2\text{--}5\text{ m}^3\cdot\text{h}^{-1}$ coupled with a fluidized bed gasifier (100 kW_{th}) and pyrolysis unit (200 kW). Scrubber is consisted of four independent columns. Water and organic liquid in the form of rapeseed oil methyl ester (RME) are used as the scrubbing liquids. Various scrubbing operating conditions were designed such as scrubbing temperature and scrubbing liquid flow rate. Suitability of these was validated in the experiments. The gas composition, the tar and dust contents were measured at inlet and outlet of mobile scrubber at different operating parameters. Mainly the tar and dust removal efficiency were determined at different operating parameters. Under the optimized conditions of scrubbing (temperature, gas flow and scrubbing liquid flow rate) high efficiencies of the tar and the dust removal were found.

Keywords: gasification, tar, wet scrubber, gas cleaning

2. Introduction

With raising societal pressure to increase the share of renewable and alternative energy sources in electricity and heat production, attention is also turning to the use of alternative syngas from various sources, such as gasification and pyrolysis products, landfill gas, coke oven gas, blast furnace gas or waste gases from the chemical industry. However, in addition to the combustible gas components CO, H₂, CH₄ and lower hydrocarbons (ethane, ethylene, acetylene, etc.), these gases also contain a number of undesirable substances (Baláš et al. 2016a; Milne et al. 1998).

Their composition and amount depend on many factors and significantly affect the subsequent methods of gas purification and its further use. Among the primary contaminants appearing in the above gases are (Baláš et al. 2017b; Choinacki et al. 2020; Milne et al. 1998):

- solid particles
- alkaline compounds
- nitrogen compounds
- sulfur compounds
- chlorine compounds
- tar.

Tar is then considered to be the key and the most problematic contaminant. It is a complex and diverse mixture of condensable hydrocarbons with a wide range of molar masses. The mechanisms of tar formation, its properties, and behavior are described in a number of publications (Neeft et al. 2004). The basic definition of tar, like “all organic substances with a boiling point higher than benzene (80.1 °C)” and the basic methodology of sampling and evaluation of tar content in-process and syngas are determined primarily by the so-called TAR PROTOCOL (Neeft et al. 2004). Tar is the most common obstacle to the broader spread of gasification. For gas turbines, tar is not a significant problem due to higher temperatures and its combustion in the chamber. If the tar is in the form of vapors, its amount is not limiting (Milne et al. 1998); in the case of condensation, the maximum amount of tar, in various publications, is in the range of 0 to 0.5 ppm (Milne et al. 1998). For the use of the produced gas in internal combustion engines, a number of values of the maximum tar content are given (Baláš 2008c); most often, this limit is in the range of 10–100 mg.m⁻³.

3. Syngas cleaning

Tar removal is an issue, especially in the development of biomass and waste gasification technologies. The production of tar in wood gasification is much higher than in coal and this tar is usually made up of heavier, more stable aromatic substances (Bridgwater, 1995). These can partially react to soot formation, which clogs filters and fittings, which is a problem, especially with biomass gasification. Therefore, the research aims to reduce tar formation during biomass gasification or remove it effectively. Measures to reduce the tar content of gas can be divided according to various criteria, the main being primary and secondary.

3.1 Wet gas Scrubbings

Wet scrubbing is a relatively effective way of secondary gas cleaning, as it effectively removes both tar and dust particles. To make the scrubbing as efficient as possible, it is essential to create a large specific surface area of the scrubbing liquid, ensuring perfect contact between the scrubbing liquid and the scrubbed gas. The passage of liquid can achieve such large contact areas through various barriers, nozzles, grids, etc. [1] The scrubber must be designed to ensure a relatively constant pressure difference and wash liquid and gas flow. Various scrubbing media are used for scrubbing impurities from gas (especially tar and solid pollutants). These are water and organic liquid. Separation of tar using a wet scrubber is carried out in two ways: condensation and absorption. (Kubiček, 2005)

3.2 Scrubbing mechanism

Two mechanisms are used to scrub impurities from the gas – condensation and absorption. During cleaning, the gas comes into contact with the liquid, the impurities pass from the gas to the liquid, thus cleaning the gas. (Kubiček, 2005)

a) Condensation

Condensation is performed by cooling the gas below its dew point temperature. Condensed drops of water and tar are trapped and entrained by drops of scrubbing liquid, usually dispersed into the gas stream by the nozzles of the scrubber. The contaminated liquid is collected in the lower part of the chamber, from where it is drained [2].

b) Absorption

During absorption, mass sharing occurs, where the components from the gas phase transfer to the liquid phase. The gas contaminants are absorbed by a suitable solvent scrubbing liquid, where they are dissolved. The driving force behind this process is the difference in the partial pressures of a given component in the gaseous mixture and above the liquid in which the components dissolve. The gaseous component is absorbed by the liquid provided that its partial pressure in the gas phase is greater than above the liquid. As the partial pressure of the component in the gas phase increases, so does its amount absorbed in the liquid. Henry's law determines this absorbed amount [3].

(eq. 1)

where p is the gas partial pressure above the solution, x is the molar fraction of dissolved gas in solution and H is Henry's constant for the given gas. Henry's constant, and therefore solubility, depends on temperature. With increasing temperature, the solubility of gases decreases. The efficiency of absorption is affected by many factors [1]:

- *the large surface of the washing liquid*, which ensures perfect contact between the liquid and gas - a large surface of the washing liquid can be achieved by passing the liquid through the grids or by spraying the liquid on the droplets through the nozzles,
- *gas velocity* – this should be such that there is a good mixing of gas and liquid phases; if the speed is too high, the scrubber could be overwhelmed,
- *liquid injection rate* – efficiency increases with increasing injection rate; the amount of liquid that can be injected is limited by the dimensions of the scrubber; the optimal amount of liquid depends on the gas flow,
- *turbulent contact between phases*,
- *sufficient contact time*.

3.3 Scrubbing liquid

Scrubbing is done with water or organic liquid. When choosing a scrubbing medium, its properties must be taken into account.

a) Organic liquid

Most of the substances contained in tar are soluble in an organic liquid. Compared to water, organic liquid has a broader field of application. Scrubbing with this scrubbing liquid works on the principle of absorption. The suitability of using an absorbent medium depends on its

ability to reduce the dew point of tar and on its ability to work even at higher temperatures. The temperature of the gas leaving the scrubber should not fall below 75-80°C to prevent water condensation. If water condenses in the gas, it will infect the scrubbing liquid and disrupt the heat and mass flow of the scrubber (Baláš et al. 2014d). The organic liquid effectively lowers the dew point of the tar below the scrubbing temperature. However, the disadvantage is the relatively high cost of the liquid, which must be constantly replenished due to its evaporation. This loss of liquid by evaporation can be minimized using the lowest possible scrubbing liquid pressure (Baláš et al. 2014d). The suitability of the organic liquid used for scrubbing is assessed according to the following properties (Heymes et al. 2006):

- ability to absorb volatile organic compounds,
- low viscosity,
- high diffusion coefficient controlling the kinetics of absorption,
- low vapor pressure to reduce losses and prevent unwanted absorbent contamination.

During scrubbing, the organic liquid becomes contaminated and needs to be regenerated. The contaminated liquid can be fed back to the gasification reactor, thereby utilizing its chemically bound heat. Regeneration can be performed by thermal desorption. The opposite effect occurs in the desorber than in the scrubber. Part of the gasification air is sprayed with the contaminated liquid and saturated with tar vapors (Kubiček, 2005).

a) Water

Scrubbing with water, unlike organic liquid, works more on the principle of condensation. Only heterocyclic compounds and the highest polyaromatic hydrocarbons (PAH) can be eliminated by absorption (Baláš et al. 2014d). It is necessary to have a cold water source or a device for its cooling for scrubbing with water. The advantage is relatively economically undemanding operation. The disadvantage is the possible clogging caused by the formation of salt on the tip or inside the nozzles and tubes of the scrubber. The problem of gas purification with a water-based scrubber is the generation of environmentally unfavorable wastewater, which must be treated before being discharged into the environment, at least to the level specified by the limits for discharge into the sewer. Regeneration of contaminated water is a demanding process. Specific tar components are complicated to remove. Mechanical phase separation is almost impossible because the specific gravity of some tar components in the liquid phase does not differ much from the particular gravity of water (Baláš et al. 2014d).

4. Experimental setup

As part of the development, a new type of technological system for the purification and treatment of gaseous media was designed to ensure efficient purification of syngas produced by various technologies (gasification, pyrolysis, coking, etc.) from various raw materials under different operating conditions. Syngas can be used for treatment as input to cogeneration units. It is a compact design in a mobile or semi-mobile version

with an autonomous control system. The English name of the system is “Syngas cleaning and treatment system,” abbreviation SCTS. The resulting SCTS technological system will usually be part of a larger technological unit, used for thermal processing of biomass and agromaterials with subsequent cogeneration of electricity and heat. The system is designed as compact, mobile, and partially modular to allow the gradual expansion or replacement of some parts of the technology and auxiliary and support systems, including measurement and control. The SCTS technological system consists mainly of the following subsystems and it is shown in figure 1.

- removal of mechanical impurities,
- gas cooling,
- tar removal,
- removal of acid components,
- preheating of purified gas,
- storage tank for scrubbing solution,
- control system and monitoring.

For real applications, the classification and design of individual subsystems will be adjusted according to the requirements for individual applications. The decisive factors will be the quality and the quantity of syngas and the expected output of the cogeneration unit. The main operating parameters of the technological system will depend mainly on the power of cogeneration units behind the SCTS system and the quality of syngas. The power and configuration range of 30–1000 kWe of the cogeneration unit output is considered. It is assumed that the guaranteed parameter will be the amount of syngas processed according to a particular specification, with the proviso that the presence of oxygen is not considered in the syngas. For the design of apparatus, piping, and other calculations, a reserve of about 10% compared to the guaranteed parameters will be considered. The inlet syngas temperature is max. 300°C, the inlet syngas temperature does not exceed 40°C. The gas at the outlet from the SCTS technological system must meet the quality requirements set by the manufacturer of cogeneration units for gaseous fuel (Baláš et al., 2008e; Kubíček, 2005)

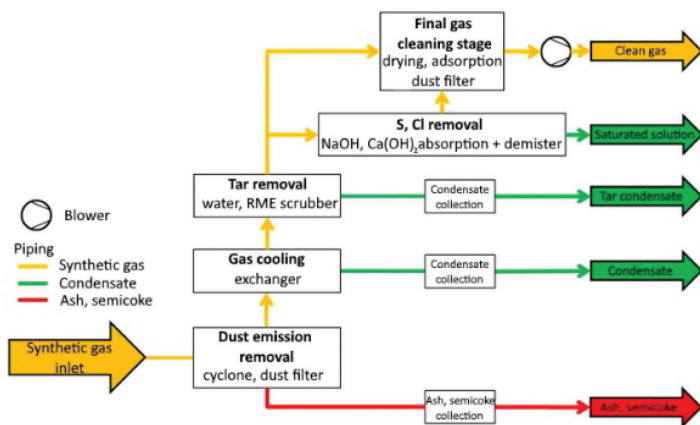


Fig. 1: Basic scheme of SCTS technology

4.1

Design of the pilot unit

A pilot unit with a 3.6 kg/hour gas flow was designed to verify the properties and the operating parameters. In particular, the critical step is the primary removal of particulate matter (PM) from the syngas source, which is usually a gasification reactor or pyrolysis plant. Dedusting of the gas is solved using a cyclone separator to separate particles above 5 μm or a filter with a suitable filter insert. In addition to secondary measures, minimizing the emission of solid particles from the reactor can also be solved by primary measures directly in the reactor, for example, by inserting a barrier, soothing zone, etc. However, high tar content in the gas increases the adhesion of dust particles, particularly in lower temperatures. Therefore, it is necessary to consider the inclusion of this process step concerning the properties of the syngas. Three subsequent critical technological operations are considered in the SCTS system:

- gas cooling,
- tar removal,
- removal of acid components.

The tar is removed in an absorption column. The choice of scrubbing liquid considers water or organic substances - mineral or vegetable oils, methyl ester of rapeseed oil, etc. The pump ensures the circulation of the scrubbing liquid from the storage tank of the scrubbing liquid; the tar fraction is collected in the storage tank. The tar-free gas then enters a droplet separator equipped with a demister. In lower gas temperatures, the cooling of the gas and the removal of tars and moisture can be carried out simultaneously in one absorption column. The last step of gas purification is adsorption in the adsorber with activated carbon. After saturation, the sorption material can be removed and the adsorber filled with a new or regenerated filling. The filter ensures the final flue gas purification. The blower provides the flue gas flow into the air conditioning system. The manufactured prototype unit is shown in Fig. 2.

4.2 Pilot tests

Pilot tests of the designed unit were carried out by connecting to three sources of syngas - a pyrolysis unit, a fixed bed gasifier, and a fluidized bed gasifier. This publication presents the conditions and results of measurements using gas from an atmospheric fluid generator. Since 2000, research into fluidized biomass gasification and sorted municipal waste is being carried out at the Institute of Power Engineering, Faculty of Mechanical Engineering, Brno University of Technology. Experiments are carried out on a fluidized atmospheric gasification reactor with a stationary fluidized layer called Biofluid 100, see Fig. 3. Starting-up the fluidized gasification generator to a steady state is carried out by way of combustion mode. The process temperature is controlled within the 750°C–900°C range by changing the fuel/air ratio. The average heating value of the generated gas ranges within 4 MJ/m³–7 MJ/m³, the content of solids is within the range of 1.5 g/m³ to 3 g/m³ and tar content is between 1 g/m³ to 5 g/m³ in relation to the fuel used and based on operating conditions.



Fuel is supplied from the bin equipped with a rake and is dosed to the reactor by a worm conveyor. Air compressed by the blower is supplied to the reactor under the grate as the primary air provides partial oxidation of fuel and maintains the fluidized layer. Air can also be supplied at two different height levels as secondary air and tertiary air. The produced gas is rid of particulates in a cyclone and then burned up in a burner fitted with a small flame holder burning natural gas and having its air supply. Ash from the reactor is intermittently discharged into ashbin by way of a specially designed travelling grate. To be able to investigate the impact of air preheating, an electric heater has been installed at the blower outlet. The form in which fuel can be supplied is limited mainly by screw conveyor dimensions and fuel moisture content. The optimum fuel moisture content is 20% to 30%. It is mostly wood shavings and small wood chips in woody biomass, size some 2 cm to 3 cm. For the experiments, spruce chips with a moisture content of 20% were chosen as fuel; the gasification temperature ranged from 780–800°C. The gas was taken after the cyclone at about 400°C, and before entering the unit, its temperature was adjusted to the required 300°C. According to the design condition, the gas flow through the unit was around 3.5 kg/hour.

Gas quality measurement was usually carried out in two ways. One consisted of online monitoring of gas composition with simultaneous gas sampling to gastight glass sample containers. The samples were subsequently analyzed using a gas chromatograph. Tar sampling was carried out in line with IEA methodology (Neeft et al., 2004) by capturing tar in a solution that was subsequently analyzed by gas chromatograph with a mass spectrometer.

5. Results and discussion

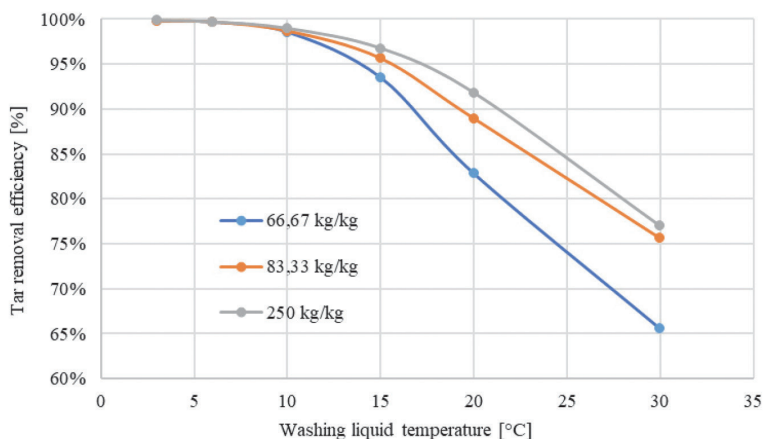
Tests were performed for the steady-state fluidized bed generator. The primary set condition was the fluidized bed temperature of 780°C during problem-free and stable gasification. At the same time, there is a higher proportion of tar in the generated gas. Other operating conditions, particularly the amount of fuel and gasification air fed, were subject to maintaining a constant temperature. The experimental work aimed to determine the efficiency of removal of contaminants from syngas depending on:

- Type of scrubbing liquid and their combination
- Scrubbing liquid temperature for three flow ratios
- The ratio of the flow rate of the scrubbing liquid

Gas samples were taken for 3 operating modes. Samples were taken simultaneously before the scrubbing (after the generator) and after the pilot unit. The effect of the scrubbing on the gas composition was tested. 3-4 gas samples were taken for each setting. The passage of gas through the wet scrubber pilot unit **does not affect the composition of the gas and its calorific value.**

5.1 Variant–water in both columns, temperature dependence

In this variant, a constant coolant flow (in this case, water) was set during the experiment. The dependence on the efficiency of conversion on temperature and the determination of the so-called breaking point of tar capture efficiency was monitored. To assess the difference in the content of individual tar compounds in the gas produced from different fuels, it was necessary to keep the temperature in the fluidized bed of the gasifier very strictly at 780°C, because the amount of tar is primarily most dependent on the temperature of the gasification reactions. The amount of tar before cleaning ranges from 3500–5500 $\text{mg} \cdot \text{m}_\text{N}^{-3}$ and after cleaning ranges from 6–1430 $\text{mg} \cdot \text{m}_\text{N}^{-3}$. Analyzes of tar compounds cover a relatively wide range of evaluated substances. It is unnecessary to distinguish the individual components to determine the scrubbing efficiency. Tar removal efficiency is shown in figure 4.



The following conclusions can be drawn from the results of the study of the use of water for tar washing and the influence of the temperature of the washing liquid:

- the tar removal efficiency of 99.7 % was achieved utilizing scrubbing,
- as expected, the highest efficiency is for the lowest temperatures,
- for low temperatures (3, 6, and 10 °C), there is no flow dependence of efficiency,
- for low temperatures (3, 6, and 10 °C), the resulting tar concentration is at an acceptable value around $50 \text{ mg} \cdot \text{m}^{-3}$.

5.2 Variant–RME in both columns, temperature dependence

In this variant, a constant coolant flow (in this case, RME) was set during the experiment. The dependence on the efficiency of conversion on temperature and the determination of the so-called breaking point of tar capture efficiency was monitored. The following conclusions can be drawn from the results of the study of the use of RME for tar washing and the influence of the temperature of the washing liquid – see Fig. 5:

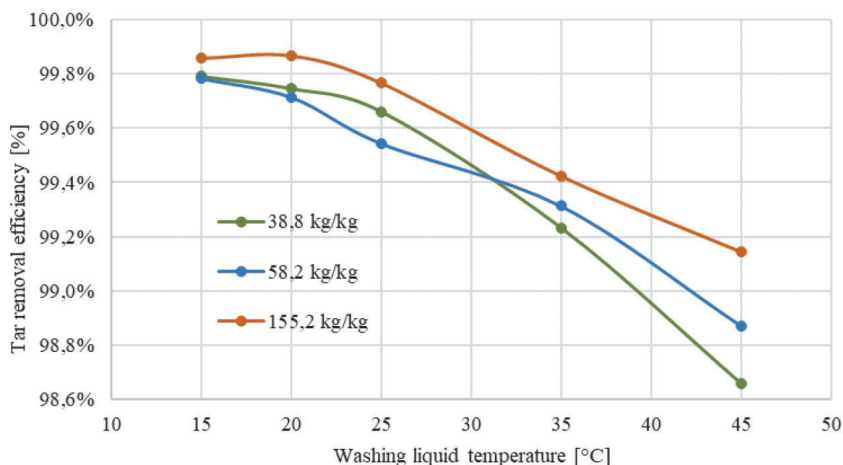


Figure 5: Dependence of tar removal efficiency on scrubbing liquid temperature-RME.

- the efficiency of the RME scrubbing reaches values of up to 99.9 %,
- scrubbing efficiency is high (99.9–98.7 %) in the whole measured temperature range (15–45 °C),
- the efficiency of scrubbing is relatively independent of the mass flows ratio of oil to gas for defined flows,
- tar concentrations for oil temperatures of 35 °C and lower are below $50 \text{ mg} \cdot \text{m}^{-3}$,
- the tar concentration for the highest examined temperature is around $100 \text{ mg} \cdot \text{m}^{-3}$,
- at the highest scrubbing temperature, the dependence of the efficiency on the mass flow rate is apparent (albeit minimal).

5.3 Variant–water in both columns, flow dependence

In this variant, a constant coolant temperature (in this case, water) was set during the experiment. The dependence on the conversion efficiency on the coolant flow and the determination of the so-called breaking point of the tar capture efficiency with respect to the amount of scrubbing liquid - water, was primarily monitored. Most experiments were performed to test the effect of the amount of scrubbing liquid on the efficiency of gas scrubbing from tar. The results can be summarized as follows (see Fig. 6):

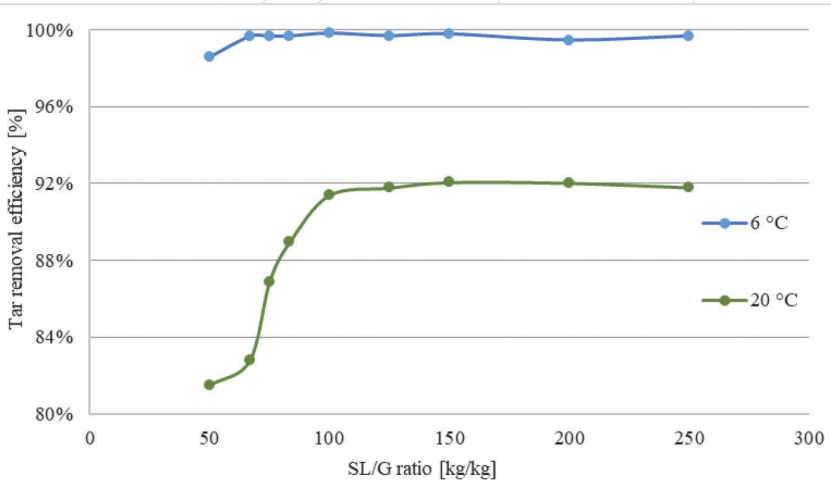


Figure 6: Dependence of tar removal efficiency on the flow of washing liquid-water

a) for temperature 6 °C

- the flow rate of the scrubbing liquid has almost no effect,
- tar elimination efficiency is high 99.7 %
- the effect is visible only for the lowest flow rate when the efficiency drops to 98.6 %,
- the final tar concentration is below $50 \text{ mg} \cdot \text{m}_n^{-3}$

b) for temperature 20 °C

- in the flow range of 50 kg/kg to 100 kg/kg, the efficiency is dependent on the washing liquid flow with almost direct proportionality,
- in the flow range of 50 kg/kg to 100 kg/kg, the efficiency is between 81.5 and 91.4 %,
- from the ratio of scrubbing liquid to gas 100 kg/kg and above, the efficiency is almost constant with an average of 91.8%,
- the resulting concentration of tar content increases with decreasing liquid ratio to gas from about $330 \text{ mg} \cdot \text{m}^{-3}$ to $1265 \text{ mg} \cdot \text{m}^{-3}$.

5.4 Variant–RME in both columns, flow dependence

In this variant, a constant coolant temperature (in this case, RME) was set during the experiment. The dependence on the conversion efficiency on the coolant flow and the determination of the so-called breaking point of the tar capture efficiency with respect to the amount of scrubbing liquid - RME, was monitored.

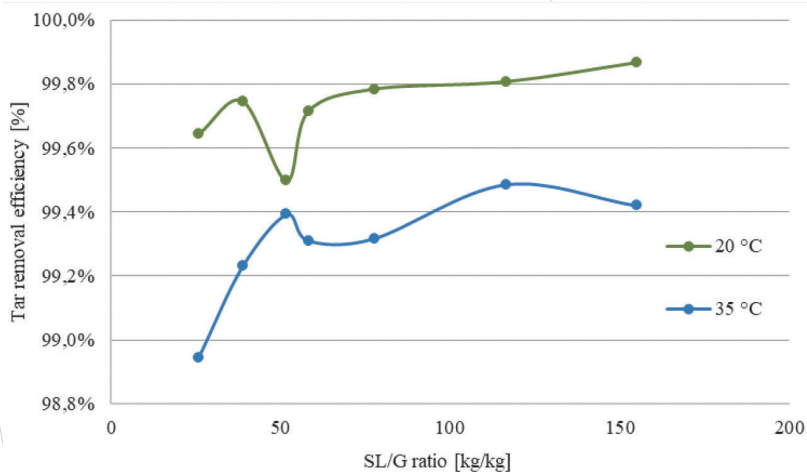


Figure 7: Dependence of tar removal efficiency on the flow of scrubbing liquid-RME.

Scrubbing with rapeseed methyl ester is very effective throughout (see Fig. 7):

- except for the lowest oil to gas ratio of 25.87 kg/kg for a temperature of 35 °C, the efficiency is above 98.9 %,
- the resulting tar concentrations in the gas after purification at 20°C are below $20 \text{ mg} \cdot \text{m}^{-3}$,
- the resulting tar concentrations in the gas after purification at 35°C are around $50 \text{ mg} \cdot \text{m}^{-3}$ (except for the lowest SL/G ratio).

6. Conclusions

A series of tests were performed to verify the scrubbing capabilities of the pilot unit. Two scrubbing liquids were tested - water and rapeseed methyl ester. The scrubber has been tested for several constant temperature settings and different flow rates at constant temperatures. The measurement results are discussed in detail in section 5, but in summary, the main conclusions are as follows:

- both liquids have a high scrubbing ability and can be used to eliminate tar impurities from the gas,
- high efficiency of tar elimination is achieved in water at temperatures close to 0 °C, during the highest degree of condensation. Under these conditions, even a minimal amount of scrubbing liquid can be used; there will be a significant reduction in

- gas humidity at such low temperatures,
- for RME, where the main principle of tar elimination is absorption, higher scrubbing liquid temperatures can be used with high efficiency, when for residual tar concentrations up to $50 \text{ mg} \cdot \text{m}^{-3}$, it is possible to use scrubbing with a temperature of 35°C , or even higher,
- higher scrubbing liquid flows have any effect only at higher scrubbing liquid temperatures,
- the worst efficiency of the scrubber is for the gas with the lowest input concentration of impurities; it is necessary to examine whether the low efficiency was not the result of the specific composition of the tar.

In conclusion, it can be stated that the pilot unit of the scrubber removes tar components with high efficiency and achieves the required parameters. Further research should be focused on optimizing the operation and management of waste liquids.

7. Acknowledgments

This research was financially supported by the Brno University of Technology, Faculty of Mechanical Engineering in frame of the Specific Research Fund, grant no.: FSI-S-20-6280.

8. References

Baláš, M., Lisý, M., Pospíšil, J. Steam Biomass Gasification - Effect of Temperature. Applied Mechanics and Materials, 2016a, no. 832, p. 49-54. ISSN: 1662-7482.

Baláš, M., Lisý, M., Kracík, P., Pospíšil, J. Municipal solid waste gasification within waste-to energy processing. MM Science Journal, 2017b, vol. 2, no. 2, p. 1783-1788. ISSN: 1805-0476.

Baláš, M., Lisý, M., Moskalík, J. Biomass Gasification: Gas for Cogeneration Unit . WSEAS e- journal Energy and Environment, 2008c, vol. 1, no. 4, p. 203-210. ISSN: 1790- 5095

Baláš, M., Lisý, M., Skála, Z., Pospíšil, J. Wet scrubber for cleaning of syngas from biomass gasification. In: Advances in Environmental Sciences, Development and Chemistry. Santorini, 2014d, s. 195-201. ISBN 978-1-61804-239-2

Baláš, M., Lisý, M., Moskalík, J. Biomass Gasification: Gas for Cogeneration Unit . WSEAS e- journal Energy and Environment, 2008e, roč. 1, č. 4, s. 203-210. ISSN: 1790- 5095.

Bridgwater, A., V. The Technical and Economic Feasibility of Biomass Gasification for Power Generation. Energy Research Group, Aston University, Birmingham, (1995) Fuel Vol.74 -No. 5

Chojnacki, J., Najser, J., Rokosz, K., Peer, V., Kielar, J., Berner, B. Syngas Composition: Gasification of Wood Pellet with Water Steam through a Reactor with Continuous Biomass Feed System. *Energies* 2020, 13, 4376. <https://doi.org/10.3390/en13174376>

Heymes, F., Manno-Demoustier, P., Charbrit, F., Fanlo, J., Moulin, P. A new efficient absorption liquid to treat exhaust air loaded with toluene. *Chemical Engineering Journal* [online]. Elsevier, 2006, (115), 225-231 [cit. 2018-04-06]. DOI: 10.1016/j.cej.2005.10.011. ISSN 1385-8947.

Kubíček, J. Mokré čištění energoplynu před jeho využitím ve spalovacím motoru. Brno, 2005. Disertace. Vysoké učení technické v Brně, Fakulta strojního inženýrství.

Milne, T. A., Evans, R. J., Abatzoglou, N. Biomass Gasifier „Tars“: Their Nature, Formation and Conversion, NREL/TP-570-25357, Colorado, USA, (1998)

Neeft, J. P. A., H.A.M Knoef, U, Zielke, Simell, P., Guideline for Sampling and Analysis of Tar and Particles in Biomass Producer Gases. Energy project ERK6-CT 1999-2002, www.ecn.nl/docs/library/report/2003/c02090.pdf

Web references

[1] Wet scrubbers for gaseous control. United States Environmental Protection Agency [online]. 2018 [cit. 2018-02-24]. Dostupné z: https://www3.epa.gov/ttnchie1/mkb/documents/Other_B.pdf

[2] Čištění plynů. Fakulta životního prostředí: Univerzita J. E. Purkyně v Ústí nad Labem [online]. Ústí nad Labem: FZP, b.r. [cit. 2018-03-19]. Cited from: http://fzp.ujep.cz/ktv/uc_texty/pt3/13%20Cisteniplynu.pdf

[3] Rostoky: Raoultův a Henryho zákon. Informační systém Masarykovy univerzity [online]. Brno: Masarykova univerzita, 2018 [cit. 2018-04-09]. Cited from: https://is.muni.cz/do/rect/el/estud/prif/js11/fyz_chem/web/idealni/roztoky.htm

Filtration of hot process gases as a key step towards larger industrial uptake of gasification technologies

Mateusz Szul¹, Tomasz Iluk¹, Jarosław Zuwała¹,

¹ Institute for Chemical Processing of Coal, Zabrze (Poland)

1. Abstract

Dedusting of hot gases, when performed on barrier filters (bag and rigid), is often perceived as the best first step in process gas conditioning. Where bag filters provide good stability of operation and ensure high reliability, their material and hence temperature limitations will never allow for integration with other high-temperature gas cleaning methods (adsorption/conversion). On the other hand, unparalleled filtration efficiency, opportunities for process intensification and simplification, stem from the development of rigid filters operating at 300 – 1200°C. This article presents process conditions of high-temperature filtration, which influence stability and reliability issues in the dedusting of process gases. The influence of filtration temperature, filter design and selection of filter materials were considered to determine conditions leading towards the failure of filter integrity or loss of filtration stability. Non-exhaustive list of guidelines and good engineering practices useful for the development of future hot gas filtration systems is herein presented.

Keywords: hot gas cleaning; high-temperature filtration; ceramic filters; metallic filters; operational issues

2. Introduction

Modern, highly efficient solutions concerning power generation, fuel production or other processes based on the physicochemical conversion of fuels are still mainly based on combustion, pyrolysis or gasification processes. On the road towards the circular economy and decarbonization of industrial, gasification and pyrolysis are leaping forwards as the most suitable methods to convert the waste and biomass feedstocks into useful chemical and fuels. Most often thermochemical conversion is the central point of any given process. However, the products of conversion, still need to be subjected to separation, cleaning or upgrading to attain high value or for the process to be efficient and environmentally friendly. Thus, gas cleaning and product upgrading methods cannot be treated with a lesser importance. In most cases, the post-conversion products demand firstly to be separated at the highest possible temperatures. For this reason, hot gas dedusting is the most often encountered as the first step in the gas treatment train. Power generation in Pressurized Fluidized Bed Combustion (PFBC) and Integrated Gasification Combined Cycle (IGCC) applications were the first, very demanding drives for the development of stable and efficient methods for HT dedusting of gasses (Heidenreich and Wolters, 2004). In both

cases, the processes demanded to deeply dedust the gases to minimum concentration levels (preferably below 5 mg/Nm³) at temperatures in the range of 300 – 1200°C. First HT dedusting methods focused primarily on robust, inertial devices and involved mainly settling chambers, cyclones, multi cyclones, or later electrostatic precipitators (in rising order of separation efficiency, Fig. 1). All methods listed above still proved to be unsatisfactory. In the development of appropriate HT particulate removal solution, such parameters as low differential pressure (dP), high range of operational temperature or resistance to thermal and chemical shocks were considered as the most important criteria. The answer was sought in the use of rigid ceramic filters and thus almost 40 years ago, the first systems started to be developed. Today filtration technologies reached technological maturity in both high temperature (>300°C) and moderate applications (<300°C) were respectively rigid and fabric filters find their applications (Tarleton, 2015).

Filtration based on particle separation methods utilized physical filtration mechanisms occurring mainly through surface or in-depth filtration on filter cakes that gather on the surface of the filter. Materials and methods applied in the production of HT filters provide required resistance to high pressure and temperature, while at the same time, allow the filtration surface to be regenerated. In commercial systems, HT filters can operate at pressures and temperatures resp. up to 80 bar and 1200°C. The first materials developed for the purpose of HT filtration were mainly based on ceramic sintered media. Throughout the years, ceramic filters have developed unparalleled chemical and thermal attack and shock resistance while simultaneously providing satisfactory filtration efficiency. Later, new filter media started to be developed for even better filtration efficiency, improved regeneration properties, lower pressure drop, a better overall stability of filtration processes and integrated operation (structured, multilayer, catalytically active etc.). Nowadays, while developing a HT filtration unit one may choose from a range of filters manufactured from pleated sheets of metallic filaments or sintered metallic powder granules as well as from a variety of ceramic filters (Heidenreich, 2015).



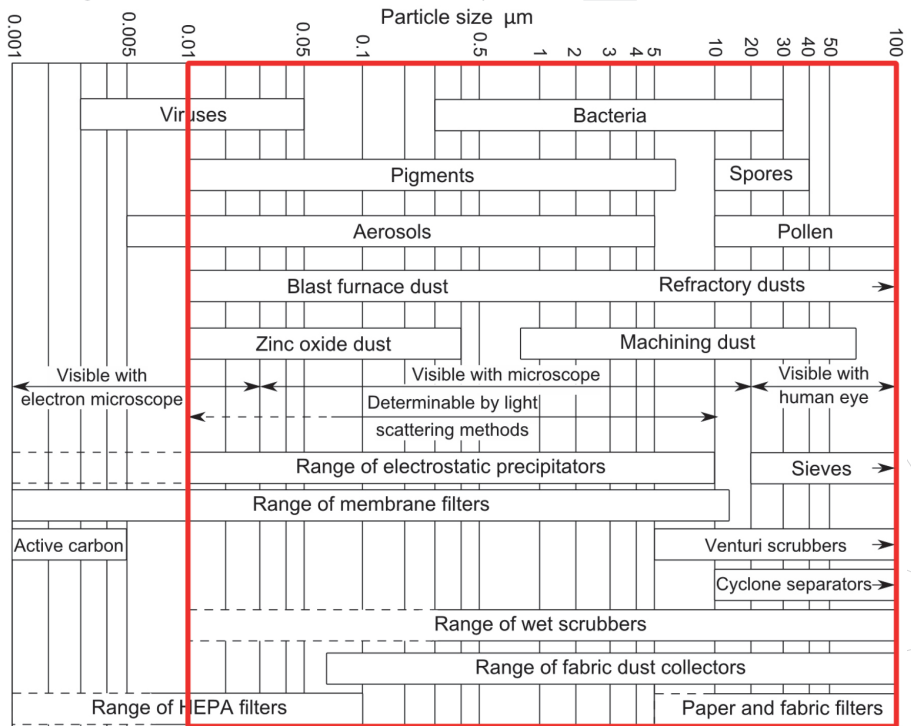


Fig. 1: Comparison of the size of particles/pollutants and the methods of their removal

From a process standpoint, it is essential to retain the useful HT heat while cleaning the gas. In HT conditions, the gas remains dry, regarding both water and organic contaminants. This is necessary to keep the filtration stable but can also be used to clean the gas from contaminants or convert them. Thus, dedusting of HT process gas allows to avoid problems of fouling of the apparatus and the risk of damage to moving parts of the installation, such as pumps, turbine blades, valves, but also nowadays provides an opportunity to clean the gases.

As mentioned above, fabric filters (PTFE and glass bags) were successfully applied in the filtration of process gases at moderate temperatures (Schmid et al., 2017). They ensure supreme operational stability and ease of maintenance, however, demand prior recovery of heat and unfortunately preclude or disadvantage most hot gas cleanup and conversion methods (adsorption, catalytic conversion). For these reasons a HT filtration system, based on rigid filter candles was developed and optimized within research conducted by ICHPW. This article presents the experience gained from the operation of a pilot-scale gasification system integrated with a HT gas filter. During the study, know-how and operational experience on all the above-mentioned types of filter media have been developed in conditions reflecting a real process environment. This text introduces operational tips and procedures as well as grounds for a better understanding of phenomena occurring at HT

filtration and provides guidelines for the development of future filtration systems.

3. Construction and operation of hot-gas filters

3.1 Principle behind the development of hot-gas filters

The general method of operation and construction of candle filters used in gasification systems is alike to bag filters. However, due to the operation at temperatures up to 1200°C and at pressures up to 80 bar, the filters have slightly different structure and use different construction materials. Vertically mounted candle filter systems make up the vast majority of designs used in industrial-scale; however, ceramic cylindrical filters also exist. Similar to bag filters, the candles are grouped into sections, which allows them to be cleaned sequentially. In high-pressure applications, cylindrical filter bodies are additionally lined with a layer of lining, while for most atmospheric systems, rectangular bodies are used, which lowers their investment costs. To avoid the problems of a limited number of filters that can be placed in one tube sheet, e.g. In the 1980s, Lurgi Lentjes Babcock and Westinghouse presented the construction of multi-level filters, the so-called multistage filters. Filters of this type worked, among others in Berrenrath (Germany) and Puertollano (Spain) (Heidenreich, 2013). The advantage of filters with a single sieve shelf is that they can be operated and repaired from the top by removable domes on the clean side of the filter and service hatches. Their limitation, however, is the small number of filter (which leads to lower filtration surface – m^2) that can be installed on a given surface of the installation (vessel footprint). Filtration with the use of candle filters usually takes place on their outer side, and the dust-free gas is recovered from their center. When operating at temperatures above 700°C, the filters often have internal ceramic linings that play a role similar to that in gasification reactors. In high-pressure applications, the lining allows using smaller thicknesses of the filter body and insulation. A basic problem associated with such filters is a large problem of adequate heating and susceptibility to damage related to heating and cooling cycles. Ceramic filters operated at temperatures above 700°C find their niche mainly in IGCC systems, and some research reactors where the filter is integrated with the gasification reactor. In most cases, gasification reactors produce gas at a max. the temperature of 850°C, which theoretically allows for its direct dedusting with the use of ceramic filters.

3.2 Operational window – upper-temperature limit

It is important to note that, in particular in biomass and waste gasification installations, the impact of heavy tar substances contained in the gas and minerals with a low condensation temperature, which are released from the ash in the reactor, often cause operational problems of filters (condensation and effective blocking of pores, impervious highly viscous layers of filter cakes). For this reason, before the candle filters, the process gas is often cooled, preferably quenched, with the use of adiabatic coolers (injection of e.g. water) or radiation coolers. As a rule, most of the minerals contained in the gas and showing a tendency to condensation constitute the same group of compounds causing problems with the fouling of steam superheaters in power boilers. The second abovementioned issue is the characterization of heavy tars, which may show a tendency to coking upon contact with the filter material. This disadvantageous feature is influenced by poor gasifier design

and operation as well as the chemical composition of the filter, which may exhibit a low catalytic activity towards the decomposition of tar compounds. Thus, based on the fuel analysis and the reactor characteristics, the upper operating temperature of the candle filter should be determined. Even though the ash chemistry and operational regime of the gasifier can give insights into the upper-temperature limit of filter operation, unfortunately, the most adequate remain experimental runs.

In the filtration process, the pressure difference between the clean and dirty side of the filter is of primary importance and it results to a large extent from the thickness and porosity of the filter cake. The value of the pressure drop on the filter does not only affect the selection of draft fans and its associated operating costs. In hot gas filtration, it also has a particularly significant influence on the stability of the filtration process itself. Since under high-temperature conditions many particles tend to form compressible filter cakes, their filtration leads to higher pressure drops. Moreover, at a higher temperature, the structure and porosity of the cake may change due to varying action of the adhesive and cohesive forces. For example, it was shown that the cake from the filtration of lime, quartz and bark ash showed higher porosity at higher temperatures than at ambient temperature (Hemmer, 2002). On the other hand, fly ash from coal combustion showed no change in cake porosity with increasing temperature (Hoff et al., 2008; Hurley and Dockter, 2003).

3.3 Characteristics of filtered particles

The literature describes methods that characterize the ceramic filter's operating window based on the analysis of the physicochemical parameters of the filtered dust. The two most discussed methods are dilatometry, high-temperature rheometry and TGA (Zimmerlin et al., 2008). However, their effective use requires having a filtered dust sample, preferably obtained from the specific reactor, fuel, and under optimal plant operating conditions. The softening point of filtered solids depends on their chemical composition. In general, ashes containing chlorides in their structure, such as NaCl, KCl or CaCl₂, tend to be problematic (Heidenreich, 2013). Filtration of dust with viscous properties not only leads to unstable filtration and problems with filter regeneration, in extreme situations it can also lead to the so-called filter cake bridging. This phenomenon is caused by incomplete regeneration of the filter elements and the continuous increase in the thickness of the cake and is visible especially in the upper part of the filters. It can lead to the formation of dead zones of the filter as well as to the breakage of the elements. The primary measure of the probability of bridging is the tensile strength of the filter cake, as a function of temperature. However, it was also determined that the tensile strength ratio related to its density as a function of temperature provides a better approximation. This parameter was called the Critical Thickness Index (CTI) (Hurley and Dockter, 2003). High values of CTI indicate that the ratio of the mechanical strength of the cake to its mass is high, which promotes bridging. In addition, hot gas filtration especially processes gas, which contains high loads of tars can lead to reactions on the surface of the filtered solid, which significantly affect the properties of the filter cake formed. Inter alia it was shown that in the CO₂ atmosphere, the filtration characteristics of limestone changes (Kanaoka et al., 2001; Kanaoka and Kishima, n.d.) and it is possible to have temperature windows in which the filtration of given dust takes place in a stable or unstable manner.

3.4 Operational window – lower temperature limit

In the case of the lower operating temperature of process gas filters, is limited to the temperature where condensing, very heavy organic compounds can lead to blockage of the filter. Laboratory measurements of the tar composition in the gas are limited to the detection capabilities offered by gas chromatography. Gravimetric tars contain compounds that are too heavy to be evaporated and analysed. It was also noticed that these compounds often show a tendency to coke before reaching the boiling point, which indicates their multi-ring structure and the content of active centres containing available hydroxyl, carbonyl groups or double bonds. It is also important that the available models approximating the value of the tar condensation point are based on the heaviest qualitatively and quantitatively analysed compounds. From the literature, it is known that the most often measurements indicate that the point of condensation of tar in the gas falls between the range of 200 – 250°C. However, in our studies, we also observed cases where condensation and coking of tars were visible on surfaces maintained at temperatures higher than 350°C. Another proof of the low precision of such determination is the fact that operation of HT filters parallel to dedusting leads also to a small reduction of the number of tars. This means that the process gas at the outlet of the filter contains less tar than at its inlet, and this difference is generally due to a slight decrease in the number of gravimetric tars. Till this point, the best indicator of the lower operating limit of a filter is the knowledge of the gasifier and the fuel with which the device will work. With a high degree of generalization, the operating point of 350°C is often assumed as the generally safe lower operating point of HT filters.

3.5 Filtration efficiency and reliability – fixing method

Due to the operating conditions, the candle filters are mounted in the tube sheet with the use of fastening plates. Metal tapes or spring clamps are not used here. To ensure the tightness of the connection and to protect the flanges of the filters, ceramic felt gaskets have used that match the structure of the filter flange (flat flanges or conical flanges). The pressure of fastening plates and their stability is maintained by using bolts or wedge connections. In each case, the selection of appropriate materials and forces is of great importance to avoid damage to the filters and the fastening system. The main problem here is a deformation of threads resulting from thermal expansion of steel and uneven distribution of pressing force resulting from deviations in the standard dimensions of the flanges of candle filters. The solution to the problem of clamping the filters is the use of expensive, high-temperature clamping nuts equipped with a set of screws tightened with low torque.

4. Filtration media

Filter materials for HT dedusting of process gases need to allow continuous operation in reducing, chemically reactive conditions at temperatures exceeding 500°C. Moreover, must show high resistance to temperature and mechanical shocks, while being resistant to chemical attacks from H_2S , COS , CS_2 , HCl , HBr , HF , NH_3 , tar (polycyclic heterocyclic, alcohols, aldehydes, ketones, acids) and chemically reactive ashes (alkalis). In such conditions, only rigid, ceramic or metal filter are used. Hot gas filtration in industrial systems is usually carried out on candle filters (in laboratory conditions also flat) and usually takes place on their outer surface. Depending on the material, the length of the filters ranges from 1 – 3 m

process gas reducing atmosphere (“Schumalith® Filter Elements - Pall Shop,” n.d.).

4.2 Metallic filter media

A niche among the materials used for hot gas filtration are filters made of sintered metal. Such filters are also built based on fibres and powders, but there are also filters where the metal non-woven fabric is applied as the filtration medium. Sintered powder filters are made in a similar way to ceramic powder filters and their porosity reaches 20 – 40%. On the other hand, the production of metal fibre filters uses the drawing process which boils down to a gradual reduction of the diameter of metal wire down to the size of approx. 2 – 40 µm. Then the wire is cut into sections of about 20 – 25 µm and braided into a net that can be sintered similarly to powders. By rolling, the final thickness of the web is formed, which controls its porosity. After sintering, the fabric is welded on top of a filter cage, which ensures the necessary mechanical strength of the filters. In this method, it is possible to produce filters with 85% porosity. In the case of metal filters, there is also a very wide range of applicable materials. However, when selecting the alloy, it is essential to consider all the related issues: atmosphere, process conditions and ash characteristics, as corrosion of the filter can lead to both clogging of pores and disruption of filter continuity. In processes with operating temperature not exceeding 420°C, filters made of stainless-steel alloys are used. However, the maximum application temperature of heat-resistant steels is 650°C. In the case of gasification systems, the use of duplexes such as Inconel 600®, Monel®, Hastelloy X® or HR 160® is also justified by the presence of sulphur and chlorine in the gas. For gases with a significant share of sulphur, filter media are specifically doped with aluminium which passivates during annealing under oxidative conditions (e.g. FeCr and FeAl alloy). Iron-aluminium alloys are applied up to a maximum temperature of 780°C and chromium-iron-chromium even up to 1000°C (“Mott Corporation - Filtration and Flow Control Engineering,” n.d.).

4.3 Opportunities for further process integration

Due to the method of preparation of candle filters and their operating conditions, the possibility of using them as a surface for catalytic gas purification processes is currently broadly investigated. In such a way, multifunctional filters have been developed mainly for NO_x and dioxins removal process from exhaust gases in SCR processes. On the other hand, concerning gasification systems, the construction of a filter enables simultaneous cracking of tar thanks to the use of particles coated with Ni. There are three basic methods of activating the multifunctionality of the filter in this regard. The first is the application of the catalyst to the surface of the inner layer of the filter during its production process. The second is the introduction of special foam cores which convert the gas just after the separation of solids. The third option is an application of a reactor upstream of the filter, and thus enable long contact times, good mixing properties and perfect separation of the sorbent/catalyst as well as ash particles. All the above-mentioned concepts can be realized while maintaining the process temperature in the range of 800-850°C. In such a reactive filter system, the possibility of reducing tar substances up to 94% was previously proven (Rhyner, 2013).

5. Regeneration process

5.1 Idea and operating conditions of a conventional regeneration system

In the case of HT candle filters, the only industrially used cleaning method is back-pulsing. Structurally, these systems do not differ significantly from solutions known from bag filters. The difference between the application of filter pulsation systems in bag and candle filtration is their much lower regeneration efficiency due to the rigid, thick walls of the filters. Where in bag filters the pressure pulse leads to deformation of the surface of the bag, and acceleration of the filter surface leads to dislodging the filter cake, rigid filters cannot change their shape during the propagation of the pulse pressure wave, thus here regeneration takes place only due to induced local pressure difference between the clean and dirty side of the filter. In candle filters, the kinetic energy of the pulse stream and the sucked clean process gas changes into the static pressure inside the filter. This overpressure between the clean side of the regenerated filter and its dirty side causes the filter cake to dislodge. The energy of the pressure pulse in candle filters is additionally dispersed inside the structure of the filter medium, which further inhibits the regeneration process. Standard pressure in the tank is within the range of 5 – 10 barg for non-pressurized installations and should be min. twice the pressure in the system operating under pressure, i.e. with gasification at 20 bar, the pressure of the pulsating system should be min. 40 bar. The dominant parameters responsible for the effectiveness of the system are the gas velocity at the nozzle outlet, its mass flow and the geometry of the system itself (pressure losses on the flow and unequal distribution between filters in sections). The upper limit of the speed of the gases leaving the pulse nozzles is the speed of sound, above which, the energy of the jet exiting the nozzle drops due to cavitation.

Commonly used conventional pulse-type systems used to regenerate candle filters operate by the principle of a nozzle directing a stream of compressed gas through a Venturi tube into the interior of the filter. A schematic representation of the filter operation and regeneration is shown in Fig. 2. The purpose of the Venturi is to create a low-pressure zone on the clean side of the filter and to use the additional volume of process gas to clean the filtration area. However, their effectiveness in conjunction with rigid filters is often debated (Rhyner, 2013).

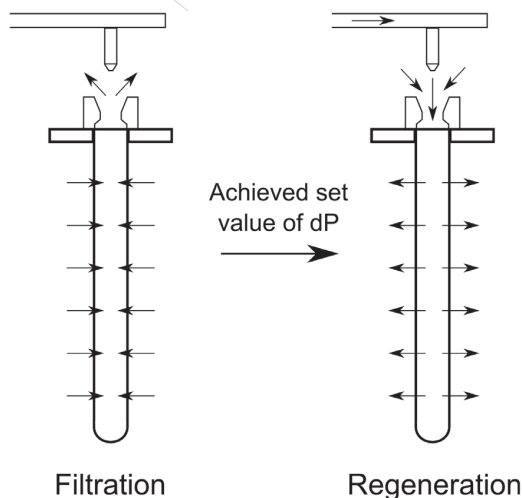


Fig. 2: Idea behind operation and regeneration of the typical rigid hot-gas filter

5.2 Reasons and solutions for low regeneration efficiency – temperature of the pulse gas

The biggest operational problem connected with the use of rigid filters is incomplete regeneration of their filtration surface, which leads to a build-up of pressure drop. Reasons for this can be sought in filtration of very fine dust, sticking of the cake to the surface of the filter, as well as in insufficient efficiency of the pulsing method. Another problem is that the temperature of the gas used for pulsation is significantly lower than that of the filtered gas. Therefore, the injection of cold pulsing gas leads to cyclical thermal shocks of the filter and may cause local condensation of tars contained in the gas, coking of the tar particles inside the filters and finally their blockage. This problem can often be partially resolved by mixing cold pulsed gas with warm clean process gas sucked in through the Venturi nozzles, thus providing slight heating of the pulsing gas. The second method is to use pulse-back systems with significant thermal ballast designed to preheat the pulsing gas. Such configuration can unfortunately adversely affect the distribution and peak values of the pulses. The best solution for this problem is preheating the pulse-back gas. However, this method is seldomly used in commercial application as it is limited by the materials used for the construction of the pulse valve (maximum 160°C) or demands the application of specially devised quick-acting high-temperature valves. A number of technical difficulties stem from such operation, i.e. the following can be listed: low tightness (loss of pulse gas and dilution of process gas), larger footprint of the valves, lowered peaks of the pulse, lower pressure of the gas reservoir, excessing mechanical stresses, noise, and vibrations.

5.2 Reasons and solutions for low regeneration efficiency – increasing efficiency of the regeneration system

To resolve the above-mentioned problems, a solution directly connecting the regeneration system to the clean side of the filters was also proposed. The pulse back system is cut off from the filter space with pulse valves, and the pulse gas is fed directly from the tank to the inside of the filters through porous ceramic pipes. Opening the pulse back valves

build overpressure in the entire clean part of the filter, which results in a more complete regeneration even when using lower regenerative gas pressures (1 – 2 bar_g).

This method also uses additional total filters located on the clean side of the filter. They serve as protection against undesirable ingress of dust to the clean side of the filter, which may occur as a result of damage of the filter element or too aggressive regeneration (Heidenreich et al., 2013, 2002).

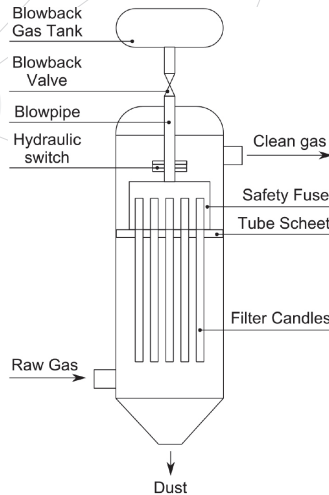


Fig. 3: Schematic diagram of a hot gas filter designed with a CPP regeneration system (Pall)

Another strategy to increase the efficiency of regeneration of rigid filters is sought in redesigning the filter and using the dirty gas stream as a mean to dislodge the filter cake or limit its built-up. Fig. 4 presented below, depicts the idea of feeding the dirty gas coaxially, directly into the outer wall space of the filter, supports blowing off the cake as well as its gravitational fall. In the event of favourable process conditions, this modification may even lead to "automatic" cleaning of the filter surface, and significantly reduce the frequency of necessary pulsations (Sharma et al., 2013, 2010). This system has been tested, inter alia, in conjunction with cyclones, with and without a pulsed system, and with additional internal gas recirculation to increase the local gas velocity at the inlet and the shear forces acting on the filter cake. However, such methods were not demonstrated in large industrial conditions. The reason might lie in the fact that the effectiveness of this method is high, only in the case of favourable physicochemical parameters of filtered solids, i.e. a low tendency to create dense, sticky filter cakes.

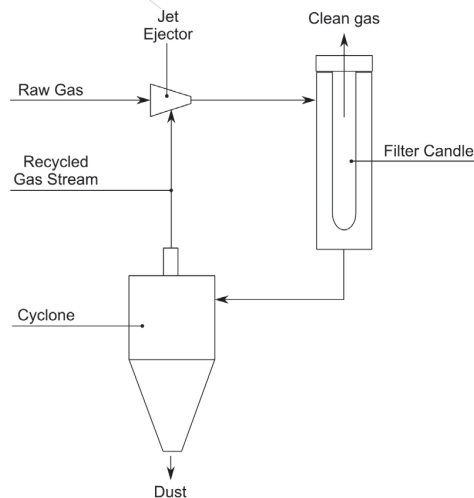


Fig. 4: Schematic representation of a concept using process gas to maintain a stable layer of filter cake

Subsequently, some methods should be treated as supplementing the main pulsing system. These include, among others mechanical and ultrasonic methods, which are often used in the operation of low-temperature bag filters. However, due to the nature of the gasification process, they find very limited application possibilities.

6. Conclusions

To this day market potential of ceramic filters depends on many factors, from which the following two should be treated as main: development of integrated hot-gas cleaning methods and the development of reliable, applicable for all types of filtered solids filtration and pulse-back systems. All the above mentioned also depend on the rate of market uptake of Waste and Biomass to Chemicals and Fuels technologies. For the past decade, in all large-scale, high Technology-Readiness-Level applications connected with gasification (but also pyrolysis), process gas filtration with the use of a bag or rigid filters predominated. Unparalleled filtration efficiency and opportunities for process intensification and simplification, boost their status as the best option for the first stage of process gas cleaning. Where bag filters provide good stability of operation and ensure high reliability, the material and hence temperature limitations will never allow to integrate them with other HT gas cleaning methods (adsorption/conversion). On the other hand, recent developments in the design of rigid hot-gas filter elements (multilayer, active filters) and highly integrated pave the way for the change in market view on the usefulness, and applicability of HT rigid filters.

Throughout the past decade, IChPW developed gasification and gas cleaning systems. The following information was herein gathered and compiled to increase the availability of knowledge on good engineering practice and operational experience connected with the use of hot gas rigid filters.

In terms of the design and selection of components included in the pulse regeneration system, experience is mainly based on bag filters. No gold standards were obtained so far for rigid filter and thus one needs to take into account the different characteristics of the filter medium. The following information applies to typical, conventional back-pulse systems:

- use pulse solenoid valves with a diaphragm with dimensions of min. 1 ½ ”(DN40),
- implement a cleaning sequence control system, which will clean sections at random, one section at a time, maintaining a gap of min. 2 – 3 rows, and time interval of min. 60 s,
- manage the operation of the filter regeneration system through the controller and the signal from a dedicated differential pressure sensor,
- install a digital pressure transducer in the air manifold,
- install the cabinet with pneumatic controllers for the pulse valves as close as possible, pref. length of lines <2m (ATEX),
- clean a maximum of 10 – 15 filters in one series,
- set the duration of pulse to 200 – 400 milliseconds,
- Regarding the design of the filter housing, its construction, distribution of nozzles and applied dust collection devices, it is advantageous to:
- control the temperature of the gas at the filter inlet (adiabatic cooling, heat removal by radiation or membrane coolers with soot blowing),
- use gas distributors at the inlet, homogeneously distribute the stream and direct it from the top-down to limit the re-entrainment of dust from filter regeneration,
- use two-layer insulations resistant to high temperature, hydrophobic and air-tight,
- use a trace heating system to eliminate temperature losses, for start-ups and pauses in operation (eg. electric trace heating),
- use a hopper angle of repose at least 5° larger than determined for the dust (often 60°),
- use a high dust level indicator, inspection door and a mechanical vibrator in the hopper of the receiver,
- min. DN200 outlet, considering the characteristics and stream of the dust.
- use of dust coolers, e.g. radiation coolers, enabling the use of a sealed sluice system based on double flap valves (Double Flap Gate Valve, Double Pendulum Valve, Double Disk Valve) or throttles,
- the use of an emergency water injection system to the receiver, preventing ignition of the dust/gas collected by sucking in air.
- Finally, regarding the issues of selecting filter media for hot process gas filtration and ensuring their tightness are one of the main issues conditioning the reliable operation of HT rigid filter, thus it is advantageous to:
- use ceramic multilayer filters as they tend to be the safest option of the

- first choice in many applications,
- use tube sheets with a minimum thickness of 5 mm, reinforce the structure on the dirty side,
- use a minimum distance of 40mm between the external surfaces of the filters,
- place the filters in such a way that the filters in the section being regenerated at the same time are placed in one plane, and the number of filters clamped with one fixing plate does not exceed 20 – 25 filters.

7. Acknowledgements

The results presented in this paper were obtained during the research project entitled: Improvement of biomass and waste gasification technology in fixed bed and fluidized bed reactors, (PL: “Doskonalenie technologii zgazowania biomasy oraz odpadów w reaktorach ze złożem stałym i ze złożem fluidalnym”) (IChPW no 11.21.009), financed by the Polish Ministry of Education and Science.

8. References

- Heidenreich, S., 2015. Chapter Eleven - Hot Gas Filters, in: Tarleton, S. (Ed.), Progress in Filtration and Separation. Academic Press, Oxford, pp. 499–525. <https://doi.org/10.1016/B978-0-12-384746-1.00011-2>
- Heidenreich, S., 2013. Hot gas filtration – A review. Fuel, 10th Japan/China Symposium on Coal and C1 Chemistry 104, 83–94. <https://doi.org/10.1016/j.fuel.2012.07.059>
- Heidenreich, S., Haag, W., Salinger, M., 2013. Next generation of ceramic hot gas filter with safety fuses integrated in venturi ejectors. Fuel 108, 19–23. <https://doi.org/10.1016/j.fuel.2011.03.007>
- Heidenreich, S., Haag, W., Walch, A., Scheibner, B., Mai, R., Leibold, H., Seifert, H., 2002. Ceramic Hot Gas Filter with Integrated Failsafe System.
- Heidenreich, S., Wolters, C., 2004. Hot gas filter contributes to IGCC power plant's reliable operation. Filtration & Separation 41, 22–24. [https://doi.org/10.1016/S0015-1882\(04\)00233-2](https://doi.org/10.1016/S0015-1882(04)00233-2)
- Hemmer, G., 2002. Grundlagenuntersuchungen zur kombinierten Abscheidung von Stäuben und gasförmigen Schadstoffen aus Biomasseverbrennungsanlagen [WWW Document]. URL <https://publikationen.bibliothek.kit.edu/642002> (accessed 6.21.21).
- Hoff, D., Meyer, J., Kasper, G., 2008. Influence of the residual carbon content of biomass fly ashes on the filtration performance of ceramic surface filters at high temperatures. Powder Technology 6.
- Hurley, J.P., Dockter, B.A., 2003. Factors affecting the tensile strength of hot-gas filter dust cakes. Advanced Powder Technology 14, 695–705. <https://doi.org/10.1163/15685520360731981>
- Kanaoka, C., Hata, M., Makino, H., 2001. Measurement of adhesive force of coal flyash particles at high temperatures and different gas compositions. Powder Technology, In Commemoration of Prof. Koichi Iinoya, edited by C. Kanaoka and H. Masuda 118, 107–112. [https://doi.org/10.1016/S0032-5910\(01\)00300-X](https://doi.org/10.1016/S0032-5910(01)00300-X)

Kanaoka, C., Kishima, T., n.d. Observation of the process of dust accumulation on a rigid ceramic filter surface and the mechanism of cleaning dust from the filter surface 10.

Mott Corporation - Filtration and Flow Control Engineering [WWW Document], n.d. URL <https://mottcorp.com/> (accessed 6.21.21).

Rhyner, U., 2013. Reactive hot gas filter for biomass gasification. ETH Zurich. <https://doi.org/10.3929/ETHZ-A-009917147>

Schmid, J.C., Fuchs, J., Benedikt, F., Mauerhofer, A.M., Müller, S., Hofbauer, H., Stocker, H., Kieberger, N., Bürgler, T., 2017. Sorption Enhanced Reforming with the Novel Dual Fluidized Bed Test Plant at TU Wien. European Biomass Conference and Exhibition Proceedings 25th EUBCE-Stockholm 2017, 421–428. <https://doi.org/10.5071/25thEUBCE2017-2BO.2.2>

Schumalith® Filter Elements - Pall Shop [WWW Document], n.d. URL <https://shop.pall.com/us/en/oil-gas/refinery/refinery-react-catalyst-protect/zidgri78lc2?CategoryName=refinery-react-catalyst-protect&CatalogID=oil-gas&tracking=searchterm:> (accessed 6.21.21).

Sharma, S.D., Dolan, M., Ilyushechkin, A.Y., McLennan, K.G., Nguyen, T., Chase, D., 2010. Recent developments in dry hot syngas cleaning processes 10.

Sharma, S.D., McLennan, K., Dolan, M., Nguyen, T., Chase, D., 2013. Design and performance evaluation of dry cleaning process for syngas. *Fuel* 108, 42–53. <https://doi.org/10.1016/j.fuel.2011.02.041>

Tarleton, E.S., 2015. Progress in filtration and separation. Academic Press, London, UK; San Diego, CA.

Zimmerlin, B., Leibold, H., Seifert, H., 2008. Evaluation of the temperature-dependent adhesion characteristics of fly ashes with a HT-rheometer. *Powder Technology* 180, 17–20. <https://doi.org/10.1016/j.powtec.2007.03.014>

Gasification of biomass for the production of electricity and heat in cogeneration

Aleksander Sobolewski, Tomasz Iluk, Mateusz Szul and Marcin Stec

Institute for Chemical Processing of Coal, Zabrze (Poland)

1. Abstract

This paper presents the technology of biomass gasification as one of the basic technologies enabling the use of renewable energy sources for the production of electricity and heat in cogeneration. The gasification process, gasification agents and gasification reactor types are described. A concept of the biomass gasification installation dedicated to small and medium CHP systems is demonstrated. In the second part of the paper, a concept of the fixed bed reactor, dedicated to the biomass gasification process and for the combustion of process gas in reciprocating CHP engines, is shown. The results of gasification tests on selected biomasses and their influence on the composition of the process gas and its calorific value have been characterised. The concept of the developed system for the treatment of process gas before its use in the reciprocating engine is explored. The gas purification system is based on a high-temperature filter system, an oil scrubber system, a gas cooler and a demister integrated with a coalescer. The degree of contaminant reduction in the purification system is analyzed. Finally, the reciprocating engine in which the purified process gas was combusted, is introduced.

Keywords: *biomass, gasification, electricity, heat, CHP*

2. Introduction

The change in energy policy which has been implemented in recent years in the European Union, as well as in some other countries around the world, is aimed at reducing the environmental impact of the energy industry. One of the main directions is to reduce CO₂ emissions. According to the declarations of representatives of several countries, the energy industry is to be completely neutral for the environment within several years. Such an approach requires the use of modern, highly efficient technologies, which are based on renewable energy sources [1] or allow a possibility to adapt the existing units to the new standards of the currently implemented energy transformation, e.g. by implementing technologies to capture CO₂ from flue gases along with its chemical utilization [2].

3. Gasification of biomass

One of the basic sources of renewable energy is biomass. The use of biomass for energy purposes can be achieved by implementing three basic technologies: combustion,

gasification and pyrolysis. [3]. The combustion of biomass in district heating water boilers enables the production of useful heat, while through its use in large power units with steam boilers, electricity is produced [4]. In smaller-scale equipment, the biomass combustion in furnaces is aimed for hot flue gas production or in water boilers for utility heat production. Of particular interest is the currently developed gasification technology, which enables in the small and medium-range scale the use of solid biomass, especially the so-called waste biomass. An important advantage of the gasification process is, among others, the multidirectional use of process gas, which is the main product of the process. Possible uses include the production of heat, electricity, or ecologically clean fuels like methanol and hydrogen [5,6].

The gasification process can be, in general terms, defined as a series of chemical reactions combined with thermal processes aimed to produce a combustible gas from organic matter. This process takes place at elevated temperatures and in the presence of a gasifying agent, which is usually air, oxygen, water vapour or carbon dioxide. The chemical composition of the gas obtained in the gasification process depends on the following process factors:

- the temperature and pressure of gasification,
- the chemical composition of the raw material, i.e. the fraction to be gasified and of the gasification agent,
- reactor type and residence time of the gas in its individual zones [3].

The gasification process is carried out in equipment called gas generators or gasification reactors. In general, these devices can be divided into the following types considering the type of the bed:

- fixed bed gasifiers,
- fluidized bed gasifiers,
- entrained bed gasifiers.

The concept of a biomass gasification installation for electricity production is shown in Figure 1. The biomass after the preliminary preparation process (including e.g. drying, grinding) is directed to the gasification reactor, where it undergoes the gasification process in the presence of a gasification agent for the production of process gas. The gas, after prior purification from e.g. tar substances, dust, is directed to a gas reciprocating engine to produce electricity and heat in cogeneration.

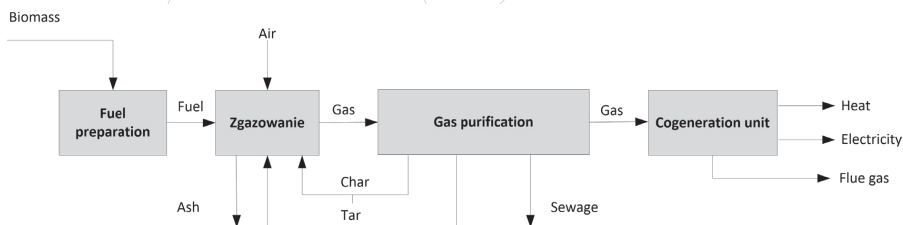


Fig. 1 Concept of biomass gasification plant for cogeneration of electricity and heat.

4. GazEla - IChPW

Institute for Chemical Processing of Coal for many years develops gasification technologies for, among others, coals, biomasses and wastes. The research and development works are carried out mainly for the energetic utilization of process gases in cogeneration units as well as for the production of synthetic gaseous and liquid fuels.

The gasification process considered in this article is carried out in a fixed bed GazEla reactor. The reactor was designed and developed for the generation of process gas from solid fuels (mainly biomass) for cogeneration of heat and power in a gas reciprocating engine. This technology is dedicated to small and medium scale energy systems e.g. district heating stations as well as heat and power stations, companies that have technological lines utilizing hot water or technological steam, as well as companies with large internal demand for electricity.

The gasification installation consists of four main technological blocks, ie. fuel preparation and feeding, GazEla fixed bed gasification reactor, gas cleaning unit and cogeneration unit based on the gas reciprocating engine.

The main equipment of the system is the GazEla reactor: a vertical, cylindrical reactor with a fixed bed. In the vertical axis of the reactor, a central pipe is fitted allowing ar recovery of process gas directly from the gasification zone. Fuel is fed into the reactor from the top, while the gasification agent is fed into three zones: under the reactor's grate, into its middle part as well as above the bed. Proper selection of type and flow of gasifying agent is crucial for the control of a load of each process zones. This mechanism provides means for control of temperature profiles within the reactor and obtaining the right process conditions in relation to physicochemical parameters of gasified feedstock [3, 7, 8, 9]. Fig. 2 presents a technological flow sheet of the reactor with denoted individual process zones.

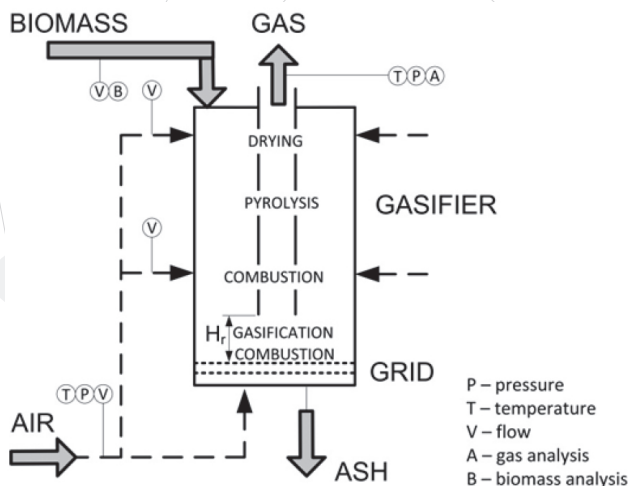


Fig. 2. Technological scheme of GazEla reactor with denoted specific process zones

Figures below show the pilot GazEla reactor, located in Clean Coal Technology Centre in the IchPW, Zabrze.



Fig. 3. The pilot-scale GazEla fixed bed reactor (upper and lower part of the reactor)

The results of reactor tests for selected types of biomass (Tab 1) are presented in Tab 2. They confirm the possibility of using different biomass raw materials in the GazEla reactor. The calorific value of the (dry) gas obtained ranged from 3.82 to 4.72 MJ/m³. For wood chips, the dry gas composition was as follows: H₂ = 6.1÷7.5%, CH₄ = 2.1÷2.5%, CO = 19.5÷25.0%, CO₂ = 9.5÷11.8%, N₂ = 55.9÷60.1%. In the case of pellets, the main gas components took up following values: H₂ = 6.7÷8.9%, CH₄ = 0.9÷2.6%, CO = 20.3÷22.0%, CO₂ = 12.8÷12.9%, N₂ = 55.4÷57.5%.

Tab 1: Characteristics of the fuel [8].

Parameter	Unit	Fuel			
		Wood chips I	Wood chips II	Wood pellets	Straw pellets
Form	-	lumps	fibrous	peletts	peletts
Size [mm]	mm	< 8	20÷50	Ø6	Ø6
Total moisture, W ^{tr}	%	21.4	14.6	4.4	9.3
Ash, A ^a [%]	%	1.3	0.5	0.3	5.5
Volatiles, V ^{daf} [%]	%	81.11	83.48	83.61	81.36
C _t ^a [%]	%	49.4	48.5	49.6	45.0
H _t ^a [%]	%	5.56	5.75	5.88	5.47
N ^a [%]	%	<0.05	0.19	0.27	0.53
Calorific value, Q _i ^r [J/g]	MJ/ kg	14.2	15.7	17.8	15.4

Table 2: Change in the composition of the process gas depending on the type of biomass [8].

Gas component	Unit	Wood chips I	Wood chips II	Wood pellets I	Straw pellets II
H ₂	% v/v	6.1	7.5	6.7	8.9
CH ₄		2.5	2.1	0.9	2.6
CO		19.5	25.0	22.0	20.3
CO ₂		11.8	9.5	12.9	12.8
O ₂		0.0	0.0	0.0	0.0
N ₂		60.1	55.9	57.5	55.4
Wd	MJ/m ³ _n	4.01	4.72	3.82	4.45

The process gas with a temperature of approx. 550÷650°C, obtained from the GazEla gasifier, is transferred to the purification system for preparation of gas for combustion in the reciprocating engine. In the system developed by IChPW, the above objective is achieved through high-temperature filtration, oil scrubbing and gas cooling followed by cleaning with a dedicated demisting system. During the tests, the ability to remove dust from process gas to the levels of 5 mg/m³_n (at the outlet after the high-temperature filter) was confirmed, while organic substances concentration was reduced to the value of approx. 100÷150 mg/m³_n [8,].

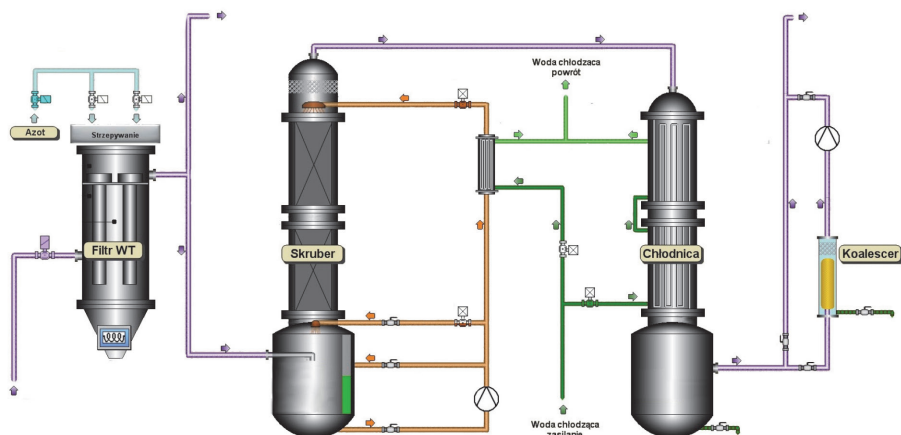


Fig. 4. Concept for purification of process gas from biomass gasification - IChPW

As a part of the research work on the biomass gasification installation with the use of GazEla gas generator, combustion tests of the produced process gas in a dual-fuel reciprocating engine were also carried out to confirm the possibility of efficient use of process gas to supply piston engines (Figure 5).



Fig. 5. Piston engine running on process gas and Diesel in dual-fuel mode, generating 15,5 kWel.

5. Conclusion

Currently, for small and medium power units, one of the most intensively developed technologies that enable the highly efficient generation of heat and power, both from energetic and environmental points of view, is the gasification of solid fuels. This technology enables the production of combustible gas from biomass, waste biomass, which after cleaning can be effectively combusted in highly efficient cogeneration units based on reciprocating engines. In the future, gasification technology will be used to produce liquid and gaseous fuels as well as for the production of substrates for chemical purposes.

The biomass gasification technology presented in this paper is based on the concept of a vertical, cylindrical fixed bed reactor, which uses a central pipe for the direct extraction of process gas from the gasification zone. The presented results of gasification tests of selected biomasses on a pilot-scale confirm the possibility to use the reactor for the production of process gas, suitable for combustion in gas piston engines for the production of electricity and heat in cogeneration. Before the combustion, in the presented concept, the gas is subjected to purification in the dedicated gas purification system.

Further development of gasification technology, which is being carried out at the IChPW, is currently focused on the use of waste raw materials such as municipal waste, RDF, sewage sludge for energy and chemical purposes introducing circular economy concepts.

6. Acknowledgements

The results presented in this paper were obtained during the research project entitled: Improvement of biomass and waste gasification technology in fixed bed and fluidized bed reactors (GazEla, IPPS, IZOP), (PL: "Doskonalenie technologii zgazowania biomasy oraz

odpadów w reaktorach ze złożem stałym i ze złożem fluidalnym (GazEla, IPPS, IZOP).”) (IChPW no 11.21.009), financed by the Polish Ministry of Education and Science.

7. References

- [1] Bartela Ł., Kotowicz J., Remiorz L., Skorek-Osikowska A., Dubiel K., Assessment of the economic appropriateness of the use of Stirling engine as additional part of a cogeneration system based on biomass gasification. *Renewable Energy* 2017;112:425-443
- [2] Skorek-Osikowska A., Bartela Ł., Kotowicz J., Thermodynamic and ecological assessment of selected coal-fired power plants integrated with carbon dioxide capture. *Applied Energy*; DOI: 10.1016/j.apenergy.2017.05.055.
- [3] Sobolewski A., Iluk T.: Zgazowanie biomasy. Monografia: Odnawialne źródła energii. Rolnicze surowce energetyczne. Pod redakcją Barbary Kołodziej i Mariusza Matyki. Wydawnictwo Rolnicze i Leśne Sp. z o.o., Poznań 2012, ISBN 978-83-09-01139-2, 550-556.
- [4] Kalisz S., Pronobis M., Baxter D., Co-firing of Biomass Waste Derived Syngas in Coal Power Boiler, *Energy* 33(12), 2008.
- [5] Basu P., Biomass Gasification and Pyrolysis. Practical Design and Theory, Burlington, 2010.
- [6] Szubel M., Filipowicz M., Biomass in Small-Scale Energy Applications Theory and Practice, CRC Press 2020.
- [7] P. Billig, M. Ściążko, A. Sobolewski, “Zgazowarka ze złożem stałym”, Patent PL-208616, 2010.
- [8] Kotowicz J., Sobolewski A., Iluk T., Energetic analysis of a system integrated with biomass gasification. *Energy* 2013, 52, 265-278.
- [9] Iluk T., Sobolewski A., Szul M.: Gasification of solid recovery fuel, biomass and sewage sludge in a fixed bed gasifier in pilot scale. *Przemysł Chemiczny* 2016 (8), 1634-1640. IF 0.367. doi 10.1519/62.2016.8.45.

The utilisation of Vehicle-to-Grid Technology in Power Engineering

Vojtech Blazek, Lukas Prokop, Stanislav Misak

ENET Centre, VSB Technical University of Ostrava, 17. listopadu 15, 70800 Ostrava, Czech Republic

1. Abstract

The article presents the potential use of Vehicle-to-Grid (V2G) technology and describes the developed testing platform of a Microgrid system with V2G support. V2G technologies enable battery capacity in an electric vehicle (EV) as a potential energy storage system for the distribution system. The platform, developed by the Centrum ENET research team, uses a control system based on Demand-side Response (DSR) methods, which seeks to optimise electricity consumption in the energy network effectively. Furthermore, by combining DSR and V2G technologies, the platform can utilise renewable electricity sources efficiently. Our iteration of DSR is named Active demand-side management (ADSM). The Microgrid control system with ADSM based on artificial intelligence methods that opt to optimise the energy sources and appliances according to the priority plan of switching appliances. Finally, the article describes a simulation of an actual Microgrid model of a V2G system with a real scenario. These results will be used in the future to develop a Microgrid system located on campus VŠB – Technical University of Ostrava.

Keywords: Vehicle-to-Grid, Microgrid, Demand-side response, Renewable energy sources

2. Introduction

There is actual electric vehicle (EV) deployment in recent years, both in local and global measure [1]. With this growth are connected newly appeared ideas and technologies to utilise EV batteries in non-traditional ways [2], [3]. Vehicle-to-Grid (V2G) includes a set of technologies that allow the use of the capacity of connected EVs, hydrogen fuel cell electric vehicles (FCEV) or plug-in hybrids (PHEV), communicate with the power grid to sell demand response services by either returning electricity to the grid or by throttling their charging rate.[3]

V2G technology utilises energy storage in EVs to store and discharge electricity generated from renewable energy sources (RES) such as solar and wind, with output fluctuating depending on the time of day and actual weather.[3] V2G technology can be used with vehicles that can be connected to a bidirectional V2G inverter. These are generally referred to as plug-in EV and PHEV. Since about 95% of cars are parked at any given time, the batteries in EV could be used to let electricity flow from the car to the electric distribution network and back. Fig. 1 shows a block diagram of the functionality of Vehicle-to-Grid technology.

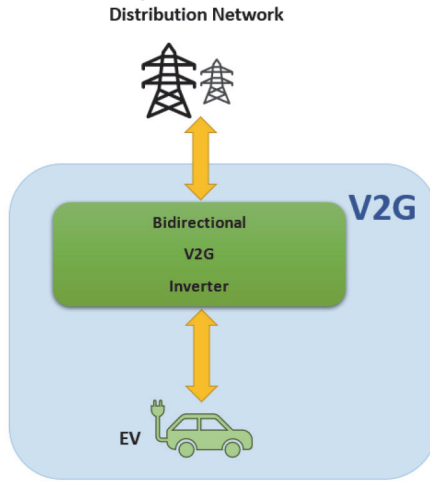


Fig. 1: V2G energy flow diagram

Fig. 2. shows the potentially ideal use of EV as a possible supporting energy service in the Czech Republic. Consumption dates from 9th March 2021.

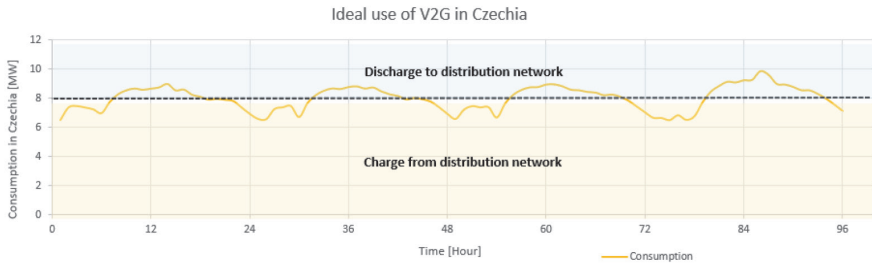


Fig. 2: Ideal use of V2G in Czechia

Today, advanced methods are used in energy to manage electricity consumption. These methods are unified under the term Demand-side response (DSR). Usually, (DSR) aims to encourage the consumer to use less energy during peak hours or to move the time of energy use to off-peak times such as nighttime and weekends.

Peak demand management does not necessarily decrease total energy consumption but could reduce the need for investments in networks and power plants to meet peak demands. An example is the use of energy storage units to store energy during off-peak hours and discharge them during peak hours. DSR with V2G technology represents a huge potential in the energy sector to streamline the production and consumption of electricity. Each method of demand-side management show in Fig.3.

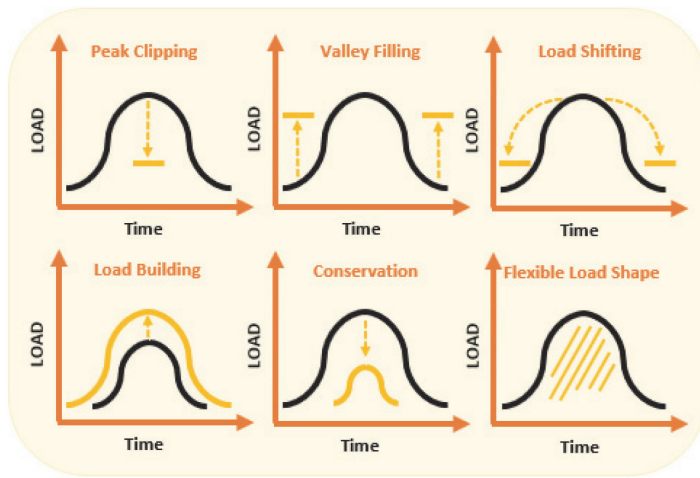


Fig. 3: DSR Methods

3. INFRASTRUCTURE DESCRIPTION

The centre of the Microgrid system is a hybrid inverter Schnieder Conext XW+ 8548 with 6.8 kW rated power. Accumulation is formed from 40 series-connected Ferak KPL 375 NiCd batteries w

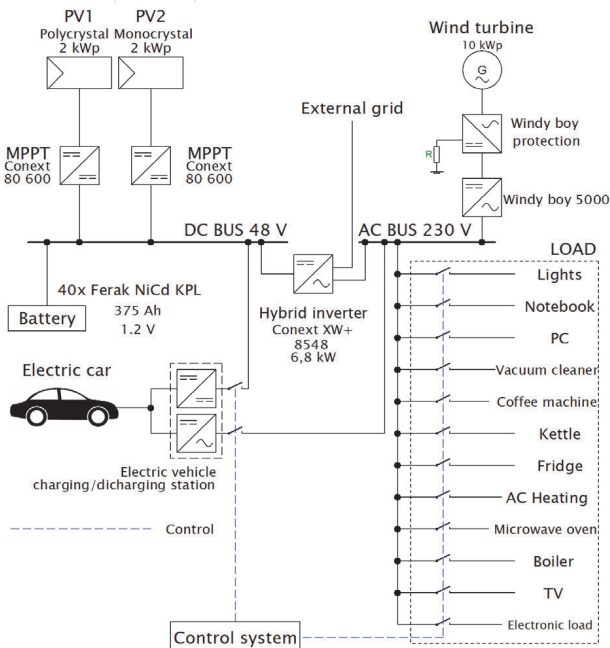


Fig. 4: Electric Scheme of a testing platform with V2G

Fig. 4 show the Electric Scheme of an actual Microgrid model with V2G. Two photovoltaic panels (monocrystalline and polycrystalline), each 2 kWp, are connected to the solar charge controller Xantrex XW MPPT 80 600. These controllers are DC coupled to the Microgrid. Another RES is a wind power plant with rated power 10 kW AC-coupled through inverter Windy Boy 5000. Fig. 5

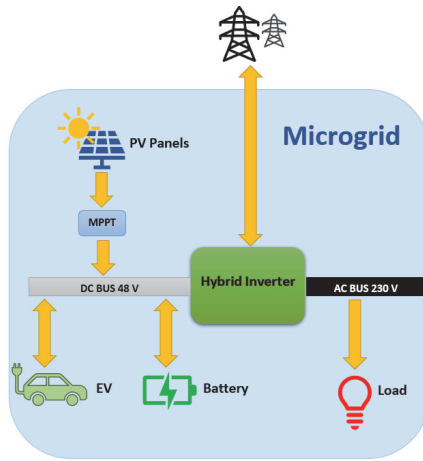


Fig. 5: Concept of energy flow in Microgrid with V2G

The Control system is driven Quido I/O module is used to control appliance switching physically. Many typical household appliances are present and connected to the system, and the programmable electronic load simulates those that are missing. The programmable electronic load has a maximum power of 4 kW with step 100 W and 5 options of power factor (1, 0.95 C or L and 0.5 C or L). Fig. 6 shows the newly developed V2G inverter that will be part of the EV charging/discharging station used to transfer energy between EV batteries and the Microgrid. Station connected EV also reports its actual state of charge of the batteries.

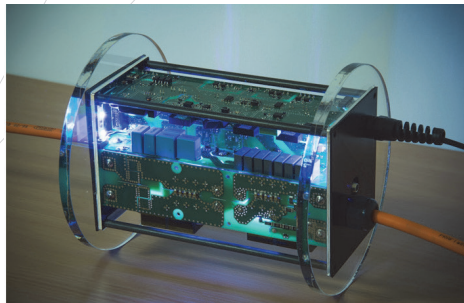


Fig. 6: Inverter for V2G application

ADSM decides appliance switching according to the following factors – remaining energy in batteries, predicting energy consumption and generation. ADSM based on multiobjective optimisation (MOO) was applied in this experiment for hyperparameter optimisation of the random decision forest algorithm (RF). In general, the MOO problem is posed as an optimisation problem of several (mostly conflicting) objective functions [4]. According to the defined equality and inequality constraints, the input value vector X defines the search space (often called a feasible design space) for solutions. MOO is mainly based on search engine optimisation, but there is one significant difference from single-objective optimisation. In MOO, the number of solutions is defined as a feasible solution (called a Pareto front). Each of its candidates is called Pareto optimal and together, forming a so-called tradeoff curve in a chart of objective values. The Pareto optimal solutions are equally distributed on this curve toward all the optimisation functions. The solutions placed in the middle of the curve ideally hold the optimisation tradeoff toward the applied cost functions.

One sample day is selected to demonstrate the ADSM function. Tab.1 contains a one-day appliance switching plan and optimisations performed by ADSM to avoid Microgrid shutdown due to lack of energy in batteries. Performed optimisations were load shifting and connecting the system to the distribution grid. Fig. 7 shows a daily load of appliances supplied from batteries before and after optimisation. Fig.9 shows available (remaining) energy in batteries over time here. We can see that the ADSM system would run out of energy around 2 AM without intervention, which would lead to a Microgrid system shutdown.

Tab. 1 Appliance plan after adsm optimisation

Appliance	Start	Stop	Change	Start	Stop
Fridge	00:00	00:00	-	-	-
AC Heating	00:00	00:00	-	-	-
Washing machine	07:00	09:00	Powered from the external grid	-	-
Kettle	08:00	08:05	-	-	-
LCD TV	09:00	11:00	-	-	-
Boiler	00:00	08:00	Powered from the external grid	-	-
PC	05:00	10:00		-	-
Notebook	05:00	10:00	Start delayed	10:15	17:30
Microwave oven	06:00	06:05	Start delayed	11:25	11:30
Boiler	20:00	21:00	Powered from the external grid	-	-
LCD TV	07:00	09:00	-	-	-
Lights	07:00	09:00	-	-	-
Kettle	17:00	17:05	-	-	-
Lights	17:00	23:00	-	-	-
Kettle	09:00	09:05	-	-	-

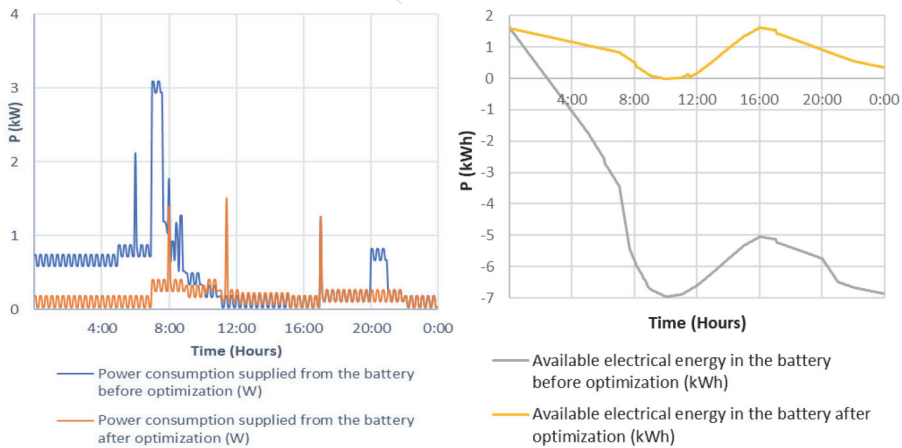


Fig. 7 Comparison of ADSM optimisation

4. Experiment description

The experiment applies the ADSM system to an actual model of the Microgrid network with V2G technology. An EV with a battery capacity of 50 kWh will be connected to the system. EV was connected from 18 PM to 6 AM. The EV was connected with a 50% SoC battery, and at the end of the simulation, there was a requirement that the EV is SoC 50% again. The minimum capacity for an electric car was 5 kWh. The entire microgrid system is connected to the energy distribution network from 0 AM to 4 AM to replenish the necessary energy for its operation. Microgrid contains batteries with a total capacity of 18 kWh. The minimum capacity of a stationary battery in a microgrid system is 1.8 kWh.

The microgrid system will have its own electricity consumption. This consumption represents the consumption of a real household with common electrical appliances. You can see the schedule of running appliances in Tab.2. In the simulation of the whole system, there are appliances with which the start of a start-up can be delayed. The schedule always shows the start time of the appliance and the time for which the appliance has been started.

The missing energy that the Microgrid will be supplied from the external energy network. The simulation took place in 5 working days on weather data from 4th May to 9th May 2020. The optimisation has 7 iterations.

Tab. 2 Schedule of appliances in the Microgrid with connected EV

Appliances	ADSM	Day	Time (h:m)	Start (min)	Day	Time (h:m)	Start (min)	Day	Time (h:m)	Start (min)			
Air conditioning	Yes	All days	5:00	60	All days	15:00	420						
Lights	No	All days	6:00	120	All days	18:00	240						
PC	No	All days	17:00	240	Fri	10:00							
Washing machine	Yes	Wed	18:00	120	Fri	18:00	120						
Fridge		All-day long											
TV	No	All days	6:00	120	Fri	16:00	360						
WiFi and standby mode in appliances		All-day long											
Boiler	Yes	All days	7:00	180	All days	20	120						
Kettle	No	All days	7:00	5	All days	15:45	5				All days	19:00	5
Microwave oven	No	All days	6:15	5	All days	16:00	5				All days	19:00	5
Vacuum cleaner	No	Wed	17:00	30									
Cooker	No	All days	10:00	180									
Dishwasher	Yes	Mon	14:00	120	Wed	14:00	120	Fri	14:00	120			

5. Results

Fig. 8 shows the energy in a Microgrid system. The figure shows the current state of the stationary battery in Microgrid, the production of energy from PV (RES-PV), the current state of the charged battery in the car (Car), the current electricity consumption (Total load) and the current supplied energy of the distribution network (Grid supply). Fig. 9 shows the energy after optimisation.

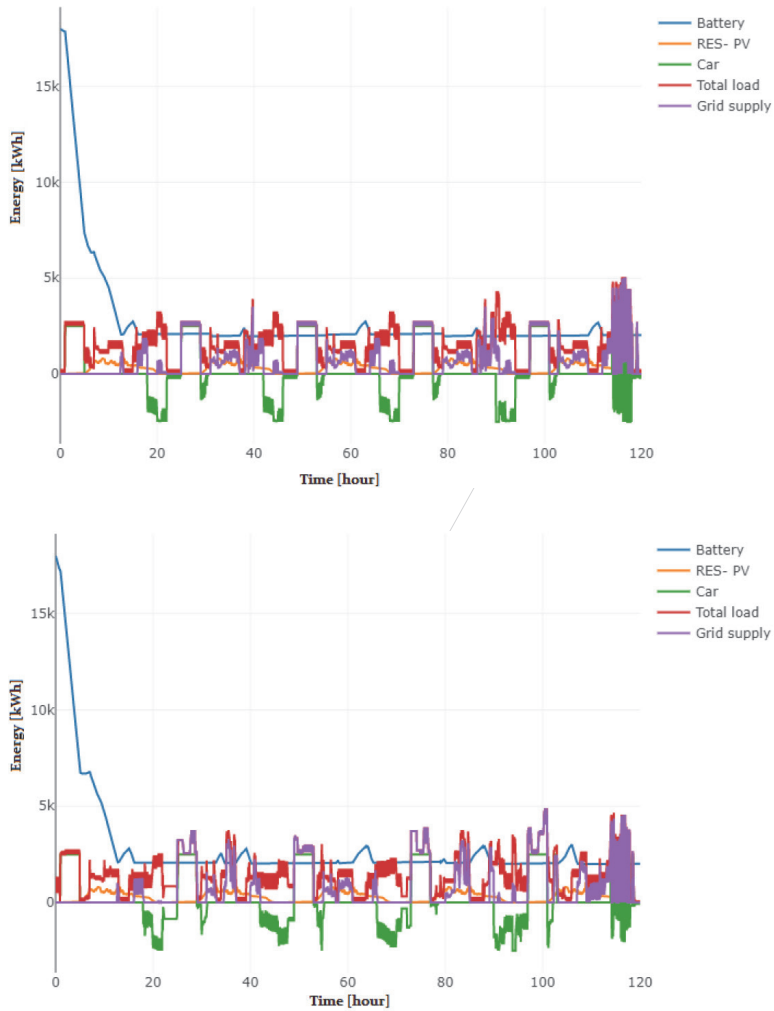


Fig. 9: Energy after optimisation

Fig.10 shows the effect of the ADSM optimisation with iteration on the energy-saving efficiency. This energy has to be supplied to the Microgrid from the external distribution network, or the regular operation of the Microgrid would be disrupted. In iteration 0, the optimisation was not started. The result of the simulation came out without optimisation came out 89.64 kWh. Results with ADSM optimisation is 67.96 kWh.

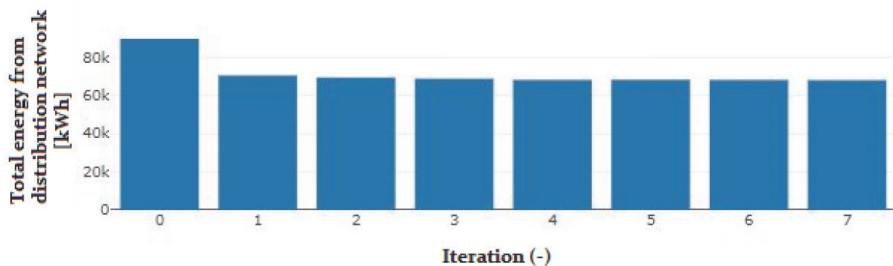


Fig. 10: Influence of optimisation iteration on optimisation efficiency

6. Conclusion

The article describes the potential use of V2G technology combined with DSR. The simulation results showed that the planned Microgrid with V2G technology could save up to 24.1% of total consumed energy over 5 days. Furthermore, according to the experiment results, the first iteration showed the highest increase in saved energy, and further iterations of optimisation no longer significantly affect the amount of saved energy.

In further work, we will continue to simulate various scenarios to create a dataset that will be used for future research purposes.

7. References

- [1.] IEA (2019), "Global EV Outlook 2019", IEA, Paris, Accessed on: Jan. 23 2020, [Online], Available: <https://www.iea.org/reports/global-ev-outlook-2019>
- [2.] C. Liu, K. T. Chau, D. Wu and S. Gao, "Opportunities and Challenges of Vehicle-to-Home, Vehicle-to-Vehicle, and Vehicle-to-Grid Technologies," in *Proceedings of the IEEE*, vol. 101, no. 11, pp. 2409-2427, Nov. 2013. doi: 10.1109/JPROC.2013.2271951
- [3.] Cleveland, Cutler J.; Morris, Christopher (2006). *Dictionary of Energy*. Amsterdam: Elsevier. p. 473. ISBN 978-0-08-044578-6.
- [4.] Vantuch, T.; Mišák, S.; Jeřowicz, T.; Buriánek, T.; Snášel, V. The power quality forecasting model for off-grid system supported by multiobjective optimization. *IEEE Trans. Ind. Electron.* 2017, 64, 9507–9516.

The Using of Fuel Cell in Micro-Cogeneration Unit in Buildings

Peter Pilat¹, Marek Patsch¹

¹ Department of Power engineering, University of Zilina, Univerzitna 1, 010 26
Zilina, Slovakia

1. Abstract

The article deals with the analysis of the results of long-term experimental operation of a micro-cogeneration unit with high-temperature fuel cells for natural gas. Due to its performance parameters, the unit is primarily intended for installation in a family house or in a small building. Long-term testing operation under laboratory conditions verified the power and emission parameters of the micro-cogeneration unit in steady and transient modes, which may occur during operation in a family house. Measured values of heat and electricity demand in a real family house served as a basis for the test operation, according to which a load algorithm was created. Long-term testing has confirmed the difficulty of correctly designing the installation of a micro-cogeneration unit in a family house for its specifics, such as the highly variable consumption of electrical and thermal energy depending, for example, on the season and the daily regime of its inhabitants.

Keywords: micro-cogeneration unit, fuel cell

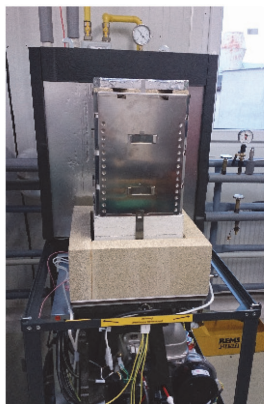
2. Introduction

Cogeneration is the combined production of electricity and heat in one technological facility. Nowadays, cogeneration units find their application also in installations where low electric and heat output is required, for example in family houses or in smaller buildings. Micro-cogeneration - cogeneration with a maximum electrical output of up to 50 kWe is used in these areas. In addition to traditional internal combustion engines, new technologies for cogeneration units such as fuel cell, Stirling engine, steam engine, micro-combustion turbines and the like are coming to market. These units are capable to achieve low electrical and thermal performance adapted for use in single-family houses. The philosophy of their use is in the production of heat to cover the heat losses of the building and to heat hot water and as a bonus the user gets electricity. The electricity produced is not primarily intended for sale, but is consumed directly at the production site, so the electrical and thermal output of the micro-cogeneration unit must accurately reflect the needs of the object. The family house, as the place of installation of the micro-cogeneration unit, is quite specific for its highly variable consumption of electric and thermal energy, which is demandingly predictable and therefore it is difficult to match the produced electrical and heat output of the micro-cogeneration unit with the family house needs. Nowadays, at the age of intelligent technologies, when designing the installation of a micro-cogeneration unit, it is possible to

know the real consumption of electric and thermal energy in a given building throughout the year from simple measurements provided by these technologies. These data are input data for the calculation of the number of operating hours of the micro-cogeneration unit in a year, the burden and the resulting amount of heat and electricity produced and last but not least the payback period. Family house, which was considered to install a micro-cogeneration unit with fuel cells for natural gas, is a new building inhabited by a family of four, located near Zilina, it is a two-floored house with a flat roof, built-up area 100 m², built in low energy standard. The family house is equipped with smart technologies for smart homes that provide not only significantly higher comfort of living, but in this case also important data on electricity and heat consumption during any period of the year.

3. Experimental laboratory operation of the micro-cogeneration unit

Electricity and heat consumption data in the family house were recorded throughout the year 2018 and served to create a load algorithm according to which the micro-cogeneration unit with fuel cells was loaded in the laboratory conditions of the University of Žilina. As the electrical load of this unit served the resistor (electrical energy is converted to heat), the heat was wasted in a hot air unit or in a plate heat exchanger cooled by a flow thermostat. Operation and measurement of electrical and thermal output of the micro-cogeneration unit took place in automatic mode, all constants and settings were obtained from the load algorithm. This algorithm currently assumes the use of heat from the micro-cogeneration unit in the heating and domestic hot water system and the electrical output of the unit only for direct consumption in a single-family house, without the possibility of selling excess electricity to the external grid to cover possible later increased electricity consumption.



a)



b)



c)

Figure 3.1.

Micro-cogeneration unit with fuel cells a) view of fuel cell module - top of unit, b) view of integrated condensing boiler - bottom of unit, c) assembly of micro-cogeneration unit. The micro-cogeneration unit used to simulate year-round operation in a family house (Fig.3.1) uses a fuel cell module with SOFC technology (high temperature ceramic fuel cell with a working temperature of 830°C), with a nominal electrical output of 1 kWe and a fuel cell thermal output of 1.8 to 3,3 kWt. The unit is complemented by a condensing boiler with a heat output of 7.0 to 20.0 kWt, which covers any increased heat demand. The unit is capable of operating in fuel cell mode, condensing boiler mode, or both. As the fuel unit uses natural gas, hydrogen for the fuel cell module is obtained by partial oxidation of CH_4 . The simulated operation of the unit was in automatic mode, the suitability of using one of the three operating modes was selected according to the load algorithm.

The micro-cogeneration unit operating in fuel cell mode is not one of the flexible sources of electric and thermal energy, because of the slow change in the output electric power, the operation at nominal electric power is optimal. Start of the micro-cogeneration unit (Fig. 3.2a), if the fuel cell module is not heated to operating temperature, takes approximately 45 hours (output power 0 We to 1000 We, fuel cell module operating temperature 20°C to 830°C), start from stand-by mode (Fig. 3.2b), when the fuel cell module is maintained at operating temperature takes approximately 2.5 hours (output power 0 We to 1000 We, fuel cell module operating temperature 830°C), response to change of required output power is approximately 2 minutes.

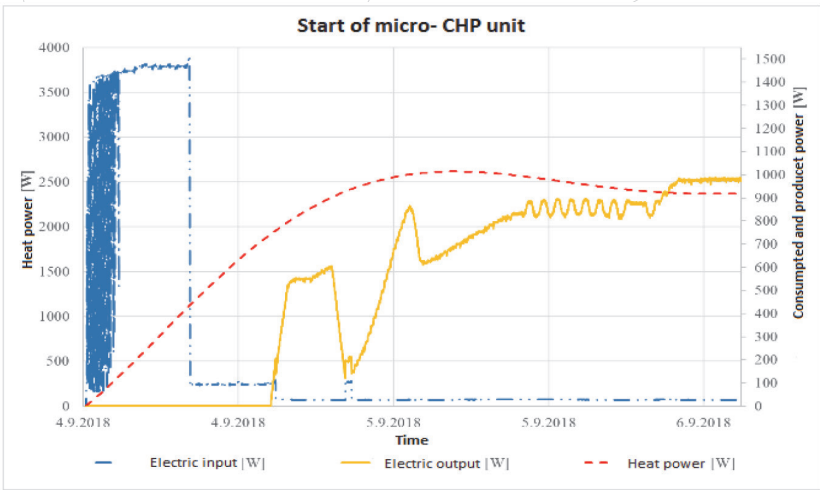


Figure 3.2. a)
Cold start of the micro-cogeneration unit

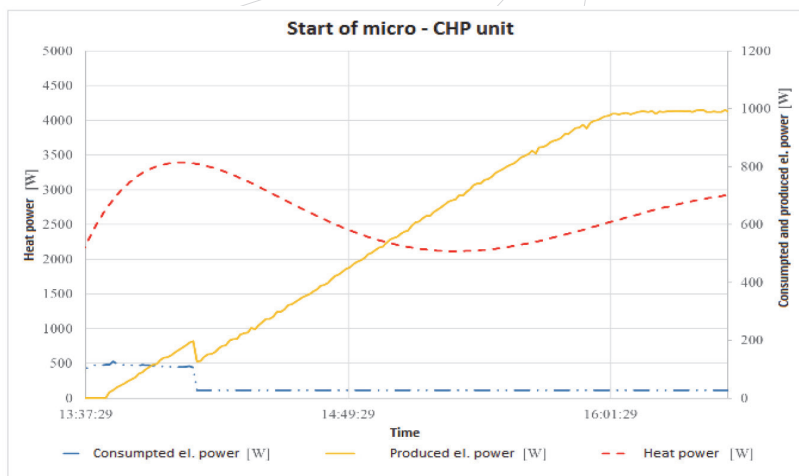


Figure 3.2. b)
Start from stand-by mode

From the year-round simulated operation, the coldest winter day in 2018 with the lowest night temperature of -15°C and the highest daily temperature of -8°C was chosen for graphic processing. During this period, the unit operated in a combined mode, since only the thermal power of the fuel cell is not sufficient to cover the heat loss of the building. Fig. 3.3 shows the output thermal and electrical output of a micro-cogeneration unit operating in a steady-state fuel cell mode and for comparison Fig. 3.4 shows the output thermal and electrical output of a micro-cogeneration unit operating in a steady-state combined mode, during which the output electrical output of the fuel cell module decreases from a nominal value of 1000 We and oscillates around 800 We. This unfavorable phenomenon is caused by a common condensation heat exchanger for the fuel cell and the integrated gas boiler. These steady-state modes of operation occur to a lesser extent during operation in a single-family home, more often transient modes occur, which, due to the characteristics of the micro-cogeneration unit described above, significantly affect the overall electrical and thermal output.

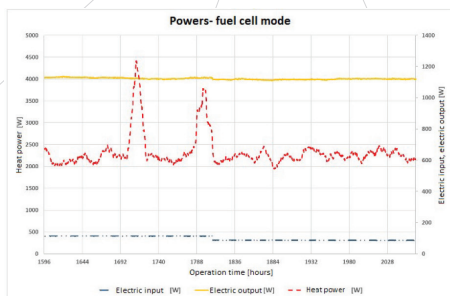


Figure 3.3
The course of electrical and thermal output during
fuel cell mode

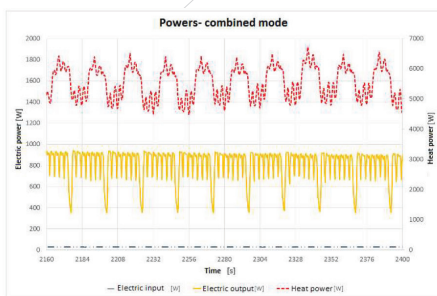


Figure 3.4
The course of electrical and thermal output during the
combined mode

Figure 3.5 shows the course of the 24-hour need and the produced electric and thermal energy in a family house and is largely influenced by the daily regime of the inhabitants and the season, thus the heat loss of the building. Continuous consumption of electricity consists of stand-by devices and variable consumption of devices whose operation is influenced by residents of the house (lighting, electric appliances of daily use, ...). The consumption of thermal energy depends on the heat loss of the building and high increases in consumption are probably caused by the preparation of hot water.

A more detailed analysis of the electricity demand in the family house and the course of the electricity produced by the micro-cogeneration unit in the combined mode shows that the unit at night and part of the day when residents are absent covers only the consumption of stand-by and cyclically switched equipment. During the rest of the day, the unit operates at maximum electrical power, but due to the combined mode operation, it does not reach the nominal electrical power of 1000 We, the remaining electricity required is supplied from the public grid. A more detailed analysis of the heat demand in the family house and the heat produced by the micro-cogeneration unit in the combined mode of operation shows that throughout the day the fuel cell module of the unit did not reach the maximum possible heat output of 3.3 kWt, its value oscillating around 1.5 kWt. During the night and part of the day when residents are not present, the low heat output is caused by the low power consumption. During the rest of the day, an increase in thermal energy was expected due to an increase in electricity production, but this did not occur. The cause approximately constant thermal power is a method of regulating the output electric power micro-cogeneration units and use burning out zone at module for fuel cells to convert the unconverted natural gas for heat. The remaining part of the required thermal energy is produced in the integrated gas boiler. Only a condensing boiler was used to heat hot water in winter. Due to the low heat output of the fuel cells, the heating time would be unacceptably long. Heating of hot water by fuel cells could be used, in particular, in the early predictive heating of the storage tank and during transitional heating periods, but the low electricity consumption at night and the resulting low heat output would further increase this time.

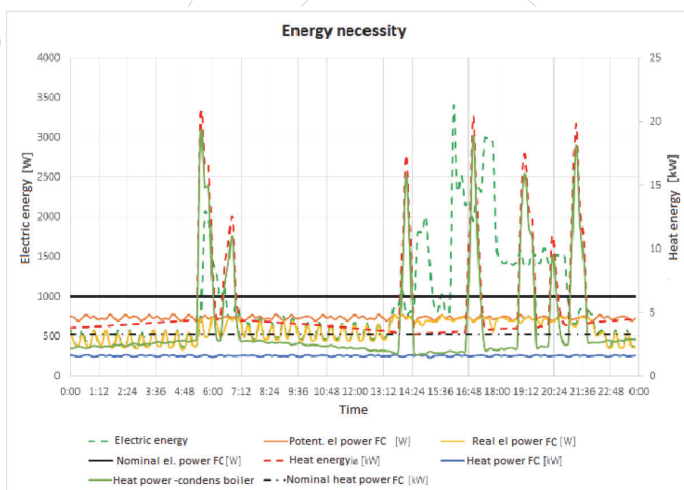


Figure 3.5.
Demand of electrical and thermal energy needs

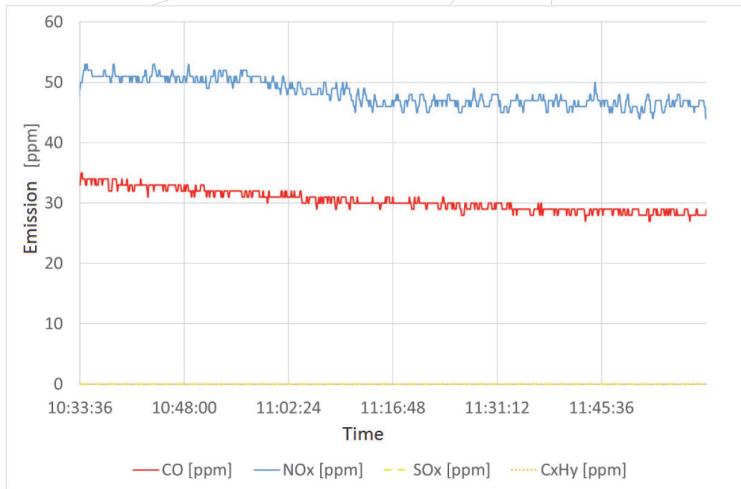


Figure 3.6.
Emissions from the operation of a fuel cell micro-cogeneration unit - fuel cell mode

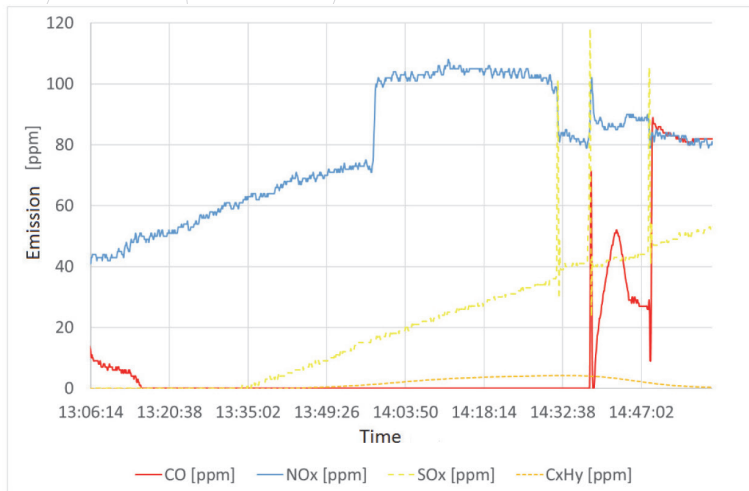


Figure 3.7.
Emissions from operation of a fuel cell micro-cogeneration unit - combined mode

The graph of figure 6 shows an example of measured NO_x, SO_x, CO emissions and unburned C_xH_y fractions in steady state fuel cell mode. The course of values has a constant character with only slight variations. SO_x and unburned fractions were not recorded in the flue gas. Zero SO_x concentrations are due to the use of a desulfurization filter at the inlet of natural gas to the fuel cell. Zero values of unburned C_xH_y fractions are due to the post-fuel cell post-deposition zone, where unused methane CH₄ and most of the CO react from the partial oxidation reaction to CO₂ and water. The graph of figure 7 shows the evolution of emission values when switching from fuel cell mode to combined mode

and subsequent operation in combined mode. The switching is manifested by fluctuations of otherwise constant values due to the change of working and chimney temperature, slight increase under normal conditions of zero unburned CxHy fractions and increase of SOx concentration. The SOx increase is due to the fact that the natural gas for the condensing boiler does not pass through the desulfurization filter and the resulting small values of sulfur compounds are due to the presence of an odorant in the natural gas. The CO and NOx concentration values in the flue gas in the combined mode are higher than in the fuel cell mode, but are still within the limits of the applicable standard.

4. Conclusion

The simulated year-round operation of a natural gas micro-cogeneration unit has demonstrated the complexity of correctly designing such a unit in a family house for its specific variable electricity and heat consumption. Nowadays, considerably energy-efficient home appliances seem to be the nominal electrical output of the unit as useless, year-round average electrical output was about 450 We, during the year-round operation the unit was able to replace only 24% of the total annual electricity consumption of the building. The return on investment is in the order of decades when using the nominal electrical output. A more suitable installation of a micro-cogeneration unit of this type would be in the case of the possibility of selling surplus electricity to the grid or in the possibility of its accumulation. A suitable installation would also be in an object where the minimum required electrical power for stand-by devices is higher than the nominal electrical power of the unit, the unit would only operate in fuel cell mode, requiring yet another separate heat source.

Emission measurements during the operation of the fuel cell micro-cogeneration unit have pointed to its ecological operation. The operation of the fuel cell micro-cogeneration unit in fuel cell mode, after recalculation of the CO concentration by volume, reached an average value of 0.0095%, which complies with the applicable standard (the allowed limit of CO concentration in dry flue gases given by the standard is 0.10%). The NOx mass concentration reached an average value of 87.77 mg.kWh⁻¹, which corresponds to a Class 4 standard with a 100 mg.kWh⁻¹ threshold. The operation of the combined fuel-cell micro-cogeneration unit, after recalculation of the CO concentration by volume, reached an average value of 0.0056%, which complies with the requirements of the applicable standard (permissible limit of CO concentration in dry combustion products given by the standard is 0.10%). After stabilization, the NOx mass concentration reached an average value of 149.89 mg.kWh⁻¹, which corresponds to a class 3 standard with a allowable limit of 150 mg.kWh⁻¹.

5. Acknowledgments

This article was created with grant KEGA 048ŽU-4/2019 „Visualization of flow in environmental engineering“.

6. References

Examples for references:

Reference to a journal publication:

Van der Geer, J., Hanraads, J.A.J., Lupton, R.A., 2000. The art of writing a scientific article. J. Sci. Commun. 163, 51-59.

E. DVORSKÝ and P. HEJTMÁNKOVÁ, Kombinovaná výroba elektrické a tepelné energie, in Technical literature BEN., Praha (2005).

P. ĎURČANSKÝ and R. NOSEK, Modelling and application of Stirling engine with renewable sources in electricity production, in Structure and Environment: Architecture, Civil Engineering, Environmental Engineering and Energy. 10,. 4 (2018).

L. KUČÁK and F. URBAN, Kogenerácia na báze palivového článku. Vykurovanie 2007. Zborník prednášok z 15. medzinárodnej konferencie. - Tatranské Matliare, 26.2. - 2.3. 2007. - Bratislava : Slovenská spoločnosť pre techniku prostredia ZSVTS, (2007).

P. ORŠANSKÝ and B. FTOREK and P. ĎURČANSKÝ, Mathematical model of a closed hot air engine cycle using MATLAB®/Simulink®, in XIX. the application of experimental and numerical methods in fluid mechanics and energetics 2014- proceedings of the international conference, Liptovský Ján, Slovakia, (9-11 April 2014)

M. PEHNT and M. CAMES and C. FISCHER and B. PRAETORIUS and L. SCHNEIDER and K. SCHUMACHER and J. P. VOß, Micro Cogeneration, Towards Decentralized Energy Systems, Springer, Berlin, (2006)

Technical documentation of micro-cogeneration unit with fuel cell Hexis Galileo, Hexis, a.g.

Experimental Investigation of Selected Parameter's Effect on Solid Biofuels Quality and Densification Process

Peter Križan¹, Miloš Matúš¹ and Michal Svátek¹

¹ Institute of Manufacturing Systems, Environmental Technology and Quality Management, Faculty of Mechanical Engineering, STU in Bratislava, Nám. Slobody 17, 81231 Bratislava, Slovakia;

1. Abstract

Paper describes the importance of experimental research of the interrelationships between the properties of input raw material, the process of mechanical treatment and the final quality of solid biofuels. The final quality of solid biofuels, which is represented by the physical properties of the solid biofuels and by the requirements related combustion process, is affected in the process of mechanical treating the input raw material with a set of parameters. The main aim of this paper is to present the importance of knowledge about the interaction of important influencing parameters during the process of mechanical treatment of input raw material and during the densification process into solid biofuels. This paper presents the research findings regarding the effect of influencing variables on the final density of solid biofuels during densification. Aim of the experimental process is to determine the mutual interaction between solid biofuels density and influencing variables during densification. Effect of input raw material parameters and technological parameters on solid biofuels density from wood sawdust was determined.

Keywords: solid biofuels, densification, particle density, compression pressure, pressing temperature, particle size, moisture content

2. Introduction

Area of biomass densification into final solid biofuels is very interesting and itself complicated. During the densification process, many various variables influence this process and thus the final solid biofuel quality. Solid biofuels quality is given by EU standards [1] and is evaluated by mechanical and chemical-thermic indicators of quality [2]. The properties of the raw material, as well as technological demands, are both very important during the solid biofuels production process [3 - 6]. In the field of biomass densification research, it is mostly about gaining knowledge related the behavior of important parameters, their effect on various aspects of the biomass densification process, and thus the effect on the final solid biofuels quality. To streamline the energy recovery process, biomass must be processed into a suitable form - densified into solid biofuels [7]. Nowadays, there are several manufacturers of densification machines with a wide range of products on the

market. However, not every machine can produce solid biofuels (briquettes, pellets) with the required quality which is given by technical standards. With today's broad expansion of densification technology, the lack of suitable raw material is beginning to emerge. The technological development of the machines and the trend in the energy recovery of a wide range of biological materials enhance the importance of experimental research in this area. In addition to the fact that biofuels producers already have to use less widely used types of biomass, they often ask whether another kind of raw material can be used. Requirements from the biofuels production are showing that another important fact is considering the possibility for a variable change of pressed material [5, 7]. These activities can cause serious problems during raw material treatment and lonely densification. Each type of raw material requires an individual approach, due to the variety of properties and chemical composition of the input raw materials [8, 9]. The input raw material needs to be treated for gaining the optimal particle size and the optimal moisture content level and we have to provide optimal technological parameters throughout the process of densification [8, 10]. Any small change in input can significantly affect the resulting quality of solid biofuels. Different properties of the input raw material require different mechanical treatment conditions and resulting in a different final quality of solid biofuels [9, 10]. Different raw material properties cause also different conditions during the densification process [11] and can influence also the pressing forces distribution along with the pressing chamber of densification machine [7, 12]. For this reason, it is appropriate to know perfectly the behavior of raw materials in the mechanical treatment process and to properly operate input technology and solid biofuel production based on knowledge. It is very important to determine the effect of each variable and their interaction and to quantify the effect of the variable on densification itself. Knowledge about densification process in the base is a necessary condition for the development and engineering of densification machines with effective production of solid biofuels.

On the base of our experiences, research studies and analyzes realized in abroad [5-12], they can be divided into the following three groups - raw material parameters, technological parameters and structural parameters of densification machine [5]. Raw material parameters is a group of parameters related to the type of raw material that is selected and used for densification. They are e.g. the type of raw material, the raw material particle size, moisture content or the temperature of the raw material. To the technological parameters belongs parameters related to the densification process itself, it's mean pressing technology. Specifically, we can include here the method of densification, the pressing temperature in the pressing chamber, the compression pressure along with the pressing chamber, the pressing speed, the holding time under acting pressure, the time and method of cooling. The group of structural parameters includes the structural parameters of a densification machine, respectively structural parameters of pressing tool. It is important to say that these parameter's effect is not an aim of this research paper.

The general purpose of this paper is to describe the research findings which were gained during experimental research on our department. This research findings is an overview of experimental investigation in biomass densification process and describes relations, interactions and effect of influencing variables on final solid biofuels quality.

3. Materials and Methods

From the densification machine construction point of view, all the above-mentioned parameters are interesting. But it is not possible to design and realize the experimental research, and also to quantify the effects of all parameters at the same time. Can imagine that in-depth research related the effects of all of these parameters is very extensive, complicated and requires a thorough analysis and understanding of the issue [5, 6]. For this reason, experimental research was divided into several phases.

During the densification process, can be recognized various acting forces [13, 14] in the pressing chamber which forms the conditions for solid biofuels pressing and releasing from the pressing chamber, e.g. axial forces, radial forces and counter forces. These parameters are very significantly changing according to basic variables (described above) [15]. The most important are interactions with compression pressure "p", pressing temperature "T", particle size "L" and raw material moisture content "w_r" [13, 15]. To obtain the correct results, was necessary to design the step by step experiment, where each investigated parameter's effect was determined separately. Experimental research conditions were adequately chosen according to the investigated parameter character, but take in mind the common, proper and interconnected evaluation of results.

3.1. Raw material in the experimental research

Experimental research in our laboratory conditions was carried out with widely known wooden, which are originating from south-western Slovakia. Softwoods and also hardwoods were chosen for this experiment and suitable raw material in sawdust form was obtained from wood processing company without bark. When the effect of raw material was determined the pine, spruce, oak and beech sawdust was chosen. When the effect of raw material parameters, technological and structural parameters were determined, the pine sawdust was used. Before the densification, it was necessary to characterize the basic properties of each used raw material, because particle size and moisture content of raw material influence the creation and value of binding forces between raw material particles, and thus the final physical properties of solid biofuel. The moisture content of sawdust before experimental research was measured by Kern MRS 120-3 balance. This measurement was based on heating the material (gravimetric method of moisture content measuring) [16] at $105 \pm 2^\circ\text{C}$ until a constant weight was achieved. Initially, the particle size distribution was analyzed by Retsch Vibrating Sieve Equipment AS 200 [17]. When the effect of particle size was determined, particle sizes 0.5, 1.0, 2.0, 4.0 mm and more than 4.0 mm were chosen according to our possibilities.

3.2 Experimental equipment and pressing procedure

Experimental research was realized for determination of technological and raw material variables effect on final solid biofuels quality during densification. Solid briquettes quality, as a final output of the densification process, was evaluated by its particle density [5, 18]. For each setting 7 briquettes were produced where the dimensions (diameter, length) [19] and weights of briquettes were measured and the particle density of briquettes was calculated.

Results and effects of lonely variables were evaluated from the final particle density point of view and graphical dependencies were created from values after stabilization. Briquette stabilization time is the time interval during which dilatation occurs. It is also the time interval during which the briquette stabilizes [5]. Briquette dilatation is an effect during which the briquettes dimensions and weight are changing (diameter, length and weight) [19]. These changes come from the internal parameters of the raw material and also external parameters of the densification technology. Dilatation directly influences the briquette particle density and therefore only obtained values after stabilization time were used for research evaluation.

Briquettes were produced by a vertical hydraulic press which was supplemented by the experimental pressing device (see Figure 1). This equipment is representing vertical single-pressing densification. The experimental pressing device consists of a base frame, a cylindrical pressing chamber with 20 mm diameter die, a heating device with a temperature sensor for temperature control and the backpressure plug. The additional pressing temperature was changed in the range from 20°C to 115°C. When the temperature into the chamber was reached the raw material was fed into the chamber and pressing by hydraulic piston was performed. The hydraulic press allowed setting the compression pressure in the range from 31 MPa to 318 MPa. Pressing chamber with various lengths were designed and prepared according to the dimensional conditions of pressing stand. Figure 1 shows the positioning and cross-section of the pressing chamber in a pressing device. The maximal dimensional limit for pressing chamber was 140 mm, shortest pressing chamber length was 80 mm.

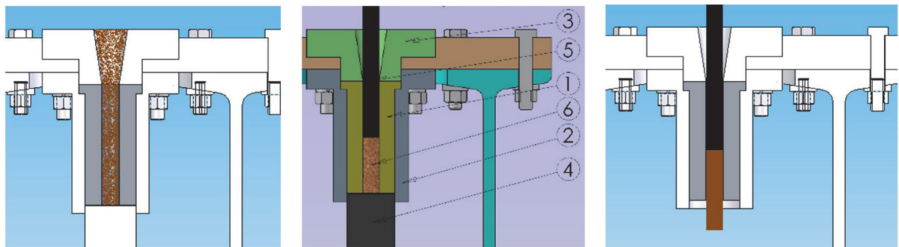


Fig. 1: Cross-view of the experimental pressing device and pressing phases (1-pressing chamber, 2-pressing chamber flange, 3-startup chamber, 4-counter pressure plug, 5-pressing piston, 6-pressed raw material).

4. Results and discussion

We have been working on experimental research in this area for several years. Since this research in the workplace has been addressed for a long time, it has been possible to obtain the results of the effects of different influencing variables on different types of biomass and to propose smaller or larger engineering designs of important densification machine parts. All results presented in this part were conducted from experiments in a similar manner on an experimental pressing device. We tried to preserve the continuity of the measurements

and the connectivity of the obtained results for the evaluation.

4.1. Effect of raw material parameters on biofuels particle density

In this part, the type of raw material, particle size and moisture content of raw material are the most influenced variables and therefore the effect of these variables on biofuels particle density was determined.

In this phase of the experiment, spruce, pine, beech and oak sawdust were used. We can see very clear differences between briquettes particle density from each type of raw material. The densification process works with different parameters (pressure, temperature, etc.) when pressing different types of materials. The main differences are in chemical composition, and not only between the group of softwoods and hardwoods but also between the individual trees [20]. With different types of materials and different input conditions, we are able to obtain different properties of final solid biofuels (particle density, mechanical durability, etc.) [22, 23]. The type of raw material which is densified is the very influencing parameter and ultimately affects the final quality of biofuels. Each type of raw material has its specific density, different from others. Raw material properties in a combination with technological parameters of the densification process very significantly influence the quality of the final briquettes. This is proven also in Figure 2.

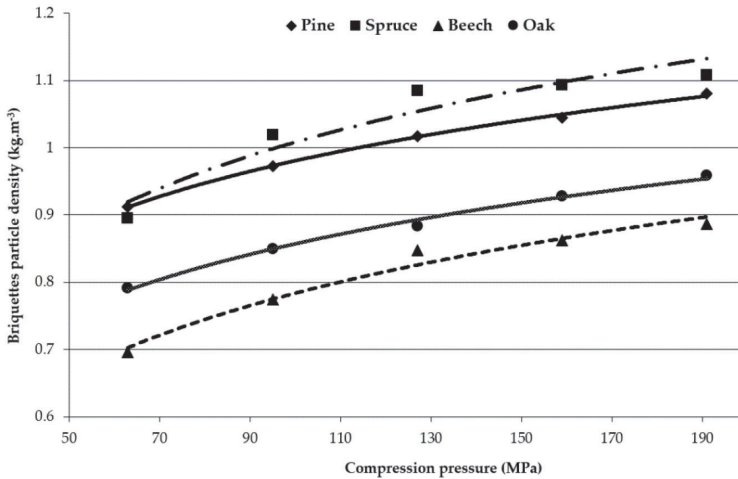


Fig. 2: Dependence of briquette particle density on the compression pressure for different types of raw material densified at the same conditions ($T=115\text{ }^{\circ}\text{C}$, $w_r=10\%$, $L=2.0\text{ mm}$).

The optimal value of moisture content in the raw material is a critical condition for densification of biomass. If we want to produce high-quality solid biofuels as required by standards, we also need to know the effect of raw material moisture content. It is possible to say that the quality of biofuels depends on the moisture content of raw material, but we cannot exactly indicate the optimal moisture content value. This optimal value has to be determined experimentally for each type of raw material being pressed separately and with respect to other influencing variables. On the following Figure 3, the dependence of briquette particle density on the raw material moisture content is displayed. In this case,

pine sawdust of particle size 2.0 mm was used. Since the objective was to determine the effect of moisture content, 8 levels of the configuration of the monitored variable were equally distributed over a range of 5% to 30 %. The compression pressure was constant and set at 286 MPa. Since we were pressing without increasing temperature, this compression pressure was selected to achieve briquettes compactness. We can observe that the two curves represent the state before and after stabilization. The briquette particle density difference is significant before and after stabilization, and the average difference in pine sawdust briquettes was around 9 %. Interesting is the interaction of raw material moisture content and pressing temperature (see Figure 4).

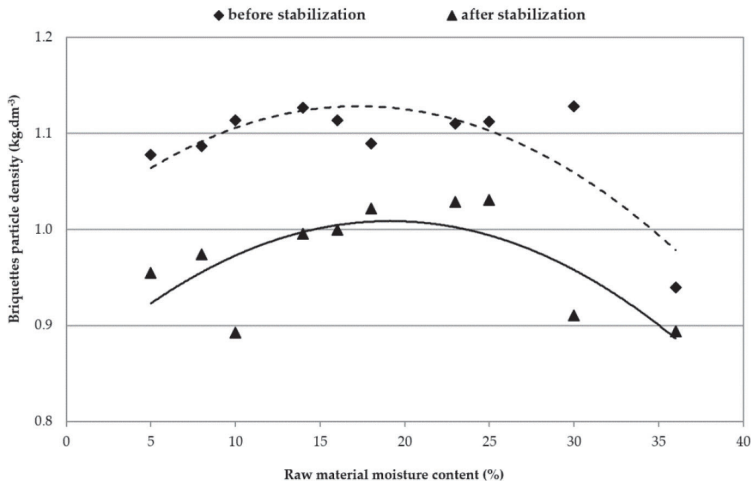


Fig. 3: Dependence of briquette particle density on the raw material moisture content – comparison state before and after stabilization (pine sawdust, T=23 °C, p=286 MPa, L=2.0 mm) [5].

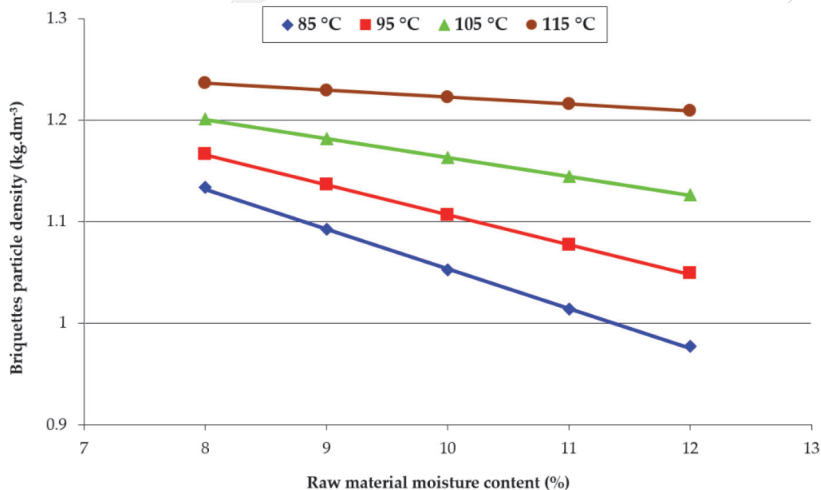


Fig. 4: Dependence of briquette particle density on the raw material moisture content at various pressing temperatures (pine sawdust, p=155 MPa, L=2.0 mm) [5].

In another experimental research, the pressing conditions were changed. Figure 4 shows the dependence between briquettes particle density and moisture content of the raw material at various pressing temperatures. The dependency tells us how the moisture content of the raw material combined with pressing temperature affects the final briquette particle density.

The particle size of raw material also has a significant effect on the densification process itself, if the particles size is large more power for densification is required [13, 15]. As can be seen in Figure 5, with increasing raw material particle density also increases the force needed for releasing the briquette from the pressing chamber. The briquette can have lower homogeneity and strength [22].

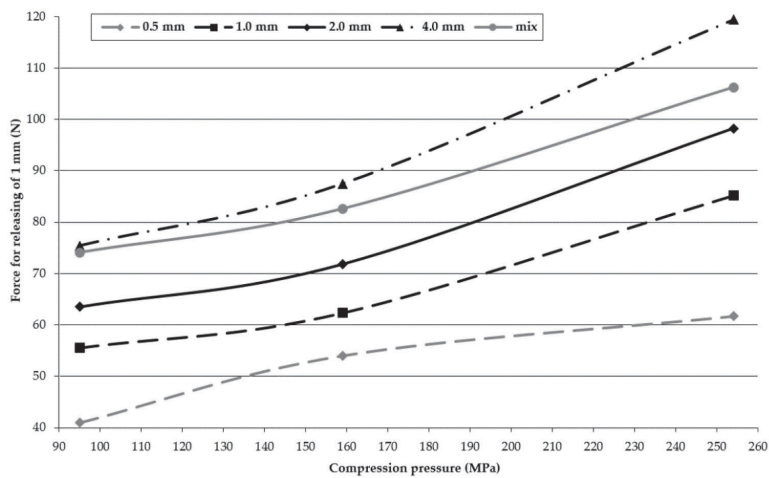


Fig. 5: Dependence of force for releasing of briquette on compression pressure for various levels of raw material particle size (pine sawdust, T=23 °C, wr=10 %) [6].

Conversely, the presence of more fine-grained particles helps to better densification of the material. Briquette is more cohesive and with better physical-mechanical properties. This effect can be supported by increasing of pressing temperature. Figure 6 shows when increasing the pressing temperature can be increased the briquette particle density. This was proven by each level of raw material particle size.

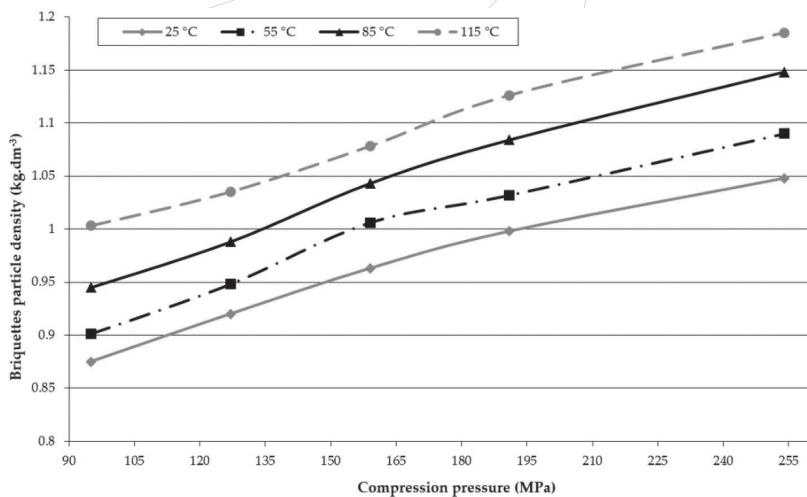


Fig. 6: Dependence of briquette particle density on the raw material particle size at various pressing temperatures (pine sawdust, $w_r = 10\%$, $L = 2.0$ mm) [6].

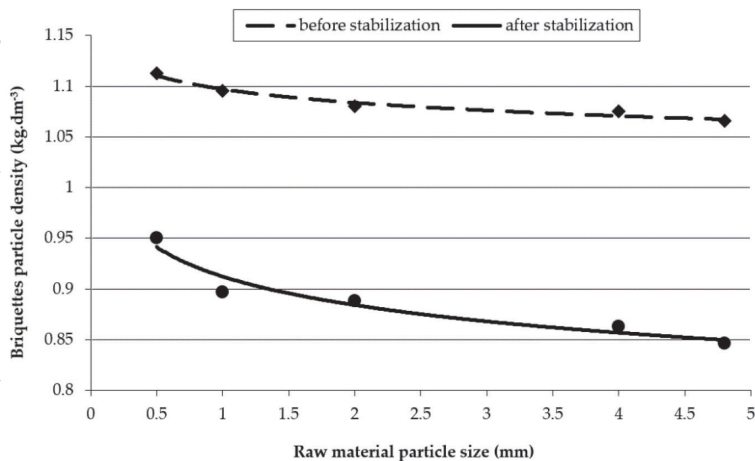


Fig. 7: Dependence of briquette particle density on the raw material particle size – comparison state before and after stabilization (pine sawdust, $T = 23$ °C, $p = 286$ MPa, $L = 2.0$ mm) [5].

On Figure 7, the dependence of briquette particle density on the raw material particle size is displayed. Can be seen that with increasing of particle size, briquettes particle density changes. It's important to notice, that for these results, the measurement was performed while pressing without any increase in pressing temperature during the process and at a constant compression pressure. A significant part of the experimental research was also studying the effect of particle size on the final quality of biofuels. The experimental results in Figure 7 have shown that decreasing particle size can positively influence the increase of briquette particle density. That is why it was important to also determine the effect of particle size change on briquette dilation. We again notice two curves, characterizing the state before and after stabilization. The briquette particle density difference before and after stabilization is very significant, the average change in density of Pinewood briquettes was around 18 %. As the size of the particles increases, the binding forces between particles decreases, resulting in the rapid break-up of the biofuels in the combustion process [23, 24]. The quality of the biofuels decreases and the necessary compression pressure increases as the particle size of the raw material increases. However, the optimal particle size of the raw material varies with respect to the densification technology used and the raw material to be densified. Research results have shown that by reducing the particle size, the increase in the physical properties of biofuels can be positively influenced.

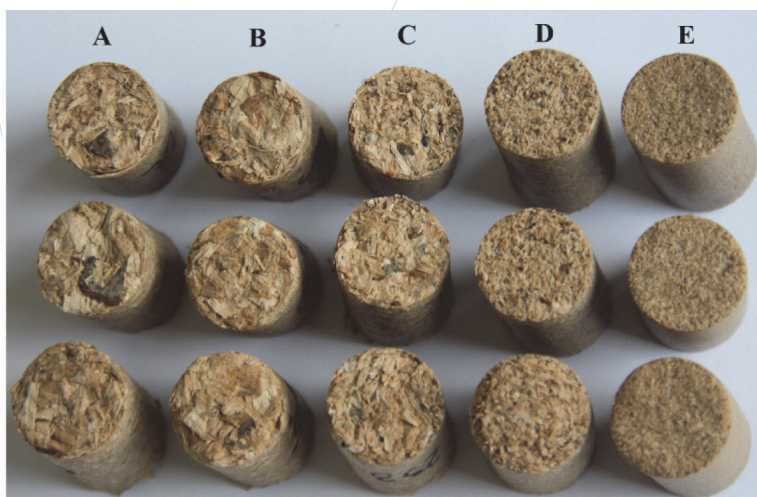


Fig. 8: Densified samples from beech sawdust with different particle size (A - mixture, B - up to 4.0 mm, C – up to 2.0 mm, D – up to 1.0 mm, E – up to 0.5 mm) [6].

4.2. Effect of technological parameters on biofuels particle density

Based on the knowledge gained in practice concerning the impact and variation of the design principles of densification machines (with their pressing tools), we can say that the densification method is a fundamental technological parameter that significantly affects the final quality of biofuels. In principle, there are only 2 basic methods of densification [14, 25]. We recognize densification in so-called “closed” pressing chamber and in an “open” pressing chamber. By changing the densification method, we can significantly influence the

resulting physical properties of the biofuels and also the formation of friction conditions in the pressing chamber. The densification method affects the distribution of the material layers in the biofuel and hence its strength. Compression pressure is a very important factor affecting mainly the biofuel strength.

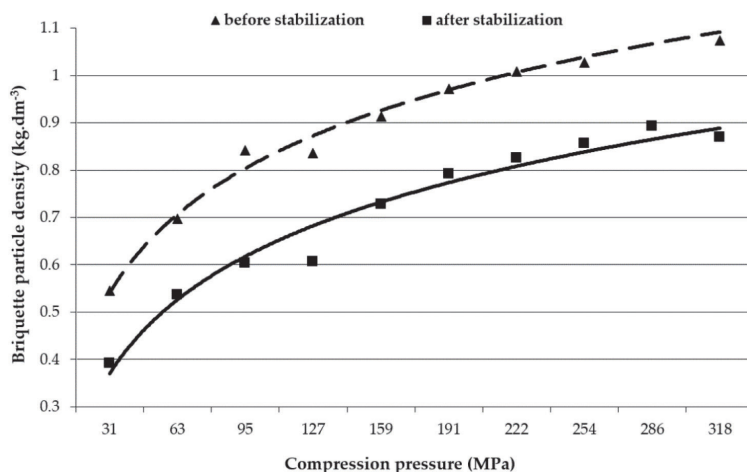


Fig. 9: Dependence of briquette particle density on the compression pressure (pine sawdust, $T=23\text{ }^{\circ}\text{C}$, $w_r=10\%$, $L=2.0\text{ mm}$).

With increasing the compression pressure, the biofuel particle density and biofuel strength increase, up to the strength of the raw material. Figure 9, also the differences between Pinewood briquettes before and after stabilization is shown. The difference is significant. Since it was proven, that briquette dilation (stabilization period) is very important, it was important to commence with the experimental research. The biggest difference in briquette density was noted at lower compression pressures. With the increase of compression pressure, these differences slightly decreased. We can say that the higher the compression pressure is during the process, the lower the briquette dilation. This can be very clearly seen in Figure 10 when the briquettes particle densities difference is displayed. This dependence shows the effect of compression pressure on dilation of briquettes. If the compression pressure is increasing the dilatation of briquettes is decreasing. When the raw material particle density is changed, the character of this effect is the same. The impact of compression pressure was noticed at each level of the monitored level of raw material particle density (see Figure 11).

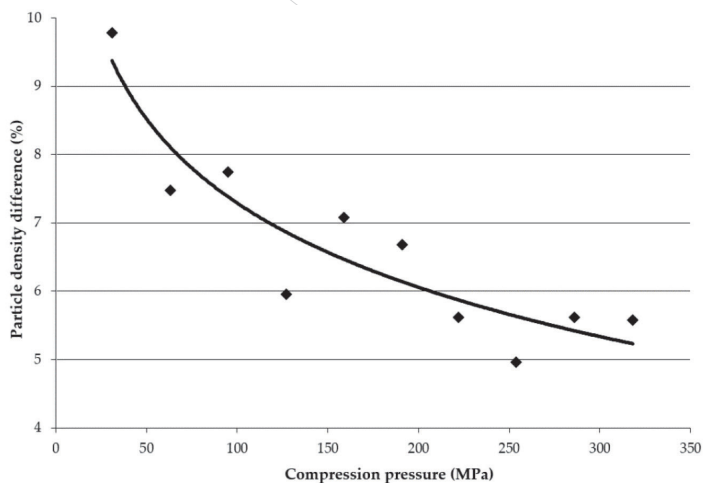


Fig. 10: Dependence of briquette particle density difference on the compression pressure (pine sawdust, $T=23\text{ }^{\circ}\text{C}$, $w_r=10\%$, $L=2.0\text{ mm}$).

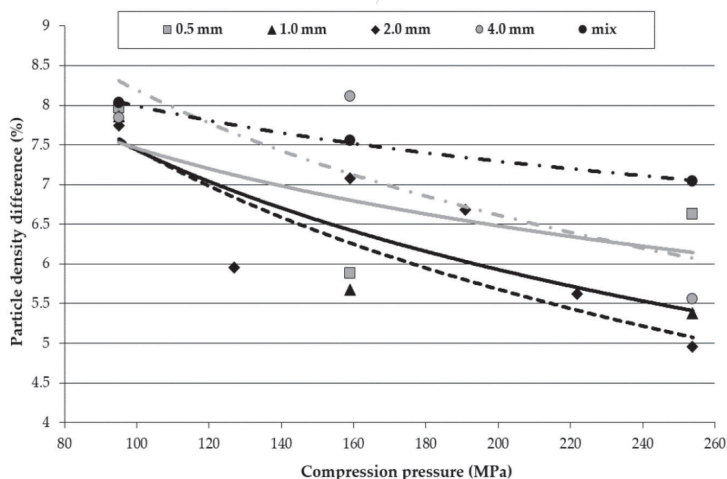


Fig. 11: Dependence of briquette particle density difference on the compression pressure for various raw material particle sizes (pine sawdust, $T=23\text{ }^{\circ}\text{C}$, $w_r=10\%$).

The pressing temperature has a significant effect on the quality and strength of biofuels [22]. This parameter determines lignin secretion from the biomass cell structure [22]. Lignin is very important during the densification process because in the pressed raw material its function is to combine the fibres and act as a strengthening factor of cellulose molecules within the cell walls [10, 11]. The more lignin the raw material contains and the more we can release it during the densification process, the higher the quality of the biofuels can be achieved. The lignin is only released at a certain pressing temperature, which has to ensure

for the densification process can work. However, this temperature also depends on the type of raw material being pressed.

In Figure 12, the effect of pressing temperature on briquette particle density can be observed. With increasing compression pressure and pressing temperature as well, briquette particle density increases. Pressing temperature during densification of wooden materials goes hand in hand with the compression pressure [25, 26]. It can be seen that the increase of pressing temperature has an effect on the higher value of briquette particle density at a lower compression pressure. The effect of pressing temperature in interaction with compression pressure and raw material moisture content can be observed in each biological raw material. Only the limited factor which influences during the densification the values of increment is lignin content. In Figure 13, the effect of pressing temperature on the particle densities difference and thus on briquette dilatation can be seen. This dependence shows the effect of compression pressure and pressing temperature as well on dilatation of briquettes. If the compression pressure and pressing temperature are increasing the dilatation of briquettes is decreasing.

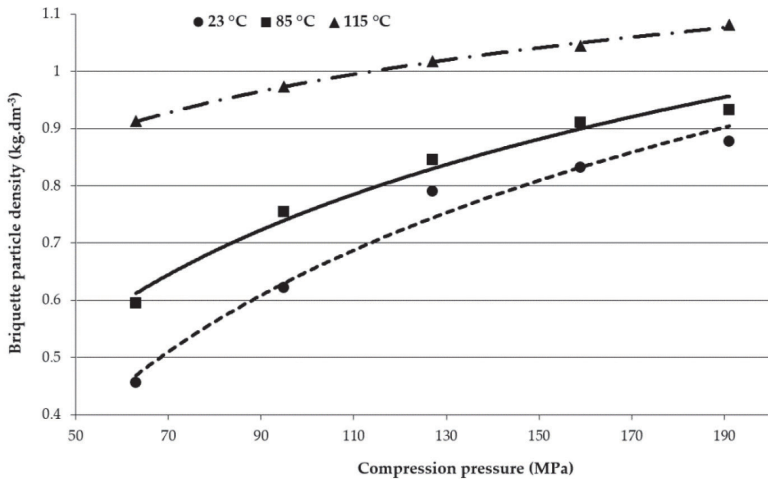


Fig. 12: Dependence of briquette particle density on the compression pressure at various pressing temperatures (pine sawdust, wr=10 %, L=2.0 mm).

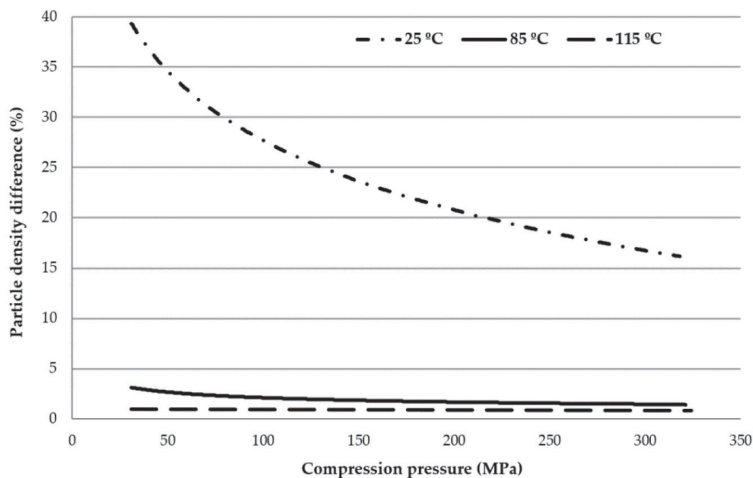


Fig. 13: Dependence of briquette particle density difference on the compression pressure at various pressing temperatures (pine sawdust, $w_r=10\%$, $L=2.0$ mm).

In Figure 14, dependence of briquettes particle densities on compression pressure executed without additional pressing temperature can be seen. In general, we can say that an obtained result (particle densities) weren't so different but proves the difference between single and multiple pressing. In the case of single pressing which represents “closed” chamber pressing were produced briquettes with highest densities at pressing chamber length 80 mm. In the case of multiple pressing which represents “open” chamber pressing were produced briquettes with highest densities at pressing chamber length 140 mm. We can see that repeated activity of compression pressure during multiple pressing positively influences the particle density of the briquettes.

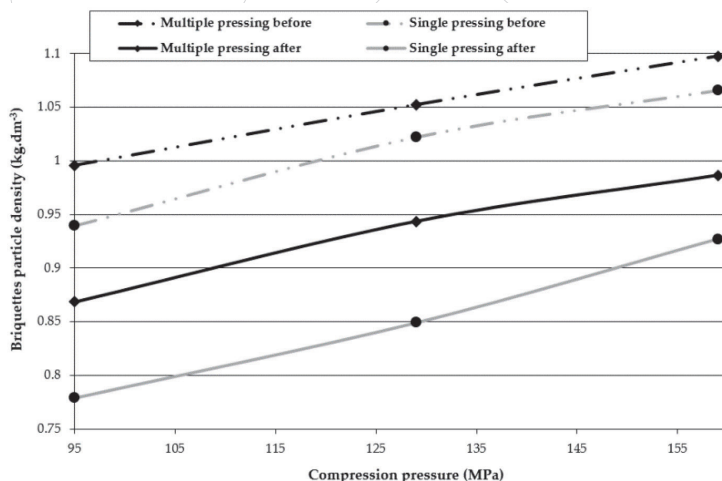


Fig. 14: Dependence of briquette particle density on the compression pressure during multiple and single pressing at 140 mm pressing chamber length (pine sawdust, $w_r=10\%$, $L=2.0$ mm).

If we compare briquette particle densities produced by single and multiple pressing for each pressing chamber lengths we can see that higher densities after dilatation were obtained during multiple pressing. Dependence of briquette particle density on compression pressure during single and multiple pressing at 140 mm pressing chamber length can be seen in Figure 14. With increasing of pressing chamber length also increases differences between briquettes densities produced during single and multiple pressing. A result presented in this part of paper proves that with multiple pressing can be achieved briquettes with higher densities.

According to the listed research findings we can see that the interaction of compression pressure and pressing temperature and properties of raw material is significant during biomass densification. Finding this functional dependence $\rho = f(p, T)$ is the “alpha and omega” of the whole densification process for the optimal construction of a densification machine [27]. In the Figure 15 the measured values of briquettes particle densities and pressure needed for releasing from the chamber related to the densification conditions are displayed. Here can imagine the positive effect of pressing temperature increasing from the final particle density point of view and forces distribution in pressing chamber as well. Also the economy point of view can be involved. If compare the added value from increasing of compression pressure and pressing temperature, very clearly we can say than greater efficiency can be achieved with increasing of pressing temperature.

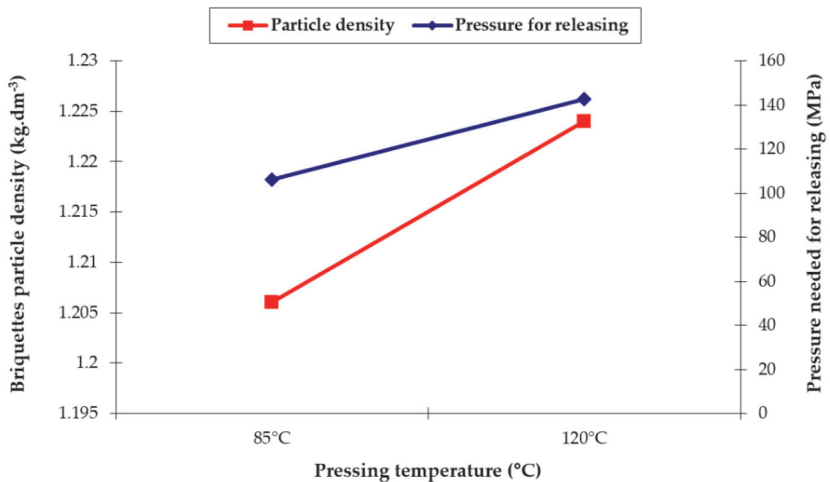


Fig. 15: Interaction of pressing temperature, the pressure needed for releasing and briquette particle density in 140 mm pressing chamber length (pine sawdust, $p = 159$ MPa, $w_r = 10\%$, $L = 2.0$ mm).

5. Conclusions

Based on the results of the experiments we can conclude that the influenced parameters significantly influence the final quality of biofuels. All investigating parameters have a significant influence on final briquette particle density. The results obtained will unconditionally find their application and use in practice. Finding the functional dependence can help when constructing a densification machine, sizing the drive, designing the mechanism [27], and sizing of the shape and dimensions of the pressing chamber, etc. The acquired knowledge about the influence of individual parameters can be used (or without) by the mathematical model at two basic levels. In the first case, after defining and setting the values of the monitored parameters, we can predict the resulting physical properties of solid biofuels. Such results are a useful tool for manufacturers of biofuels. In the second mode, the acquired knowledge can be used as a tool for the optimization of structural parameters. Engineers can use this knowledge, for example, to predict the compression pressure and pressing temperature, which can be very useful in optimizing machine and tool designs.

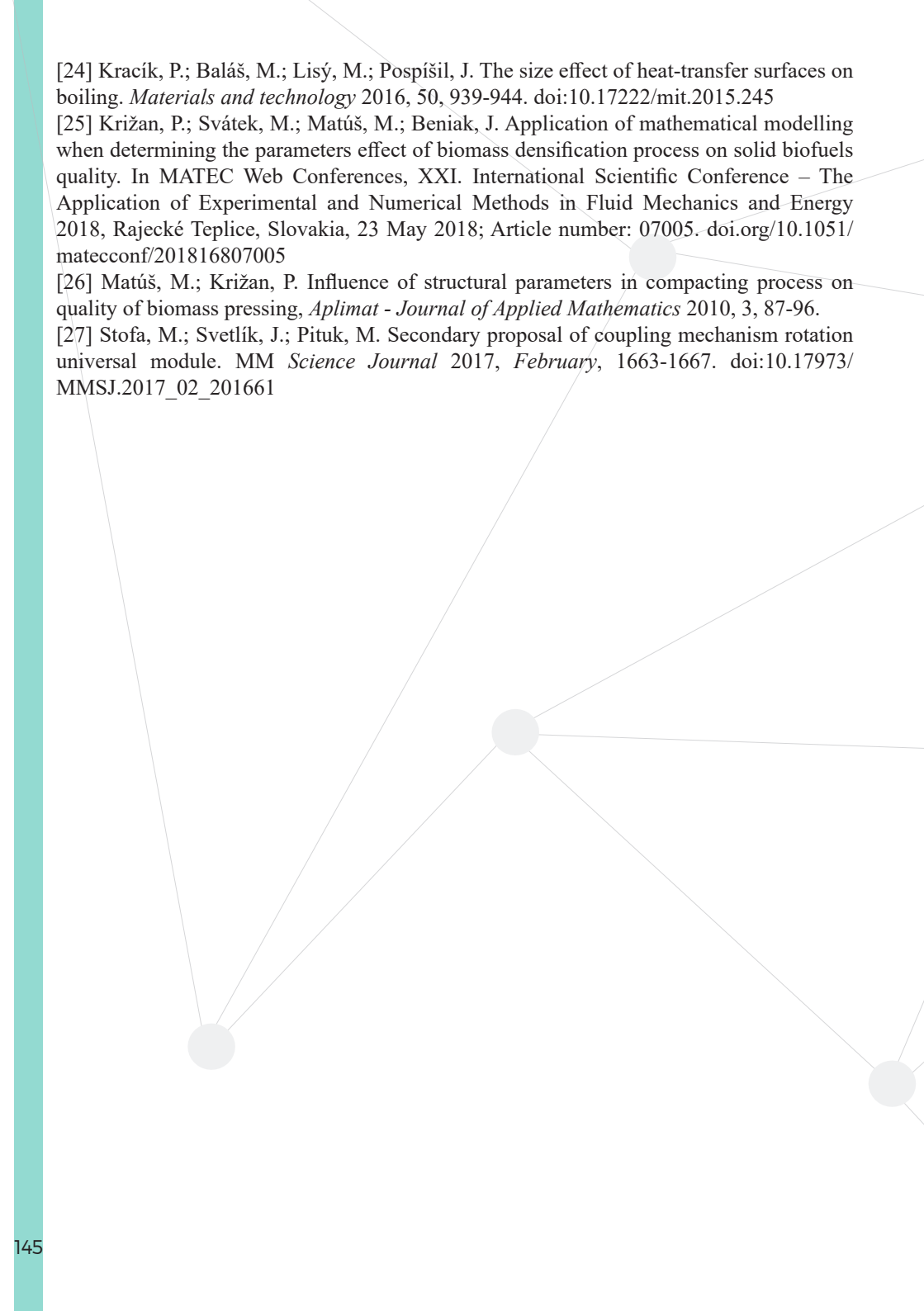
6. Acknowledgments

The paper is a part of the research done within the project VEGA 1/0085/19 – “Research of acting forces interaction during densification of biomass and shape optimization of pressing tools of densification machines” and within the project APVV- 18-0505 “Development of an original design of a compaction press with reversed kinematics”. The authors would like to thank the Ministry of Education of Slovak Republic, to the Slovak Academy of Sciences and to the Slovak Research and Development Agency.

7. References

- [1] European Committee. *Solid Biofuels—Fuel specifications and classes – Part 2: Graded wood pellets*; EN 17225-2:2014; European Committee for Standardization: Brussels, Belgium, 2014.
- [2] Nosek, R.; Holubčík, M.; Jandačka, J. The impact of bark content of wood biomass on biofuel properties. *BioResources* 2016, 11, 44-53. doi: 10.15376/biores.11.1.44-53
- [3] Arce, M.E.; Saavedra, A.; Míguez, J.L.; Granada, E.; Cacabelos, A. biomass fuel and combustion conditions selection in a fixed bed combustor. *Energies* 2013, 6, 5973–5989. doi:10.3390/en6115973
- [4] Thoreson, C.P.; Webster, K.E.; Darr, M.J.; Kapler, E.J. Investigation of process variables in the densification of corn stover briquettes. *Energies* 2014, 7, 4019–4032. doi:10.3390/en7064019
- [5] Križan, P. *The densification process of wood waste*, 1st ed.; De Gruyter Open: Berlin, Germany, 2015; p. 184.
- [6] Križan, P.; Matúš, M.; Šooš, Ľ.; Beniák, J. Behaviour of beech sawdust during densification into a solid biofuel. *Energies* 2015, 8, 6382-6398. doi.org/10.3390/en8076382

- [7] Holm, J.; Henriksen, U.; Hustad, J.; Sorensen, L. Towards an understanding of controlling parameters in softwood and hardwood pellets production. *Energy Fuels* 2006, 20, 2686-2694. doi.org/10.1021/ef0503360
- [8] Serrano, C.; Monedero, E.; Lapuerta, M.; Portero, H. Effect of moisture content, particle size and pine addition on quality parameters of barley straw pellets. *Fuel Processing Technology* 2011, 92, 699-706. doi.org/10.1016/j.fuproc.2010.11.031
- [9] Mani, S.; Tabil, L.G.; Sokhansanj, S. Effects of compressive force, particle size and moisture content on mechanical properties of biomass pellets from grasses. *Biomass and Bioenergy* 2006, 30, 648-654. doi.org/10.1016/j.biombioe.2005.01.004
- [10] **Kaliyan, N.; Morey Vance, R. Factors affecting strength and durability of densified biomass products. *Biomass and Bioenergy* 2009, 33, 337–359. doi.org/10.1016/j.biombioe.2008.08.005**
- [11] Lehtikangas, P. Quality properties of pelletized sawdust, logging residues and bark. *Biomass and Bioenergy* 2001, 20, 351-360. doi.org/10.1016/S0961-9534(00)00092-1
- [12] Nielsen, N.P.K.; Gardner, D.J.; Poulsen, T. Importance of temperature, moisture content, and species for the conversion process of wood residues into fuel pellets. *Wood Fiber Science* 2009, 41, 414-415.
- [13] Horrihgs, W. The dimensioning of an extrusion press. *Powder Technology* 1988, 56, 13-20. doi.org/10.1016/0032-5910(88)80017-2
- [14] Samuelsson, R.; Thyrel, M.; Sjostrom, M.; Lestander, T.A. Effect of biomaterial characteristics on pelleting properties and biofuel pellet quality. *Fuel Processing Technology*, 2009, 90, 1129-1134. doi: 10.1016/j.fuproc.2009.05.007
- [15] Horrihgs, W. Control of ram extruders for obtaining steady compaction pressures. *Aufbereitungs-Technik*, 1987, 28, 378-382.
- [16] European Committee. Solid Biofuels—Determination of moisture content. Oven dry method. Part 3: Moisture in general analysis sample; EN ISO 18134-3:2016; European Committee for Standardization: Brussels, Belgium, 2016.
- [17] European Committee. Solid Biofuels—Determination of particle size distribution for uncompressed fuels. Part 1: Oscillating screen method using sieves with apertures; EN ISO 17827-1:2016; European Committee for Standardization: Brussels, Belgium, 2016.
- [18] European Committee. *Solid Biofuels—Determination of particle density of pellets and briquettes*; EN ISO 18847:2017; European Committee for Standardization: Brussels, Belgium, 2017.
- [19] German Institute for Standardization. *Testing of wood; Determination of density*; DIN 52182:1976, Testing of wood, 1976.
- [20] Miranda, T.; Montero, I.; Sepúlvera, F.J.; Arranz, J.I.; Rojas, C.V.; Nogales, S. A review of pellets from different sources. *Materials* 2015, 8, 1413-1427. doi: 10.3390/ma8041413
- [21] Castellano, J.M.; Gómez, M.; Fernández, M.; Esteban, L.S.; Carrasco, J.E. Study on the effects of raw materials composition and pelletization conditions on the quality and properties of pellets obtained from different woody and non woody biomasses. *Fuel* 2015, 139, 629-636. doi:10.1016/j.fuel.2014.09.033
- [22] Li, Y.; Liu, H. High-pressure densification of wood residues to form an upgraded fuel, *Biomass and Bioenergy* 2000, 19, 177-186. doi: 10.1016/S0961-9534(00)00026-X
- [23] Balás, M.; Lisý, M.; Štelcl, O. The effect of temperature on the gasification process. *Acta Polytechnica* 2012, 52, 7-11.

- 
- [24] Kracík, P.; Baláš, M.; Lisý, M.; Pospíšil, J. The size effect of heat-transfer surfaces on boiling. *Materials and technology* 2016, 50, 939-944. doi:10.17222/mit.2015.245
- [25] Križan, P.; Svátek, M.; Matúš, M.; Beniak, J. Application of mathematical modelling when determining the parameters effect of biomass densification process on solid biofuels quality. In MATEC Web Conferences, XXI. International Scientific Conference – The Application of Experimental and Numerical Methods in Fluid Mechanics and Energy 2018, Rajecké Teplice, Slovakia, 23 May 2018; Article number: 07005. doi.org/10.1051/mateconf/201816807005
- [26] Matúš, M.; Križan, P. Influence of structural parameters in compacting process on quality of biomass pressing, *Aplimat - Journal of Applied Mathematics* 2010, 3, 87-96.
- [27] Stofa, M.; Svetlík, J.; Pituk, M. Secondary proposal of coupling mechanism rotation universal module. *MM Science Journal* 2017, February, 1663-1667. doi:10.17973/MMSJ.2017_02_201661

Biomass gasification and gas cleaning: combined utilization of in-situ catalyst and continually working filter for complete gas cleaning

Lisý M.¹⁾, Baláš M.¹⁾, Milčák P.¹⁾, Lisá H.¹⁾,

¹⁾Brno University of Technology, Faculty of Mechanical Engineering, Institute of Power Engineering

1. Abstract

The article deals with the possibility of purification of the gas produced by biomass gasification, especially tars removal by means of catalytic cracking. A brief classification of methods used to eliminate the tars is made in the introduction. The emphasis of the following text is on the description of a pilot plant of continually working hot catalytic moving bed filter employed tar and dust reduction. The basic parameters of the filter, basic operating conditions and the results achieved so far are introduced, including the primary measure based on direct catalyst loading into the fluidized bed generator. Although the mechanism is still in development, and the operating conditions, in particular, are still being optimized, gas tar content of under 10 mg.m⁻³n has been achieved by the hot catalytic filter using, with dust content ranging from 10 to 90 mg.m⁻³n. The results are sufficient to meet the objective – using the gas in the internal combustion engine.

Keywords: gasification, hot gas cleaning, tar removal

2. Introduction

Current trends in the power industry indicate toward wider application of renewable energy sources (RES). Biomass is currently regarded as the most promising RES in the Czech Republic. A wide range of processes is available for transforming biomass into more significant fuels. Gasification with subsequent combustion of the syngas in cogeneration units is one of the fast-growing technologies for future extensive application of biomass.

Thermochemical aerial gasification with air is a conversion of organic matter into low-energy gas, which after some modification is suitable for use in boilers, combustion engines or turbines. The composition of the gas is influenced by a number of factors, e.g. input composition, water content, reactive temperature, and oxidation range of pyrolytic products. The gas typically contains minute quantities of certain heavy hydrocarbons, such as ethane and ethene, fine particles of charcoal and ash, tars and other substances.

The presence of tar is one of the principal barriers to using the gas in cogeneration units. The tar concentration is primarily a function of the gasification temperature, decreasing

when the temperature increases. The relation between temperature and tar content is a function of reactor type and processing conditions. Tars originating in the pyrolysis thermal-crack mostly into heat-resistant tars, soot and gases. Testing has shown that the production of tars in wood gasification greatly exceeds that of coal or peat, and that wood tars are typically heavier and more stable aromatic hydrocarbons. This implies that the technologies developed for tar removal by coal gasification may not be directly transferable to biomass gasification. A number of research projects are therefore investigating the possibilities of reducing tar generation or of its effective elimination.

3. Tar elimination methods

Above all, devices to reduce tar content in gas can be divided into primary and secondary.

3.1 Primary methods

Primary methods are applied within the reactor. They are intuitively attractive as there is a potential to increase the total efficiency of the energy transformation, while reducing the need to eliminate tar from the gas outside the reactor, which can help reduce investment and operational costs. The two following processes are generally applied.

Thermal decomposition is the first, where tars can be cracked with success in the absence of catalysts at temperatures exceeding 1000°C, or above 1200°C in the ideal case, which imposes great requirements on the materials used in the construction [1]. The minimum temperature for the required efficiency of the destruction is not described, and will be dependent on the type of tars originating in the reactor.

Catalytic tar cracking is the second option. Various materials are added into the reactor bed to support the fission reaction as catalysts, such as dolomite, olivine, limestone, quartz sand, and another mineral or metallic materials. Dolomite and olivine are the most suitable in terms of availability, price and quality; the latter, however is not available in the Czech Republic [2,3]. The reactions in the fluid bed are very intensive thanks to the relatively high temperatures and turbulent flow; catalyst abrasion occurs, however. Current research indicates, anyway, that use of the above mentioned so-called in-situ catalysts may reduce tar content, nonetheless is viewed as inefficient in terms of complete tar elimination, at least in large-scale gasification systems.

3.2 Secondary methods

The so-called secondary devices represent subsequent tar elimination. The secondary devices may be divided into two groups: dry methods (catalysts), and wet methods (gas elution). The method of gas elution is based on artificial condensation of tar elements. This method of gas cleansing and cooling is simple and tried, but it has two fundamental disadvantages. Firstly, it degrades the heat contained in the gas, whereby a significant part of the thermal energy is lost. Secondly, and most importantly, wastewater contaminated with tars, phenols and other chemicals (NH₃, HCl, HCN) is produced, making biological water treatment impossible.

The effect and attributes of catalysts are described in detail in [2,3]. A separate reaction vessel allows better temperature control and reduces the turbulence in the bed, which can help prolong the reactive period. Dolomites, olivines, and calcites are generally used in tar cracking, as well as various metal catalysts based on Ni, Mo, Co, Pt, Ru and other elements [4,5]. The overwhelming majority of metal catalysts, however, are sensitive to deactivation by sulphur (so-called sulphur ragging-off), rendering their useful life short. Even low concentrations of hydrogen in the produced gas reduce the catalytic activity of metal-based systems. Their relatively lower operating temperatures are the advantage, achieving maximum tar conversion at 450-550°C. Under laboratory conditions, 95-99% conversion using dolomite has been achieved at 750-900°C.

4. Experimental unit biofluid 100

Research into biomass and solid waste gasification in an atmospheric fluidized bed commenced in the author's workplace in 2000. The fluid atmospheric reactor of the following parameters was built there:

•	output (syngas)	100 kWt
•	input (fuel)	150 kWt
•	wood consumption	40 kg/h
•	air flow	150 mn3/h



Fig. 1: Experimental unit Biofluid 100

The mechanism can work either in a gasification mode or a combustion mode. The gasification mode can be engaged with a stationary or circulating fluid layer. The fuel is taken from a feeder tank by a poker arm and fed to the reactor by a screw feeder fitted with a frequency converter. The primary air is compressed by a blow pump and fed to the reactor passing through a fan grate. The secondary and tertiary air intakes enter the reactor throughout its height. Flue dust is separated from the syngas produced in a cyclone and returned by an auxiliary screw feeder just under the reactor grate. The reactor ash is discharged into a storage vessel. To enable monitoring the effect of air pre-heating, an electric heater is engaged behind the blow pump. The low heating value of the produced gas ranges between 4 and 7 MJ/mn³, the solid particle content ranges between 1500 and 2800 mg/ mn³, and the tar content between 1 and 8 g/ mn³, depending on the fuel used and the operating conditions. A water sprinkling column was used to the syngas cleaning in the initial years of operation. A pilot plant of hot catalytic filter was added behind the gasifier in 2004.

5. Hot catalytic filter pilot plant

5.1 Description of the Hot Catalytic Filter

The design of the continually working hot catalytic filter (HCF) was oriented toward functional industrial technology from the very start. To achieve this, several structural and operating difficulties had to be eliminated. Ensuring long-term operation while changing the deactivated catalyst was the most difficult task. The novel two-part rotating grate serves this purpose by expelling it. The top conical surface of the grate and the bottom flat one have involute ribbing that move the catalyst first toward the perimeter of the reactor, where it falls through to the bottom of the grate. Subsequently, the bottom ribbing move the catalyst toward the centre of the reactor, where it falls out into a collector. The operation of the grate is discontinuous. A proportion of the filling is expelled when the filter pressure drop increases, whereby the deposits in the lower part of the reactor are disturbed.

The main dimensions were formulated on the assumed gas flow rate and pressure drop: diameter $D = 0.25$ m, height $H = 2$ m. The filter is heated with electricity, the input of which is 25 kW. In the development, this heating method is being replaced with partial combustion of the syngas within the filter. Air is introduced into the filter at three levels in the grate area. Oxidation in process should also remove the deposits of captured soot and fly ash.

The overall design of the HCF can be viewed in Fig. 2. Fresh dolomite is fed to the reactor from the container 1, fitted with the periodically switched slides 2 on its inlet and outlet. The reactor 3 is a cylindrical vessel with a rotating grate which expels deactivated filling into the collector 4, which also has a pair of alternatively operative slide valves 2 on its inlet and outlet. The gas is introduced in the lower part of the HCF, flows upwards through the catalyst bed and leaves the filter at the top. The HCF is fitted with an electrical heater 5 and air intake 6. The pressure drop of the HCF is measured, along with three temperature readings along the outer case of the filter which control the electrical heater (marked T201-T203 from above), four temperature readings along the filter axis (marked T211-T214 from below), and the temperatures of the input and output gas.

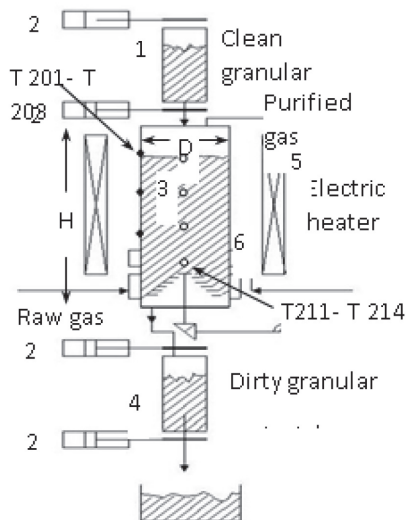


Fig. 2: Hot catalytic filter scheme

1.3 Operating Conditions

Various forms of dolomite are used for the filter filling. The above quoted literature lists dolomite as a material with good tar-cracking qualities. What is more, unlike olivine it is readily available in the Czech Republic, which would allow widespread industrial application. Experiments have shown, however, that the various materials marked as dolomite are of differing composition and physical qualities. Two of the laboratory samples were selected for testing in the filter. Table 1 shows their composition. Both the materials tested showed good effect in tar elimination, but only one of them (marked Material 1) was sufficiently resistant to abrasion and granulation. Therefore, not all the materials marked as dolomite are suitable for use in hot filters.

Tab. 1: Chemical composition of granular materials

Material Diameter [mm]	1 2,0 – 5,0	2 2,8 – 4,0
content: % wt.		
Na ₂ O	0,00	0,55
K ₂ O	0,24	0,42
MgO	17,63	5,66
CaO	32,87	40,31
SiO ₂	2,44	10,79
Al ₂ O ₃	1,34	3,06
Fe ₂ O ₃	0,31	0,97
CO ₂	45,03	37,97
Other	0,14	0,45

The pressure drop of the filter depends on the flow rate, i.e. speed, of the flowing gas, the filling and granularity of the material inserted. The gas flow rate through the HCF was about 25 m³n/h, with a corresponding pressure drop of 2.5-3 kPa. The behavior of the pressure drop (see Figure 3) shows that it increases as the filter is clogged with dust and the development of the so-called filter cake, while the pressure drop decreases sharply with the expelling of a proportion of deactivated dolomite. If the dolomite is not partially exchanged in the filter, the filter pressure drop will increase sharply up to 10 kPa, while the gas flow rate through the filter decreases accordingly.

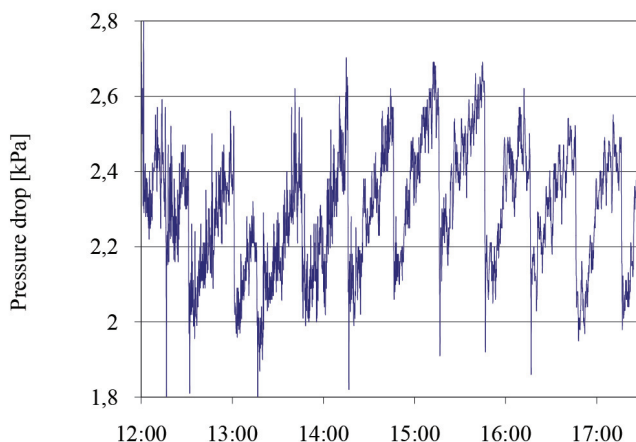


Fig. 3: Pressure drop of HCF

The active zone thermal characteristic is best evident from Figure 4. It shows the standard behavior in the filter thermal characteristics. Temperatures marked 201 to 203 are taken from the side wall of the filter and control the electrical heater. They are typically set to 1000°C. The effect of the cold newly inserted catalyst is evident from the filter top temperature 201. Thermocouples marked 211 to 214 are inserted in a tube placed in the filter axis (see Fig.2). Temperature 211 is taken approximately 20 cm above the grate, below the electrical heater. The gas input is roughly at this same height. The three other thermocouples are then positioned at 50 cm intervals.

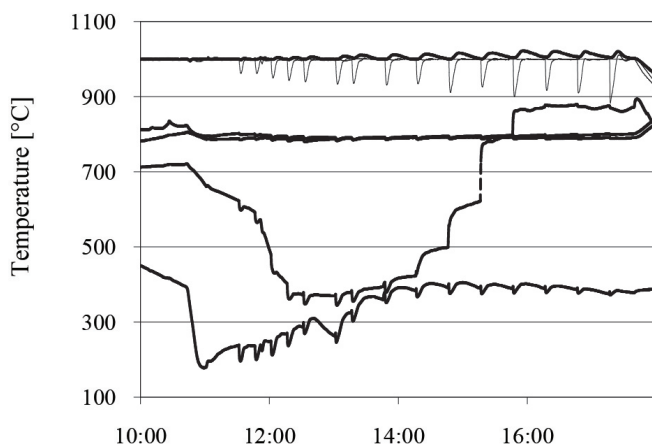


Fig. 4: Temperature in the HCF

5.3 Brief Overview of Results

Table 2 below summarises the changes in the gas composition before and after the catalytic filter. Some characteristic changes can be seen in the gas composition, caused by reforming reactions: an increase in the proportion of carbon monoxide and hydrogen due to the catalytic reactions. The increased carbon dioxide content is, among other reasons, generated by calcination of the added catalyst. The decrease in hydrocarbons is evident and logical.

The bed temperature is of decisive effect on the tar elimination. Best results are achieved when the catalyst temperature reaches near 900°C, or exceeds it in the better case. Table 3 below shows the various levels of tar elimination effectiveness and tar concentration before and after filtering. Table 4 shows the corresponding filter temperatures during the sampling instances. The tar was sampled by capturing in organic solvent and then analysed in a gas chromatograph.

Tab. 2: Average gas composition before and after HCF

Component	Before filter	After filter
	Content % vol.	
CO ₂	16,330	17,720
H ₂	12,875	16,115
CO	16,030	20,660
CH ₄	2,750	1,680
N ₂	50,580	43,740
ethane	0,101	0,006
ethylene	0,910	0,035
acetylene	0,183	0,021
propane	0,002	0,000
n-butane	0,002	0,000
cyklopentadiene	0,012	0,000
n-hexan	0,002	0,000
1,3-butadien	0,024	0,000
benzen	0,140	0,023
toluen	0,025	0,000
Other	0,034	0,000

Tab. 3: Tars content before and after

	Before filter	After filter	Catching efficiency
No.	[mg .m ⁻³ _n]	[mg .m ⁻³ _n]	[%]
1	3286	3	99,91
2	3167	211	93,34
3	2654	136	94,87
4	1141	6	99,47
5	3782	3	99,92

Tab. 4: Average temperature in HCF during sampling

	T 211	T 212	T 213	T 214
No.	[°C]	[°C]	[°C]	[°C]
1	506,5	796,1	802,5	801,2
2	283,1	375,6	784,8	792,2
3	394,3	508,3	790,5	793,5
4	386,4	873,5	789,6	798,1
5	327,6	430,7	921,5	833,7

As was mentioned above, catalysts can be used in two ways: they can be inserted directly into the fluidized bed, or engaged in a subsequent hot catalytic filter. Both ways were researched into experimentally, although more attention was given to the development of a hot catalytic filter. Other experiments were carried out to examine the effect of loading the catalyst into the fluidized bed. The objective was to reduce the loading of the hot filter, thus reducing its size. Since a variety of literature deals with this method of tar reduction, we applied the findings summarised in [2,3,4]. Different fractions and amounts of catalyst were used. After the loading was optimised for the current experimental unit, better results were achieved using a fine dolomite fraction (0.1-0.5 mm) dosed at 70 gdol/kgfuel. The tar reduction in the gas was approximately 60%, enabling a significant reduction in the catalytic filter loading.

Dust concentration in the filtered gas was measured using an isokinetic heating probe. The concentration ranged from 10–90 mg/m³. Escaping dolomite abrasion constituted a substantial proportion of the solid particle catch, but that can be separated from the de-tarred gas using regular cloth filters, as the gas needs to be cooled down to 30–40°C for use in the combustion engine anyway.

6. Conclusion

The results achieved show that the continually working hot catalytic filter combined with an effective primary measure (loading catalyst into the fluid bed) that is being developed provides an efficient and cheap method of syngas cleaning at high temperatures without loss in the total effectiveness. The effectiveness of separating solid particles depends on the granularity of the bed material, the speed of the flowing gas, and the character of the particles. The effectiveness of tars reduction, in turn, depends mainly on the operating temperatures of the HCF, the qualities of the material loaded into the HCF, and the level of its calcination.

Once the operating conditions are optimised, the continuous hot catalytic filter presented will enable efficient and effective of syngas cleaning to make it usable in the combustion engine. The significant benefit is that no liquid contaminated waste is generated. Deactivated dolomite is the only waste product. Soot and dust clogging is the main cause

of its deactivation. Such deposits can be removed by high-temperature oxidation, and the catalyst regenerated in such a way can be reused for primary feeding into the gasifier.

Another benefit of the filter is the fact that most of the potential heat of the gas can be used. In gas elution, a proportion of the heat contained in the gas is transferred into low-temperature water, thus being wasted.

7. Acknowledgments

This work was supported by the Ministry of Education, Youth and Sports of the Czech Republic under OP RDE grant number CZ.02.1.01/0.0/0.0/16_019/0000753 "Research centre for low-carbon energy technologies"

8. References

- [1] D. J.Stevens: Hot Gas Conditionig: Recent Program With Larger-Scale Biomass Gasification Systems. National Renewable Energy Laboratory – Colorado, (2001) NREL/SR-510-29952
- [2] Corella J.,Toledo J.M., Padilla R.: Olivine or Dolomite as In-Bed Additeve in Biomass Gasification with Air in a Fluidized Bed: Which is better?, *Energy&Fuels*, (2004),18, 713-720
- [3] Delgado J.,Aznar P.M., Corella J.: Calcined Dolomite, Magnesite, and Calcite for Cleaning Hot Gas from a Fluidized Bed Biomass Gasifier with Steam: Life and Usefulness, *Ind. Eng. Chem. Res.*, (1996), 35, 3637 - 3643
- [4] Caballero M.A., Corella J.,Aznar P.M., Gill J.: Biomass Gasification with Air in Fluidized Bed. Hot Gas Cleanup with Selected Commercial and Full-Size Nickel Based Catalysts, *Ind. Eng. Chem. Res.*,(2000), 39, 1143-1154
- [5] Simell P.: Catalytic Hot Gas Cleaning of Gasification Gas, Technical Research Centre of Finland, Espoo, 2000, 68s.



The project is co-financed by the Governments of Czechia, Hungary, Poland and Slovakia through Visegrad Grants from International Visegrad Fund.

The mission of the fund is to advance ideas for sustainable regional cooperation in Central Europe.